CHANNEL ESTIMATION AND PRECODING FOR MASSIVE MIMO DOWNLINK TIME –DIVISION DUPLEX SYSTEM

Tedros Salih Abdu

(EE300-0001/15)

A thesis submitted to the Pan African University Institute of Science, Technology and Innovation in partial fulfillment of the requirements for the award of the degree of Master of Science in Electrical Engineering (Telecommunication option) of the Pan African University

February 2017

DECLARATION

This thesis is my original work, except where due acknowledgement is made in the text, and to the best of my knowledge has not been previously submitted to the Pan African University or any other institution for the award of a degree or diploma.

NAME: Tedros Salih Abdu

REG. No. EE300-0001/15

SIGNATURE---------- DATE ----------

TITLE OF THESIS: Channel estimation and precoding for massive MIMO downlink time-division duplex system

PROGRAMME: MASTER OF SCIENCE IN ELECTRICAL ENGINEERING

SUPERVISOR CONFIRMATION:

This thesis has been submitted to the Pan African University Institute of Science, Technology and Innovation with our approval as the supervisors:

1. Name: …… Signature:……. Date:……..

2. Name: …… Signature:…… Date:…….

ABSTRACT

The massive MIMO technology uses a large number of antennas at the base station to transmit and receive signals using a Time Division Duplex (TDD) to/from users at the same time and the same frequency but with different time slot for uplink and downlink transmission. This gives a high spectral efficiency and improves reliability. In a massive MIMO downlink system the channel is estimated using uplink training by sending an orthogonal pilot sequence from users to the base station. The orthogonal pilot sequence is known at the base station and can be used to estimate the channel. This estimated channel is used to precode data at the base station for downlink transmission. Due to the coherence time limitation, the orthogonal sequence are re-used in different cells, causing the base station to receive non-orthogonal pilot sequence from adjacent cells which have an impact in estimating the channel. This channel estimation error is known as pilot contamination**.** In this thesis, a pre-coder technique for massive MIMO downlink TDD system is developed by considering the impact of pilot contamination in the estimating of a channel. Considering the impact of pilot contamination, a pilot reuse factor is designed to develop a novel uplink training scheme which enables an optimal estimate of the channel. The optimal estimated channel is used to develop a large scale fading precoder. A large scale fading precoding system is applied together with pilot reuse factor to mitigate the pilot contamination effect. This achieves a higher transmission rate over existing method. From simulation results obtained using MATLAB, an improvement on the 5% outage rate 10 times over the existing method has been realized. This is a significant improvement but obtained at the expense of sub-array BS installation and power consumption.

ACKNOWLEDGEMENT

First of all, I am thankful to God for the good health and well-being that has enabled me to complete this work. I am also grateful for the financial assistance received from the Africa Union during the period of my studies.

Secondly, I would like to express my heartfelt gratitude to my supervisors, Prof. Elijah Mwangi and Dr. Kibet Langat for their continuous support and motivation. My sincere thanks also go to the Pan African University staff, JICA, and the department of Electrical Engineering of Jomo Kenyatta University of Agriculture and Technology, for providing me with all the necessary facilities for the research.

Finally, I would like to express my deep gratitude to my family, colleagues, friends and others whom directly or indirectly support me in many ways for successful accomplishment of this thesis.

Contents

LIST OF FIGURES

ABBREVIATIONS AND ACRONYMS

3GPP	3rd Generation Partnership Project
BS	Base Station
CDF	Cumulative Distribution Function
CSI	Channel State Information
ELECOM	Emerging Trends in Electrical, Electronic and Communications Engineering
i.i.d.	Independent and Identically Distributed
JICA	Japan International Cooperation Agency
LMMSE	Linear Minimum Mean Square Error
LSFP-CC	Large scale fading precoding with cell cooperation
LSFP-NCC	Large scale fading precoding without cell cooperation
MATLAB	Matrix Laboratory
MIMO	Multiple Input and Multiple Output
ML	Maximum Likelihood
MMSE	Minimum Mean Square Error
MU-MIMO	Multi User Multiple Input and Multiple Output
MRT	Maximum Ratio Transmission
PCP	Pilot Contamination Precoding
PCE	Pilot Contamination Effect
PF	Pilot factor
SISO	Single Input Single Output
SNR	Signal-to-Noise Ratio
SINR	Signal-to-Interferance-Puls-Noise-Ratio
TDD	Time –Division Duplex
ZF	Zero Forcing

CHAPTER ONE

INTRODUCTION

The effect of multipath fading, limited power at the transmitter and scarce spectrum makes the task of designing high data rate, high reliability wireless communication systems extremely challenging. A solution to this challenge is the use of Multiple Input and Multiple Output (MIMO) technology that uses multiple antennas both for transmission and reception. When the number of antennas at the transmitter and receiver increases the degree of freedom in propagation channel increases and gives an improvement in the data rate or link reliability [1] [2].

MIMO techniques were first investigated in point-to-point MIMO where a multiple antennas at the transmitter communicated with multiple antennas at the receiver and gives significant performance enhancements in terms of data transmission rate and transmission reliability with respect to single input and single output wireless systems. But in point-to-point MIMO, the hardware complexity and energy power consumption of the signal processing units also increase at both the transmitter and receiver sides [2]. It is also not scalable and has unfavorable propagation. The unfavorable propagation can be minimized using multi user MIMO (MU-MIMO) in which the multiple antenna at the receiver side is divided into many independent terminal users. But MU-MIMO is not a scalable technology since it was first designed to have an equal number of service-antennas and terminals and to operate in frequency division duplex mode [3]. It also uses dirty-paper coding/decoding, and both ends of the link has to know the CSI which causes complexity as the number of antennas increased [4]. The massive MIMO technology has been proposed as a solution to scalability. It is a system where a base station (BS) with a large number of antennas array simultaneously serve many user terminals, each having a single antenna, in the same time-frequency resource [5][6]. The basic advantages offered by the features of massive MIMO can be summarized as follows:

I. High capacity: Massive MIMO can increase the capacity 10 times or more. The capacity increase results from the aggressive spatial multiplexing used in massive MIMO [3] [5].
II. Energy efficiency: The fundamental principle that makes the dramatic increase in energy efficiency possible is that with large number of antennas, energy can be focused with extreme sharpness into small regions in space [3] [5] [7] [8].
III. Increased robustness and reliability: Massive MIMO uses large number of antennas which allows for more diversity gains that the propagation channel can provide. When the number of antennas increases without bound, uncorrelated noise, fast fading, and intra cell interference vanish [2] [9]. This in turn leads to better performance in terms of data rate or link reliability.
IV. Simple linear processing: Because it uses large number of antennas at BS, simplest linear pre-coders and detectors are optimal [9] [10].
V. Massive MIMO can be built with inexpensive, low-power components. It uses hundreds of low-cost amplifiers with output power in the milli-Watt range. Several expensive and bulky items, such as large coaxial cables, can be eliminated completely [3].

1.1 Problem Statement

Generally, the massive MIMO system operates in Time –Division Duplex (TDD) mode and uses the same frequency for uplink and downlink transmission with separated time. In TDD mode the channel is reciprocal, meaning that the channel response is the same in both directions and by taking this advantage uplink training is used for estimating of the channel at the base station. In uplink training the user sends orthogonal pilot signals that are known to the base station then the base station estimates the channel. But the number of orthogonal pilot sequences are limited because the coherence time of the channel is small. These orthogonal signals need to be re-used at different cells. When two or more users uses non-orthogonal pilot sequence at the adjacent cells, interference occurs when the pilot sequences are received at the base stations causing an error in the estimation of the channel which is known as pilot contamination. This thesis is focused on developing an optimal

precoding technique for massive MIMO downlink TDD system by considering the impact of pilot contamination in the estimation of a channel.

1.2 Motivation

Massive MIMO is the most promising technology for 5^{th} generation wireless networks due to its high spectral efficiency. This is because massive MIMO uses the same frequency to serve users at the same time but different time slots for uplink and downlink transmission. As the number of antennas at the base station increases, the channels become asymptotically orthogonal. This allows the use of energy efficient and low complexity linear pre-coders. Such techniques will serve to improve the quality of future cellular mobile networks. However, the system can be deployed only if the problem of pilot contamination is efficiently resolved.

1.3 Objectives

1.3.1 General Objective

The main objective in this thesis is to design a precoder for downlink Massive MIMO TDD system to mitigate the effect of pilot contamination in the wireless channel estimation.

1.3.2 Specific Objectives

The specific objectives are:

i. To investigate the effect of Pilot contamination on estimation of the channel.
ii. To optimally estimate the channel by considering the pilot contamination effect.
iii. To design a precoder for massive MIMO using the estimated channel.
iv. To validate the designed precoder by comparing with existing methods.

1.4 Scope of Work

In this thesis a practical precoder design has not been carried out rather a mathematical precoder model has been developed by considering the impact of the pilot contamination in channel estimator. Since the thesis is focused in precoder designing for downlink massive MIMO TDD system then the uplink Massive MIMO TDD system is not considered.

1.5 Thesis Organisation

The rest of the thesis is organized as follows. In chapter 2 literature review in MIMO wireless communication and method of mitigation of pilot contamination effect that has been done previously are discussed. The pilot contamination analysis is presented in chapter 3. In chapter 4, the model of massive MIMO system is given. A detailed discussion of large scale fading precoding is also given. In addition, the derivation of the achievable rate with a finite number of base station antennas is presented. In chapter 5, the computer simulation results that support the proposed method are presented. Finally, chapter 6 gives a conclusion and suggestions for future extension of the work.

1.6 Note on Publication

The work in this thesis has been published as a paper entitled "Large Scale Fading Precoder for Massive MIMO without Cell cooperation" at the first international conference on Emerging Trends in Electrical, Electronic and Communications Engineering (ELECOM 2016) held in Mauritius from 25th to 27th November 2016. The paper was later published in the Springer Lecture Notes in Electrical Engineering series, vol 416. pp 239-251, 2017. A copy of a paper given in the appendix C.

CHAPTER TWO

LITERATURE REVIEW

2.1 MIMO Wireless Communication

Wireless communication is a communication between a transmitter and receiver through an air interface medium. The information signals propagate through space in the form of electromagnetic waves where they are reflected, scattered, and diffracted by walls, terrain, buildings, and other objects. Due to multiple reflections from various objects, the electromagnetic waves travel along different paths of varying lengths and arrive at the receiving antenna by two or more paths which leads to multipath propagation. Reflection occurs when the electromagnetic waves impinge on objects which are much greater than the wavelength of the travelling wave. Diffraction is a phenomena occurring when the wave interacts with a surface having sharp irregularities. Scattering occurs when the interface medium contains objects that are much smaller than the wavelength of the electromagnetic wave. These varied phenomena leads to large scale and small scale propagation fading. The Large-scale fading occurs due to path loss of signal as a function of distance and shadowing by large objects such as buildings and hilly or mountainous terrain. This happens as the cell-phone user moves through a distance of the order of the cell size, and is typically frequency independent. Small-scale fading occurs due to the constructive and destructive interference of the multiple signal paths between the transmitter and receiver. This happens at the spatial scale of the order of the carrier wavelength, and is also frequency dependent.

Fading can cause poor performance in a communication system because it can result in a loss of signal power without reducing the power of the noise. Fading can also be a problem as it is time variant. Although communication systems are often designed to adapt to such impairments, the fading process can change faster than the adaptation rate. In such cases, the probability of experiencing a fade (and associated bit errors as the signal-to-noise ratio drops) on the channel becomes the limiting factor in the performance of the link [11]. In this regard, multi-user multiple-input multiple-output

(MIMO) techniques have been a solution to combat multipath fading [12]. It is a wireless communication technology that uses multiple antennas at the transmitters and receivers to send more data signal at the same radio channel by exploiting multipath fading.

2.2 Benefits of MIMO Technology

Some of the benefits of MIMO technology are to be discussed here. These are:

I. Array gain

Array gain is the improvement of signal-to-noise (SNR) due to a coherent combining effect of signals at the receiver. The coherent combining can be realized using spatial processing at the receiver multiple antennas and/or at the transmitter multiple antennas [1] [13].

II. Spatial diversity gain

Spatial diversity gain improves the reliability of communication. Copies of an information signal are transmitted over multiple antennas so that the probability of at least one of the copies does not experience a deep fade when the signal is received [1].

III. Spatial multiplexing gain

Spatial multiplexing is used to achieve a high data rate by transmitting multiple, independent data streams over a multipath channel by exploiting multipath. These signals are transmitted over the same frequency band thereby enabling high data rate to be achieved [1] [14].

IV. Interference reduction and avoidance

In a MIMO system, increasing the separation between users by exploiting the spatial dimension reduces interference. The spatial dimension can also help in the avoidance of interference by directing the signal energy towards the desired user and reducing interference from other users [1].

Generally, it is difficult to achieve all the above benefits simultaneously due to parameter inter-relationship and there should be a tradeoff between these benefits.

2.3 Point-to-point MIMO System Model

Consider a MIMO system with M_t antennas at the transmitter and M_r antennas at the receiver as shown in figure 2.1.

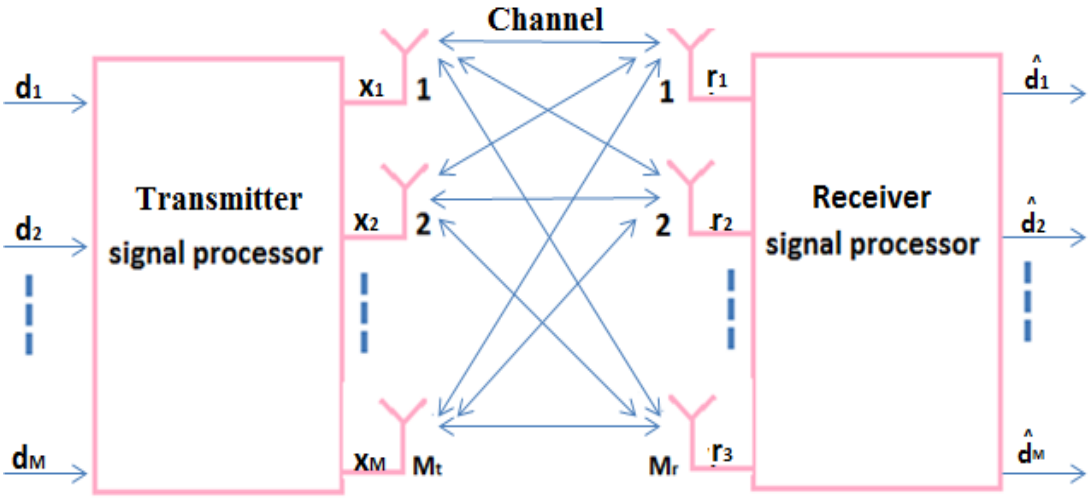

Figure 2.1 Block diagram of a MIMO system

Assuming the channel to be a Gaussian channel such that the elements of x are considered to be independent identically distributed (i.i.d.) Gaussian variables [13]. At the jth receiving antenna, the signal is:

$$r_j = \sum_{j=1}^{M_t} h_{ij} x_i + N_j\,, \quad i = 1, \dots, M_r \tag{2.1}$$

Where

h_{ij} is the channel response between the ith transmit antenna and the jth receive antenna

r_j is the received signal at the jth antenna

x_i is the symbol transmitted from the ith antenna

N_j is the noise signal at the jth receive antenna

In matrix form equation (2.1) becomes,

$$\boldsymbol{R} = \boldsymbol{HX} + \boldsymbol{N} \tag{2.2}$$

Where $\boldsymbol{R} = \lfloor r_1, \dots, r_{M_t} \rfloor^T$

$\boldsymbol{X} = \lfloor x_1, \dots, x_{M_t} \rfloor^T$

$\boldsymbol{N} = \lfloor N_1, \dots, N_{M_t} \rfloor^T$, and

$$\boldsymbol{H} = \begin{pmatrix} h_{1,1} & \cdots & h_{1,M_t} \\ \vdots & \ddots & \vdots \\ h_{M_r,1} & \cdots & h_{M_r,M_t} \end{pmatrix}$$

The channel matrix $\boldsymbol{H}$ can be normalized and equation (2.2) can be given as:

$$\boldsymbol{Y} = \sqrt{\rho}\boldsymbol{HX} + \boldsymbol{N} \tag{2.3}$$

Where ρ is the Signal to Noise ratio (SNR).

If the channel state information (CSI) is unknown at the transmitter and that the transmitted signals from each antenna are assumed to have equal powers of $\frac{E_x}{M_t}$ then the channel capacity is given by [4] [14] :

$$C = \log_2 \left| I_{M_r} + \frac{\rho}{M_t} \boldsymbol{H}\boldsymbol{H}^H \right| \tag{2.4}$$

$\boldsymbol{H}^H$ is the transpose conjugate matrix of $\boldsymbol{H}$ and I_{M_r} is $M_r \times M_r$ identity matrix.

If the channel state information (CSI) is known at the receiver and using the eigen decomposition technique, then equation (2.4) becomes:

$$C = \sum_{i=1}^{r} \log_2\left(1 + \frac{\rho}{M_t}\lambda_i\right) \quad \textbf{(2.5)}$$

Where r is the rank of the channel matrix given as $min(M_t\ ,\ M_r)$ and λ_i $(i = 1,2,\cdots,r)$ are the positive eigenvalues of $\boldsymbol{HH}^H$.

In equation (2.5), it is shown that the capacity of the MIMO channel is the sum of the capacities of r single input single output (SISO) channels, each having a power gain of λ_i $(i = 1,2,\cdots,r)$ and transmit power $\frac{E_x}{M_t}$.

The capacity of a SISO channel is given by [13][14]:

$$C_{SISO} = \log_2(1 + \rho) \quad \textbf{(2.6)}$$

For an orthogonal MIMO channel and where $M_t = M_r = M$ then the channel capacity is given by:

$$C = M \log_2(1 + \rho) \quad \textbf{(2.7)}$$

From equation (2.7), it can be concluded that a MIMO system has more capacity than a SISO system. This is achieved by using spatial multiplexing techniques.

If both the transmitter and the receiver have CSI, the channel capacity can be determined by a water-filling algorithm under the rule that more power is allocated to the channel that is in good condition and less or none at all to the bad channels [13].

2.4 Channel Estimation

To estimate the CSI based on the above techniques, the configuration given in Figure 2.2 can be considered. It is a quasi-static flat fading environment and K user terminals each with a single antenna that transmitting a sequence of P training symbols. The result is a $K \times P$ transmission pilot matrix, that is represented by $\boldsymbol{S}_P$. The BS receives the signal $\boldsymbol{S_P}$ which is a $K \times P$ matrix with noise $\boldsymbol{N}$ as given by [14] :

$$\boldsymbol{R}_P = \sqrt{\rho}\boldsymbol{H}\boldsymbol{S}_{\boldsymbol{P}} + \boldsymbol{N} \tag{2.8}$$

Where ρ is the SNR, $\boldsymbol{H}$ is the $M \times K$ channel matrix, and $\boldsymbol{N}$ is the $M \times P$ received noise matrix. Under the quasi-static fading assumption, the channel is assumed to be fixed over the period of P modulation symbols.

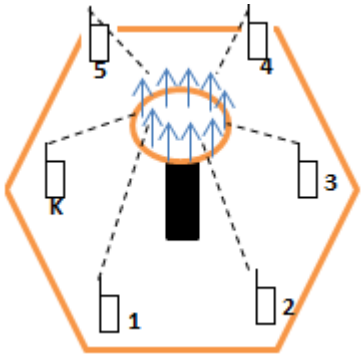

Figure 2.2 single cell MIMO system

There are different channel estimation techniques used in MIMO system and some of them are discussed here. These are:

2.4.1 Maximum Likelihood Channel Estimation

Given the received signal in equation (2.8) and using the maximum likelihood (ML) technique, the estimated channel is given by [4]:

$$\widehat{H}_{ML} = \arg\ \min \left\| \boldsymbol{R}_P - \sqrt{\rho}\boldsymbol{H}\boldsymbol{S}_{\boldsymbol{P}} \right\|_{\mathrm{F}}^2 \tag{2.9}$$

Taking the derivative of equation (2.9) with respect of $\boldsymbol{H}$ and setting the resulting equation to 0, and solving that equation for $\boldsymbol{H}$, the estimated channel becomes**:**

$$\widehat{H}_{ML} = \frac{1}{\sqrt{\rho}}\left(\boldsymbol{R}_P \boldsymbol{S}_{\boldsymbol{P}}{}^H\right)\left(\boldsymbol{S}_{\boldsymbol{P}} \boldsymbol{S}_{\boldsymbol{P}}{}^H\right)^{-1} \tag{2.10}$$

2.4.2 Least Squares Channel Estimation

In Least squares channel estimation, the channel $\boldsymbol{H}$ is estimated by taking a value that minimizes the squared error between the actual receive signal, $\boldsymbol{R}_P$, and the estimated received signal, $\widehat{\boldsymbol{R}}_P = \sqrt{\rho}\widehat{\boldsymbol{H}}\boldsymbol{S_P}$. The estimated channel is given by [4]:

$$\widehat{H}_{LS} = \arg\min \left\| \widehat{\boldsymbol{R}}_P - \boldsymbol{R}_P \right\|_{\mathrm{F}}^2 \tag{2.11}$$

Taking the partial derivative of equation (2.11) with respect to $\widehat{\boldsymbol{H}}$ and setting to zero, then the estimated channel becomes:

$$\widehat{H}_{LS} = \frac{\mathbf{1}}{\sqrt{\boldsymbol{\rho}}}\left(\boldsymbol{R_P S_P}^{\boldsymbol{H}}\right)\left(\boldsymbol{S_P S_P}^{\boldsymbol{H}}\right)^{-\mathbf{1}} \tag{2.12}$$

Comparing equation (2.10) and equation (2.12) it can be seen that the maximum likelihood and least square channel estimators are the same.

2.4.3 Linear Minimum Mean Square Channel Estimation

The linear minimum mean square channel estimation (LMMSE) seeks to obtain the channel matrix that minimizes the mean square error between the true channel and the estimate of the channel $\widehat{\boldsymbol{H}}$. In the case of LMMSE, the matrix $\widehat{\boldsymbol{H}}$ is assumed to be a linear superposition of the received signals. This assumption can be expressed mathematically as [4]:

$$\hat{h}_{i,j} = \sum_{k=1}^{P} r_i(k) w_{i,j} \tag{2.13}$$

Where $\hat{h}_{i,j}$ is the (i,k)th channel element of $\widehat{\boldsymbol{H}}$, $r_i(k)$ the (i,k)th element of the receive matrix $\boldsymbol{R}_P$ and $w_{i,j}$ values are complex weights chosen to minimize the mean square error between the true value of $\boldsymbol{H}$ and the estimate.

The equation (2.13) can be written in general form as:

$$\widehat{\boldsymbol{H}} = \boldsymbol{R}_P \boldsymbol{W} \tag{2.14}$$

Where (i,k)th element of $\boldsymbol{W}$ is $w_{i,j}$. The LMMSE estimate of the channel given by:

$$\widehat{\mathrm{H}}_{\mathrm{LMMSE}} = \arg\min \mathrm{E}\left[\left\|\boldsymbol{H} - \widehat{\boldsymbol{H}}\right\|_{\mathrm{F}}^2\right] \tag{2.15}$$

Assuming that $\boldsymbol{H}$ and $\boldsymbol{N}$ consist of independent, complex Gaussian components with zero mean and unit variance and then taking the partial derivative equation (2.15) with respect to $\boldsymbol{W}$, then the estimated channel becomes:

$$\widehat{H}_{LMMSE} = \sqrt{\rho}\boldsymbol{R}_P\left(I_p + \rho \boldsymbol{S_P}^H \boldsymbol{S_P}\right)^{-1} \boldsymbol{S_P}^H \tag{2.16}$$

Where $\mathrm{I_p}$ is the identity matrix.

2.5 Linear Precoding Techniques

A pre-coder system is illustrated in Figure 2.3. The pre-coder $\boldsymbol{T}$ is an $M_r \times M_t$ matrix which is uses to map the given data $\boldsymbol{D}$ $(M_t \times 1)$ matrix into a matrix $\boldsymbol{X}$ $(K \times M_t)$. The received signal can be written as follows:

$$y_j = h_j \sum_{i=1}^{k} \boldsymbol{T_i d_i} + N_j \tag{2.17}$$

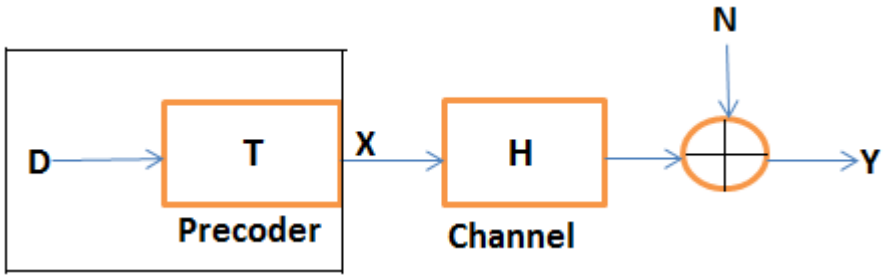

Figure 2.3 Block diagram of a pre-coder system

Where $h_j = (h_{1j}, h_{2j}, \ldots\ h_{Mj})$

The signal vector received at the jth user is given by:

$$y_j = \boldsymbol{h_j T_j d_j} + \boldsymbol{h_j} \sum_{i=1, i \neq j}^{k} \boldsymbol{T_i d_i} + N_j \quad \textbf{(2.18)}$$

The general form equation (2.17) can be written as:

$$\boldsymbol{Y = HX + N} \quad \textbf{(2.19)}$$

Where $\boldsymbol{X = TD}$

Then,

$$\boldsymbol{Y = HTD + N} \quad \textbf{(2.20)}$$

In order for the data $\boldsymbol{D}$ to be received accurately at the receiver, the channel matrix $\boldsymbol{H}$ should be cancelled out by the pre-coder $\boldsymbol{T}$ matrix. Some techniques that are used for linear precoding are discussed below.

2.5.1 Maximum-Ratio Transmission (MRT)

The Maximum-Ratio Transmission (MRT) is also referred to as a matched filter or conjugate beamforming. The precoding matrix $\boldsymbol{T}$ is given in [15] by:

$$\boldsymbol{T = H^H} \quad \textbf{(2.21)}$$

2.5.2 Zero Forcing (ZF) Precoding

The ZF uses a precoding matrix $\boldsymbol{T}$ to obtain a pseudo-inverse of the $\boldsymbol{H}$ matrix such that the combined channel $\boldsymbol{HT}$ results in interference-free reception. Precoding matrix $\boldsymbol{T}$ given in [15] [16] by:

$$\boldsymbol{T = H^H (H^H H)^{-1}} \quad \textbf{(2.22)}$$

2.5.3 Minimum Mean-Square Error Precoder

The Minimum Mean-Square Error (MMSE**)** precoder approach tries to find a coefficient $\boldsymbol{T}$ which minimizes the following criterion:

$$\in= \mathrm{E}[(\boldsymbol{TY}-\boldsymbol{X})(\boldsymbol{TY}-\boldsymbol{X})^{H}] \tag{2.23}$$

And solving equation (2.23), the precoding matrix $\boldsymbol{T}$ which is given in [15] [16] becomes:

$$\boldsymbol{T}=\boldsymbol{H}^{H}(\boldsymbol{H}^{H}\boldsymbol{H}+N_{o}I)^{-1} \tag{2.24}$$

Where N_o regularization factor.

2.6 Massive MIMO

Massive MIMO is a multi-user MIMO technology where each base station (BS) is equipped with an array of M active antenna elements and utilizes these to communicate with K single-antenna terminals over the same time and frequency band [4] [17-19].

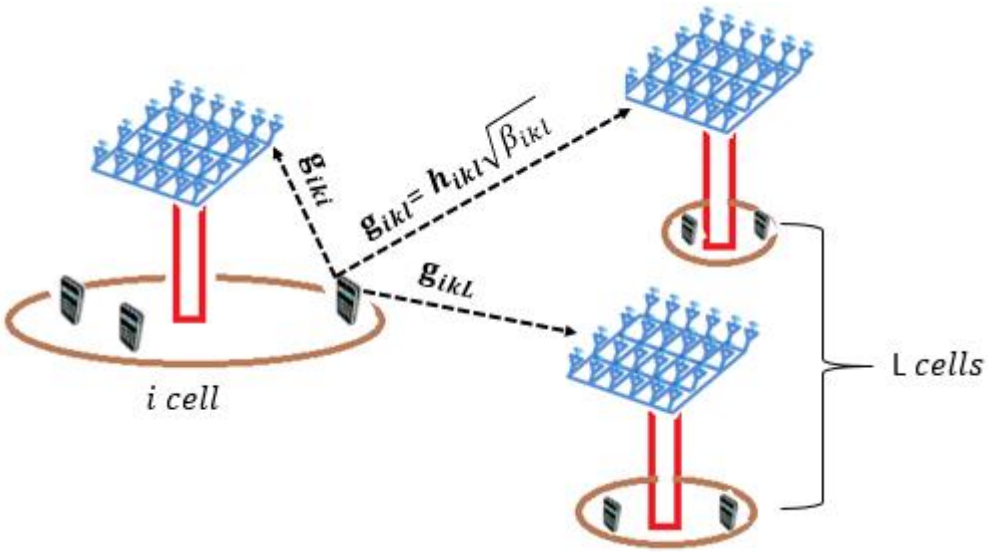

Figure 2.4 Massive MIMO communication system

The propagation channel between the BS of the i-th cell and k user of the l-th cell contains a fast fading and a slow fading component. The channel coefficient can be modeled [9] [20-24] as:

$$\mathbf{g_{ikl}} = \boldsymbol{h_{ikl}}\sqrt{\beta_{ikl}} \tag{2.25}$$

$$\boldsymbol{h}_{ikl} = (h_{1ikl}, h_{2ikl}, \dots, h_{Mikl})^T \in \mathbb{C}^{M\,x\,1}$$

$$\mathbf{g}_{ikl} = (\mathrm{g}_{1ikl}, \mathrm{g}_{2ikl}, \dots, \mathrm{g}_{Mikl})^T \in \mathbb{C}^{M\,x\,1}$$

Where $\boldsymbol{h_{ikl}} \rightarrow \mathcal{CN}(0, \mathbf{I}_{\mathrm{M}})$ and β_{ikl} are fast fading and slow fading components respectively. Since the distance between the antennas of the BS is very small compared to the distance between the kth user and the BS, then slow fading (β_{ikl}) can be considered to be independent of the M antennas of the BS. The slow fading component contains a log-normal and geometric decay part.

It operates in a TDD system (Time Division Duplex) where the uplink channel and downlink channel can be considered to be reciprocal of each other for a given coherence time [25-27]. This coherence time is divided into a number of time slots using TDD protocol for uplink training, uplink data and downlink data as shown Figure 2.5. Since the coherence time is limited then time slot that is allocated for uplink training is very small. If the amount of time required for uplink training increases then the time required to send data for uplink and downlink will decrease. This causes the data rate to decrease and hence the orthogonal signal that are used for uplink training are limited. The k user of different cells cannot have unique assigned orthogonal signals rather the orthogonal signals are re-used within a cell or adjacent cell. Using the same orthogonal signals for different users causes imperfect channel estimation. This channel estimation error is referred to as pilot contamination.

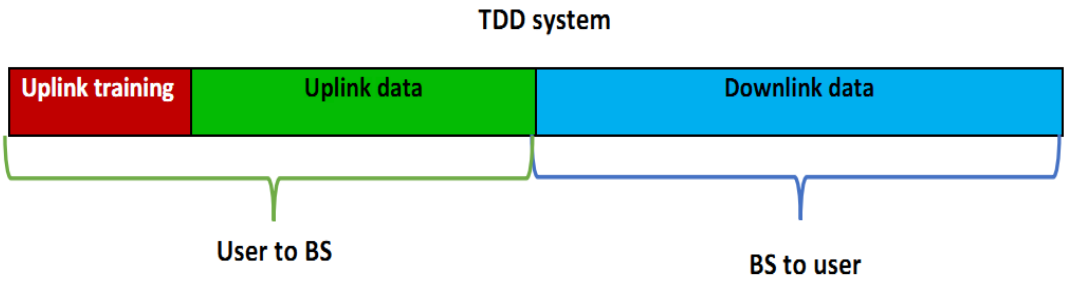

Figure 2.5 TDD protocol

2.7 Mitigating Pilot Contamination

The problem of pilot contamination in massive MIMO occurs even though the above channel estimation (section 2.4) and precoding methods (section 2.5) are used. In [25] it is shown that for non-cooperative cellular network in the asymptotic regime when the number of base station antennas tends to infinity, the SINR does not grow indefinitely. This limits the achievable rate of the system. Different methods have been developed to alleviate the pilot contamination effect. Some of them are:

2.7.1 Blind Methods

The eigenvalue-decomposition-based approach to mitigate pilot contamination has been proposed in [28]. It estimates the channel blindly from the received data. Each user channel is estimated by determining the eigenvector from the covariance matrix of the received signals up to a remaining scalar multiplicative ambiguity. A short pilot sequence is required to resolve this ambiguity. This method uses a large number of antenna to mitigate pilot contamination.

With the help of power-controlled hand-off procedure, a subspace projection has been proposed to improve channel estimation in massive multi-antenna systems [29]. The proposed algorithm can mitigate the pilot contamination problem without the need for coordination among cells. The limitation of the algorithm is an assumption that all desired channels are stronger than all interfering channels. But this assumption is not always true in practice.

2.7.2 Protocol-Based Methods

To reduce pilot contamination in multi-user TDD systems, a time-shifted protocol is proposed in [12] [23]. This protocol enables users that are at adjacent cells to send their intended pilot signal in a different time frame. The pilot contamination problem can be mitigated using the proposed protocol as long as the pilots do not overlap in time. In the paper [23], the authors have reported that some improvement can be obtained by applying power allocation algorithms in combination with the time-shifted protocol. The major challenge of the protocol is in the control mechanism needed to dynamically synchronize the pilots across adjacent cells so that they do not overlap in time.

2.7.3 Pilot Sequence Allocation

A pilot sequence allocation has been proposed to mitigate the pilot contamination in [30]. These sequences are allocated by dividing the cell into two. All users at the center of the cells are assigned the same pilot sequences, but edge users in different cells are allocated mutually orthogonal sequences. The results show that the proposed pilot sequence allocation scheme achieves better capacity than the traditional pilot sequence allocation. Since the same pilot sequences are at the center of the cell, then the pilot contamination is not eliminated.

A pilot technique scheme that allows simultaneous data and pilot transmission is proposed in [31]. It makes use of insertion of shifted pilot locations in slots, i.e., different users transmit pilots in different slots. In the first coherence interval, when the first user transmits a pilot sequence the other users are mute so that BS can estimate the first user's channel without contamination from other users. When the second user transmits a pilot sequence the first user transmits data while the other users still remain quiet, and so forth. But this scheme suffers from pilot contamination due to inter-cell interference.

A smart pilot assignment scheme is proposed in [32] to improve the performance of users with severe pilot contamination. Specifically, by exploiting the large-scale

characteristics of fading channels, the BS first measures the inter-cell interference of each pilot sequence caused by the users with the same pilot sequence in other adjacent cells. Then, in contrast to the conventional schemes which assign the pilot sequences to the users randomly, the proposed smart pilot assignment method assigns the pilot sequence with the smallest inter-cell interference to the user having the worst channel quality. This is done in a sequential manner so as to improve the performance.

2.7.4 Precoding Methods

A pilot contamination mitigation scheme based on large scale fading precoding has been proposed in [20] [21]. It is based on the assumption that the signals from all terminals in all cells are accessible at each BS and that slow-fading coefficients are accessible to all the BS or alternatively to a network hub. Instead of mitigating interference caused by pilot contamination in estimating of the channel, each BS uses the pilot contamination for transmitting information to all terminals. This mitigation technique has a high computational complexity since it uses cooperation between cells.

A pilot contamination elimination precoding is proposed in [33]. It uses the same orthogonal signals within a cell but different sequences in adjacent cells. This method mitigates the pilot contamination effect by using distributed sub-array antennas within the cell. The main problem in the method is the increase in the sub-array antennas with an increase with the number of users.

To avoid the above limitations, a cell specific precoder for downlink Massive MIMO communication system is proposed in this research to mitigate the pilot contamination effect.

CHAPTER THREE

PILOT CONTAMINATION ANALYSIS

3.1 Inter-cell Pilot Contamination

When orthogonal signals are re-used in adjacent cells an inter-cell pilot contamination occurs. Figure 3.1 shows an inter-cell pilot contamination process. The base station of the ith cell receives signals not only from its own k users but also from k users of the adjacent l cells. This causes an error when the channel is estimated at the BS of the i-th cell.

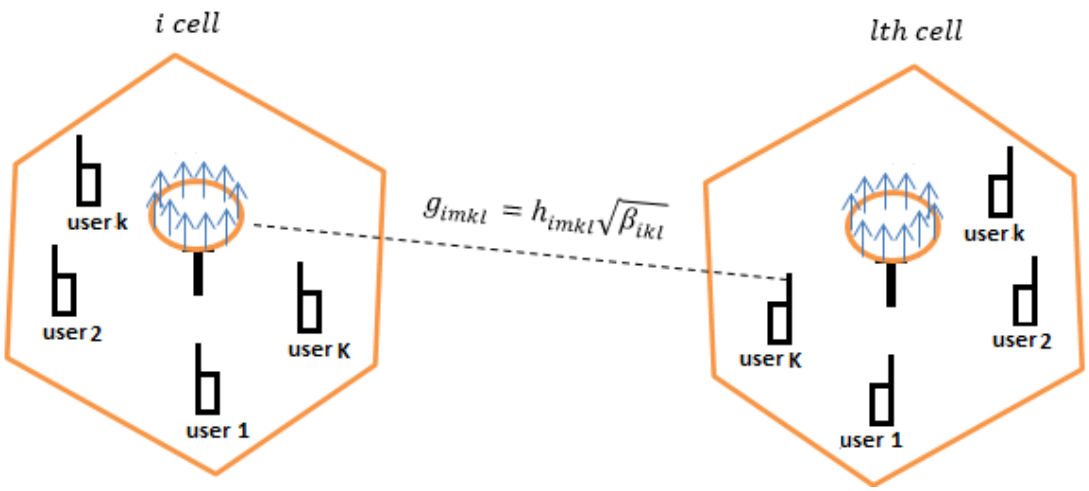

Figure 3.1 Signal reception at the BS of the ***i***-th cell from users in the ***l***th cell.

The propagation channel between m-th antenna of the ith cell and user k of the lth cell contain fast fading and slow fading components. The channel coefficient can be modeled [9] [20-24] as:

$$g_{imkl} = h_{imkl}\sqrt{\beta_{ikl}} \qquad \textbf{(3.1)}$$

Where $h_{imkl} \rightarrow \mathcal{CN}(0,1)$ is the fast fading component and β_{ikl} is the slow fading component. The slow fading component is considered to be to be independent of M antennas of the BS.

The received signal at the BS for the ith cell from all k users of l cell is given by:

$$\boldsymbol{Y_i} = \sum_{l=1}^{L}\sum_{k=1}^{K}\sqrt{\tau\rho_r}\mathbf{g_{ikl}}\phi_k + \boldsymbol{n_i} \tag{3.2}$$

$$\boldsymbol{h}_{ikl} = (h_{1ikl}, h_{2ikl}, \dots, h_{Mikl})^T \in \mathbb{C}^{M\,x\,1}$$

$$\mathbf{g}_{ikl} = (\mathrm{g}_{1ikl}, \mathrm{g}_{2ikl}, \dots, \mathrm{g}_{Mikl})^T \in \mathbb{C}^{M\,x\,1}$$

Where ϕ_k the orthogonal signal of user k and $\boldsymbol{n_i} \in \mathbb{C}^{M \times K}$ is the additive white Gaussian noise. ρ_r is the power received at the BS.

The BS of the ith cell estimates the vector $\mathbf{g_{ikl}}$ for its own k users by multiplying the received signal equation (3.2) by $\frac{\phi_k^{\dagger}}{\sqrt{\tau\rho_r}}$ i.e.

$$\hat{\mathbf{g}}_{\boldsymbol{ikl}} = \boldsymbol{Y_i}\,\frac{\phi_k^{\dagger}}{\sqrt{\tau\rho_r}} = \mathbf{g_{iki}} + \sum_{\boldsymbol{l=1, l\neq i}}^{\boldsymbol{L}} \mathbf{g_{ikl}} + \boldsymbol{n_i'} \tag{3.3}$$

Where $\boldsymbol{n_i'} = \boldsymbol{n_i}\frac{\phi_k^{\dagger}}{\sqrt{\tau\rho_r}}$.

The BS can be use a precoder conjugate beamforming [9][20-22] for $M \longrightarrow \infty$, the precoder is given by:

$$w_{ki} = \frac{\hat{\mathbf{g}}_{\boldsymbol{ikl}}^{\dagger}}{\|\hat{\mathbf{g}}_{\boldsymbol{ikl}}\|} \tag{3.4}$$

The BS multiplies the desired signal q_{ki} by equation (3.4) and sends the vector T_i

$$T_i = w_{1i}q_{1i} + w_{2i}q_{2i} + \cdots + w_{ki}q_{ki} \tag{3.5}$$

The k-th user of the i-th cell receives the signal:

$$x_{ki} = \sum_{l=1}^{L}\sum_{k'=1}^{K}\mathbf{g_{ikl}}w_{k'i}q_{k'i} + \boldsymbol{n_i} \tag{3.6}$$

Lemma 1. Let $\boldsymbol{x}, \boldsymbol{y}\ \mathbb{C}^{M\times 1}$ be two independent vectors with distribution $\mathcal{CN}(0, cI)$. Then

$$\lim_{M\to\infty} \frac{\boldsymbol{x}^{\dagger}\boldsymbol{y}}{M} = 0 \text{ and } \lim_{M\to\infty} \frac{\boldsymbol{x}^{\dagger}\boldsymbol{x}}{M} = c \tag{3.7}$$

Using *Lemma 1*, equation (3.6) becomes;

$$\lim_{M\to\infty} \frac{x_{ki}}{M} = \lim_{M\to\infty} \sum_{l=1}^{L}\sum_{k'=1}^{K} \frac{\mathbf{g_{ikl}} w_{k'i} q_{k'i}}{M} + \frac{\boldsymbol{n_i'}}{M} \tag{3.8}$$

$$\lim_{M\to\infty} \frac{x_{ki}}{M} = \sum_{k'=1}^{K} \lim_{M\to\infty} \frac{\mathbf{g_{ik1}} w_{k'i} q_{k'i}}{M} + \sum_{k'=1}^{K} \lim_{M\to\infty} \frac{\mathbf{g_{ik2}} w_{k'i} q_{k'i}}{M} + \cdots + \sum_{k'=1}^{K} \lim_{M\to\infty} \frac{\mathbf{g_{ikL}} w_{k'i} q_{k'i}}{M} \tag{3.9}$$

$$\lim_{M\to\infty} \frac{x_{ki}}{M} = \beta_{ik1} q_{k1} + \beta_{ik2} q_{k2} + \cdots + \beta_{ikL} q_{kL} \tag{3.10}$$

The k-th user at i-th cell not only receives the intended signal from the BS of the i-th cell but also receives signals from the BS of the l-th cell and causes the signal to interference ratio to be constant even though the number of M antenna increases. This interference occurs due to pilot contamination error estimation of the channel at the BS. The signal to interference plus noise ratio (SINR) decreases as given below:

$$SINR_{ki} = \frac{\beta_{ik1}^2}{\beta_{ik2}^2 + \beta_{ik3}^2 + \cdots + \beta_{ikL}^2} = \frac{\beta_{ik1}^2}{\sum_{l=2}^{L} \beta_{ikl}^2} \tag{3.11}$$

3.2 Intra-cell Pilot Contamination

Intra-cell Pilot contamination occurs when a user in one cell employs the same orthogonal signals but different from the k users in adjacent cells.

The received signal at the BS of the ith cell from all k users in the l cell is given by:

$$\boldsymbol{Y_i} = \sum_{l=1}^{L}\sum_{k=1}^{K}\sqrt{\tau\rho_r}\mathbf{g_{ikl}}\phi_l + \boldsymbol{n_i} \tag{3.12}$$

The BS at $i\,cell$ estimates the vector $\mathbf{g_{iki}}$ for its own k users by multiplying the received signal equation (3.12) by $\frac{\phi_i^{\dagger}}{\sqrt{\tau\rho_r}}$ i.e

$$\hat{\mathbf{g}}_{\boldsymbol{iki}} = \boldsymbol{Y_i}\,\frac{\phi_i^{\dagger}}{\sqrt{\tau\rho_r}} = \sum_{k=1}^{K}\mathbf{g_{iki}} + \boldsymbol{n'} \tag{3.13}$$

Where $\boldsymbol{n'} = \boldsymbol{n_i}\frac{\phi_i^{\dagger}}{\sqrt{\tau\rho_r}}$.

The BS can use a precoder conjugate beamforming [9] [20-22] for $M \longrightarrow \infty$ which is given by an expression similar to equation (3.4) as given below:

$$w_i = \frac{\hat{\mathbf{g}}_{\boldsymbol{iki}}^{\dagger}}{\|\hat{\mathbf{g}}_{\boldsymbol{iki}}\|} \tag{3.14}$$

The BS maps the signal q_{ki} using equation (3.14) and sends the vector T_i to the k users

$$T_i = w_i q_{1i} + w_i q_{2i} + \cdots + w_i q_{Ki} \tag{3.15}$$

The k-th user of the i-th cell receives the signal:

$$x_{ki} = \sum_{k'=1}^{K}\mathbf{g_{ikl}}w_i q_{k'i} + \boldsymbol{n_i} \tag{3.16}$$

Using *Lemma 1*, then*:*

$$\lim_{M\longrightarrow\infty}\frac{x_{ki}}{M} = \lim_{M\longrightarrow\infty}\sum_{k'=1}^{K}\frac{\mathbf{g_{ikl}}w_i q_{k'i}}{M} + \frac{\boldsymbol{n_i}}{M} \tag{3.17}$$

$$\lim_{M\longrightarrow\infty}\frac{x_{\mathrm{ki}}}{M} = \beta_{iki}(q_{1i} + q_{2i} + \cdots + q_{Ki}) \tag{3.18}$$

$$SINR_{ki} = \frac{\beta_{iki}^2}{\beta_{iki}^2 + \beta_{iki}^2 + \cdots + \beta_{iki}^2} = \frac{1}{k} \quad \textbf{(3.19)}$$

The pilot contamination effect when M approaches infinity is shown in equation (3.11) and equation (3.19). However, in practice the number of antennas is finite.

In this section, the achievable rate of Massive MIMO system with pilot contamination when the number of antennas is finite will be derived. If the system uses MMSE to estimate the propagation channel from the received signal, then the k-th user of the l-th cell receives the signal:

$$x_{ki} = \sqrt{\rho_b} \sum_{l=1}^{\mathrm{L}} \sum_{\mathrm{j}=1}^{K} \mathbf{g}_{lki} \frac{\hat{\mathbf{g}}_{lji}^{\dagger}}{\zeta_{lji}} \; s_{jl} + \mathbf{n}_{ki} \quad \textbf{(3.20)}$$

$$\hat{\mathbf{g}}_{\boldsymbol{lji}} = \boldsymbol{x_{kl}}\left(\phi_j^{\dagger}\varphi'_{lji}\right) = \varphi'_{lji}\sqrt{\tau\rho_t}\sum_{z=1}^{L}\mathbf{g}_{ljz} + \boldsymbol{n'_k} \quad \textbf{(3.21)}$$

Where**;**

$$\varphi'_{lji} = \frac{\sqrt{\tau\rho_t}\beta_{lji}}{\zeta_{lji}^2}\,, \qquad \zeta_{lji}^2 = 1 + \rho_t\tau\sum_{z=1}^{L}\beta_{ljz}$$

The vectors $\mathbf{g}_{lji}$ and $\hat{\mathbf{g}}_{lji}$ have the following distributions [21]**:**

$$\mathbf{g}_{lji} = \mathcal{CN}\left(0, \beta_{lji} I_M\right) \quad \textbf{(3.22)}$$

$$\hat{\mathbf{g}}_{lji} = \mathcal{CN}\left(0, \left(\frac{\sqrt{\tau\rho_t}\beta_{lji}}{\zeta_{lji}}\right)^2 I_M\right) \quad \textbf{(3.23)}$$

After some manipulation, equation (3.20) can be written as:

$$x_{ki} = v_1 + v_2 + v_3 + v_4 + v_5 \quad \textbf{(3.24)}$$

Where;

$$v_1 = \mathrm{E}\left[\sqrt{\rho_b}\mathbf{g}_{\boldsymbol{i}ki}\frac{\hat{\mathbf{g}}_{\boldsymbol{iki}}^{\dagger}}{\zeta_{iki}}\, s_{ki}\right]$$

$$v_2 = \left(\sqrt{\rho_b}\mathbf{g}_{\boldsymbol{iki}}\frac{\hat{\mathbf{g}}^{\dagger}_{\boldsymbol{iki}}}{\zeta_{iki}}\, s_{ki} - \mathrm{E}\left[\sqrt{\rho_b}\mathbf{g}_{\boldsymbol{iki}}\frac{\hat{\mathbf{g}}^{\dagger}_{\boldsymbol{iki}}}{\zeta_{iki}}\, s_{ki}\right]\right)$$

$$v_3 = \sqrt{\rho_b}\sum_{\substack{l=1\\ l\neq i}}^{L}\mathbf{g}_{\boldsymbol{lki}}\frac{\hat{\mathbf{g}}^{\dagger}_{\boldsymbol{lkl}}}{\zeta_{lkl}}\, s_{kl}$$

$$v_4 = \sqrt{\rho_b}\sum_{l=1}^{L}\sum_{\substack{\mathrm{j}=1\\ j\neq k}}^{K}\mathbf{g}_{\boldsymbol{lki}}\frac{\hat{\mathbf{g}}^{\dagger}_{\boldsymbol{ljl}}}{\zeta_{ljl}}\, s_{jl}$$

$$v_5 = \boldsymbol{n}_{ki}$$

The achievable rate is then given by:

$$\mathrm{C} = \mathbf{log_2}\left(\mathbf{1} + \frac{\mathrm{E}[|v_1|^2]}{\mathrm{E}[|v_2|^2] + \mathrm{E}[|v_3|^2] + \mathrm{E}[|v_4|^2] + \mathrm{E}[|v_5|^2]}\right)$$

$$\mathrm{C} = \mathbf{log_2}\left(\mathbf{1} + \frac{\rho_b \mathrm{M}^2\left|\frac{\rho_t\tau\beta^2_{iki}}{\zeta^3_{iui}}\right|^2}{M^2\psi_1 + M\psi_2 + \sigma^2_{ki}}\right) \qquad \textbf{(3.25)}$$

Where;

$$\psi_1 = \rho_b\left|\sum_{\substack{l=1\\ l\neq i}}^{\mathrm{L}}\frac{\rho_t\tau\beta^2_{lki}}{\zeta^3_{iki}}\right|^2$$

$$\psi_2 = \rho_b \mathrm{M}\sum_{l=1}^{\mathrm{L}}\sum_{\mathrm{j}=1}^{K}\frac{\rho_t\tau\beta_{lki}\beta^2_{ljl}}{\left(\zeta^3_{ijl}\right)^2}$$

Equation (3.25) is the achievable rate of the system when there is a pilot contamination effect for a finite number of antennas. Full derivation of the achievable rate equation (3.25) given in appendix A.

CHAPTER FOUR:

CHANNEL ESTIMATION AND PRECODING

4.1 Pilot Reuse Factor

A novel pilot reuse factor is designed to have each cell within a cluster to use unique orthogonal signals. This enables the mitigation of inter-pilot contamination effect. Even though pilot contamination effect from adjacent cells is mitigated, intra-pilot contamination effect still exist. Mitigation of intra-pilot contamination will be considered in Section 4.4. The pilot reuse factor is calculated in a similar manner to the cellular frequency reuse factor [11] given as**:**

$$N = i^2 + ij + j^2 \,. \tag{4.1}$$

Where i and j are any positive integers and with $N > 1$ **.**

From equation (4.1) the following pilot reuse factor values are possible $\{3,4,7,9,12 \ldots\}$. Figure 4.1 shows a hexagonal geometric arrangement of cells with a pilot reuse factor $N = 7$. Each cell within a cluster assigned unique orthogonal signals $PF_n = \{PF_1, PF_2, \ldots PF_7\}$. Similarly, figure 4.2 shows a hexagonal cellular system with $N = 3$ and $N = 4$. The number of unique orthogonal signals assigned for each cell within cluster is PF_n.

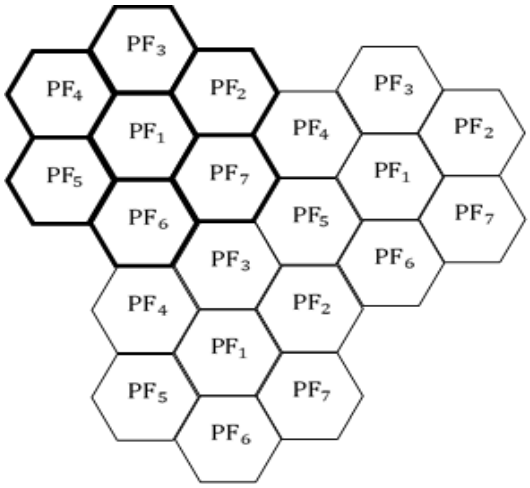

Figure 4.1 Cellular hexagonal cell with $\boldsymbol{N = 7}$

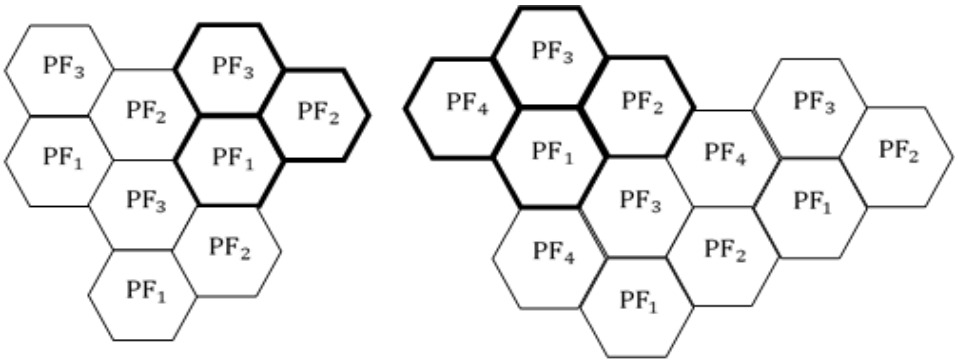

Figure 4.2 Pilot reuse factor with $\boldsymbol{N = 3}$ and $\boldsymbol{N = 4}$

4.2 System Model

Consider L hexagonal cells, each consisting of one BS and K single antenna users. In each cell, the BS consists of W distributed sub-array antennas and each sub-array has Mantennas, as shown in Figure 4.3.

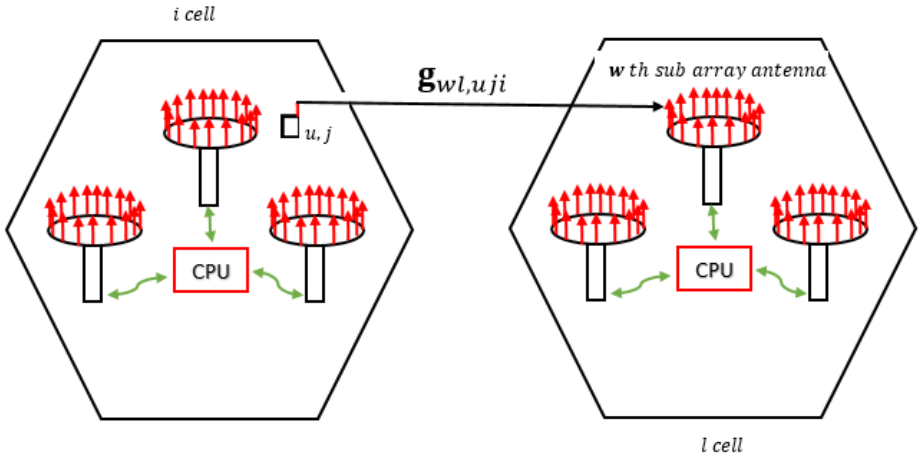

Figure 4.3 Multi-cell Massive MIMO

The uplink training scheme is developed based on the pilot reuse factor so that each cell has U orthogonal signals, where $U = \frac{K}{L}$. Since $K > U$, then all U orthogonal signals are reused within the cell J times. The parameters J,L, and W are assumed to be equal. Each orthogonal signal will have a length of $\tau = K$ and the U orthogonal signals $\{\phi_{1,l}, \phi_{2,l} \ldots \phi_{U,l}\}$ have the following property:

(i). Within the cell $\phi_{n,l}\phi_{r,l}^{\dagger} = \delta_{nr}$

(ii). For adjacent cells $\phi_{n,l}\phi_{r,i}^{\dagger} = 0$.

The propagation channel is modelled as the product of the small scale fading (fast fading) and large scale fading (slow fading) components [9] [20-24].The propagation channel coefficient from i-th cell of (u, j) user to the l-th cell of w-th sub-array sub array of antenna given as:

$$\mathbf{g}_{wl,uji} = \boldsymbol{h}_{wl,uji}\sqrt{\beta_{wl,uji}} \tag{4.2}$$

$$\boldsymbol{h}_{wl,uji} = (h_{1wl,uji}, h_{2wl,uji}, \dots, h_{Mwl,uji})^T \in \mathbb{C}^{M\,x\,1}$$

$$\mathbf{g}_{wl,uji} = (\mathrm{g}_{1wl,uji}, \mathrm{g}_{2wl,uji}, \dots, \mathrm{g}_{Mwl,uji})^T \in \mathbb{C}^{M\,x\,1}$$

Where $\boldsymbol{h}_{wl,uji} \sim \mathcal{CN}(0, \mathbf{I}_{\mathrm{M}})$ for small scale fading and $\beta_{wl,uji}$ is a large scale fading factor. The slow fading is considered to be different at all the w sub-arrays of the BS. However, since the distance between the sub-array antennas of the BS is very small compared to the distance between the (u, j) user and the sub-array BS, the slow fading parameter ($\beta_{wl,uji}$) can be considered to be independent of the M antennas of the sub-array of BS.

The received signal at the w-th sub-array of the BS that comes from users in the cell is given by:

$$\mathbf{Y}_{l,w} = \sum_{i=1}^{\mathrm{L}} \sum_{j=1}^{\mathrm{L}} \sum_{u=1}^{\mathrm{U}} \sqrt{\tau\rho_t}\,\mathbf{g}_{wl,uji}\,\phi_{u,l} + \mathbf{n}_{l,w} \tag{4.3}$$

Where $\mathbf{n}_{l,w} \epsilon \mathbb{C}^{M \times U}$ is the additive noise with distribution $\mathbf{n}_{l,w} \sim \mathcal{CN}(0,1)$ and ρ_t is the average transmitted power at each user.

The w-th sub-array of BS estimates the channel $\mathbf{g}_{wl,uji}$ from its own U users by multiplying $\mathbf{Y}_{l,w}$ in equation (4.3) by $\frac{\phi_{u,l}^{\dagger}}{\sqrt{\tau\rho_t}}$ i.e.

$$\hat{\mathbf{g}}_{wl,uwl} = \mathrm{Y}_{l,w}\frac{\phi_{u,l}^{\dagger}}{\sqrt{\tau\rho_t}} = \mathbf{g}_{wl,uwl} + \sum_{j=1, j\neq w}^{L} \mathbf{g}_{wl,ujl} + \frac{\phi_{u,l}^{\dagger}}{\sqrt{\tau\rho_t}}\mathbf{n}_{l,w} \tag{4.4}$$

The w-th sub-array of BS precodes the desired signal s_{uwl} using a conjugated beamforming precoder T_{wu} [9], [20-22]. The precoder T_{wu} is given by:

$$T_{wu} = \frac{\hat{\mathbf{g}}_{wl,uwl}^{\dagger}}{\left\|\hat{\mathbf{g}}_{wl,uwl}\right\|} \tag{4.5}$$

The w-th sub-array of BS sends the transmitted signal vector T_w to the intended user (u, j). The vector T_w given by:

$$T_w = T_{wu}s_{uwl} = T_{w1}s_{1wl} + T_{w2}s_{2wl} + \cdots + T_{wU}s_{Uwl} \tag{4.6}$$

The sub-group user (u, j)receives the signal:

$$x_{ujl} = \sqrt{\rho_b}\sum_{i=1}^{\mathrm{L}}\sum_{w=1}^{\mathrm{L}}\mathbf{g}_{wl,uji}T_w + \mathrm{w}_{ujl}\ , \mathrm{w}_{ujl} \in \mathcal{CN}(0, \sigma_{ujl}) \tag{4.7}$$

$$x_{ujl} = \sqrt{\rho_b}\sum_{i=1}^{\mathrm{L}}\sum_{w=1}^{\mathrm{L}}\sum_{q=1}^{\mathrm{U}}\mathbf{g}_{wl,uji}T_{wq}s_{qwl} + \mathrm{w}_{ujl} \tag{4.8}$$

Where ρ_b is the average transmit power from w-th sub-array of BS.

When the number of antenna approaches infinity, equation.(4.8) becomes

$$\lim_{M\to\infty}\frac{x_{ujl}}{\sqrt{M}} = \lim_{M\to\infty}\sqrt{\rho_b}\sum_{i=1}^{\mathrm{L}}\sum_{w=1}^{\mathrm{L}}\sum_{q=1}^{\mathrm{U}}\frac{\mathbf{g}_{wl,uji}T_{wq}s_{qwl}}{\sqrt{M}} + \frac{\mathbf{w}_{ujl}}{\sqrt{M}} \tag{4.9}$$

$$\lim_{M\to\infty}\frac{\mathbf{g}_{wl,uji}T_{wq}}{\sqrt{M}} = \lim_{M\to\infty}\left(\frac{\mathbf{g}_{wl,uji}\hat{\mathbf{g}}_{wl,qwl}^{\dagger}}{M}\frac{1}{\frac{\left\|\hat{\mathbf{g}}_{wl,qwl}^{\dagger}\right\|}{\sqrt{M}}}\right) \tag{4.10}$$

$$\lim_{M\to\infty}\frac{\mathbf{g}_{wl,uji}\hat{\mathbf{g}}_{wl,qwl}^{\dagger}}{M} = \begin{cases}\beta_{wl,ujl} & for\ \mathrm{q} = u\ , i = l\\ 0 & for\ \mathrm{q} \neq u\end{cases} \tag{4.11}$$

$$\lim_{M\to\infty} \frac{\left\|\hat{g}^{\dagger}_{wl,qwl}\right\|}{\sqrt{M}} = \mathcal{B}_{ujl} = \left(\sum_{i=1}^{L} \beta_{wl,uji} + 1\right)^{\frac{1}{2}} \quad \textbf{(4.12)}$$

$$\lim_{M\to\infty} \frac{x_{ujl}}{\sqrt{M}} = \sqrt{\rho_b} X_{ujl} = \sqrt{\rho_b} \sum_{w=1}^{\mathrm{L}} \beta'_{wl,ujl} s_{uwl} \quad \textbf{(4.13)}$$

Where $\beta'_{wl,uji} = \frac{\beta_{wl,ujl}}{\mathcal{B}_{ujl}}$.

Equation (4.13) reveals two outcomes. The first is that the signals that comes from adjacent cells vanish when M approaches infinity. The second is that the (u, j)-th user in the l-th cell receives not only the intended signal but also from other sub-arrays in the BS of the l-th cell. This causes signal interference. This interference happens due to pilot contamination error estimation of the channel at the sub-array of BS of the l-th cell. The signal-to-interference-plus-noise ratio (SINR)is given in equation (4.14) and from this it can be observed that the SINR is limited as M approaches infinity. However, this limitation can be avoided by using large scale fading precoding [21].

$$SINR_{u1} = \frac{\beta'^2_{1l,ujl}}{\beta'^2_{2l,ujl} + \beta'^2_{3l,ujl} + \cdots + \beta'^2_{Ll,ujl}} = \frac{\beta'^2_{1l,ujl}}{\sum_{i=2}^{L} \beta'^2_{wl,ujl}} \quad \textbf{(4.14)}$$

4.3 Large Scale Fading Estimation

Firstly, each sub-group has unique orthogonal signals. The users in each sub-group then send the same orthogonal signals. The w-th sub-array estimate the channel by multiplying the received signal with known conjugated orthogonal signal. The received signal at the w-th sub-array of the BS that comes from users in the cell is given by:

$$\mathbf{Y}_{l,w} = \sum_{i'=1}^{\mathrm{L}} \sum_{j'=1}^{\mathrm{L}} \sum_{u'=1}^{\mathrm{U}} \sqrt{\tau\rho_t}\mathbf{g}_{wl,u'j'i'}\phi_{j',l} + \mathbf{n}_{l,w} \quad \textbf{(4.15)}$$

$$\hat{\mathbf{g}}_{wl,u'j'i'} = \mathrm{Y}_{l,w}\frac{\phi^{\dagger}_{j',l}}{\sqrt{\tau\rho_t}} = \sum_{u'=1}^{U}\mathbf{g}_{wl,u'j'i'} + \frac{\phi^{\dagger}_{j,l}}{\sqrt{\tau\rho_t}}\mathbf{n}_{l,w} \qquad \textbf{(4.16)}$$

Secondly, the same orthogonal signals are assigned to the sub-groups. Then each sub-group users are assigned unique orthogonal signals. The users in each sub-group sends the orthogonal signals to the BS and the w-th sub-array estimate the channel by multiplying the received signal with a known conjugated orthogonal signal. The result will be the same as equation (4.4). Multiplying equation (4.4) with equation (4.16) and assuming the number of antennas approaches infinity, then;

$$\lim_{\boldsymbol{M}\to\infty}\hat{\mathbf{g}}_{wl,u'j'i'}\left(\hat{\mathbf{g}}_{wl,uwl}\right)^{\dagger} = \left(\sum_{u'=1}^{U}\mathbf{g}_{wl,u'j'i'} + \frac{\phi^{\dagger}_{j,l}}{\sqrt{\tau\rho_t}}\mathbf{n}_{l,w}\right)\left(\sum_{j=1}^{L}\mathbf{g}_{wl,ujl} + \frac{\phi^{\dagger}_{u,l}}{\sqrt{\tau\rho_t}}\mathbf{n}_{l,w}\right)^{\dagger} \qquad \textbf{(4.17)}$$

Finally equation (4.17) becomes;

$$\lim_{\boldsymbol{M}\to\infty}\hat{\mathbf{g}}_{wl,uwl}\left(\hat{\mathbf{g}}_{wl,uwl}\right)^{\dagger} = \beta_{wl,ujl} \qquad \textbf{(4.18)}$$

4.4 Large Scale Fading Precoding

To mitigate the pilot contamination, the w-th sub-array can add to a pre-coder some unknown variables from the set $\{ \mathrm{A}_1,\ \mathrm{A}_2 \ldots \mathrm{A}_\mathrm{L} \}$ so as to get the received signal as:

$$\begin{aligned}
X_{u1} &= \beta'_{1l,u1l}A_1 s_{u1l} + \beta'_{2l,u1l}A_2 s_{u2l} + \cdots + \beta'_{Ll,u1l}A_L s_{uLl} = s_{u1l} \\
X_{u2} &= \beta'_{1l,u2l}A_1 s_{u1l} + \beta'_{2l,u2l}A_2 s_{u2l} + \cdots + \beta'_{Ll,u2l}A_L s_{uLl} = s_{u2l} \\
&\vdots \qquad\qquad \vdots \qquad\qquad \vdots \qquad\qquad \vdots \qquad\qquad \vdots \\
X_{uL} &= \beta'_{1l,uLl}A_1 s_{u1l} + \beta'_{2l,uLl}A_2 s_{u2l} + \cdots + \beta'_{Ll,uLl}A_L s_{uLl} = s_{uLl}
\end{aligned} \qquad \textbf{(4.19)}$$

Then equation (4.15) can then be written in matrix form as:

$$\begin{pmatrix} \beta'_{1l,u1l} & \beta'_{2l,u1l} & \cdots & \beta'_{Ll,u1l} \\ \beta'_{1l,u2l} & \beta'_{2l,u2l} & \cdots & \beta'_{Ll,u2l} \\ \vdots & \vdots & \ddots & \vdots \\ \beta'_{1l,uLl} & \beta'_{2l,uLl} & \cdots & \beta'_{Ll,uLl} \end{pmatrix} \begin{pmatrix} A_1 s_{u1l} \\ A_2 s_{u2l} \\ \vdots \\ A_L s_{uLl} \end{pmatrix} = \begin{pmatrix} s_{u1l} \\ s_{u2l} \\ \vdots \\ s_{uLl} \end{pmatrix} \quad \textbf{(4.20)}$$

$$\begin{pmatrix} v_{u1l} \\ v_{u2l} \\ \vdots \\ v_{uLl} \end{pmatrix} = \begin{pmatrix} a_{1l,u1l} & a_{2l,u1l} & \cdots & a_{Ll,u1l} \\ a_{1l,u2l} & a_{2l,u2l} & \cdots & a_{Ll,u2l} \\ \vdots & \vdots & \ddots & \vdots \\ a_{1l,uLl} & a_{2l,uLl} & \cdots & a_{Ll,uLl} \end{pmatrix} \begin{pmatrix} s_{u1l} \\ s_{u2l} \\ \vdots \\ s_{uLl} \end{pmatrix} \quad \textbf{(4.21)}$$

Where

$\mathrm{A_w} s_{uwl} = v_{uwl}$ and

$$\begin{pmatrix} a_{1l,u1l} & a_{2l,u1l} & \cdots & a_{Ll,u1l} \\ a_{1l,u2l} & a_{2l,u2l} & \cdots & a_{Ll,u2l} \\ \vdots & \vdots & \ddots & \vdots \\ a_{1l,uLl} & a_{2l,uLl} & \cdots & a_{Ll,uLl} \end{pmatrix} = \begin{pmatrix} \beta'_{1l,u1l} & \beta'_{2l,u1l} & \cdots & \beta'_{Ll,u1l} \\ \beta'_{1l,u2l} & \beta'_{2l,u2l} & \cdots & \beta'_{Ll,u2l} \\ \vdots & \vdots & \ddots & \vdots \\ \beta'_{1l,uLl} & \beta'_{2l,uLl} & \cdots & \beta'_{Ll,uLl} \end{pmatrix}^{-1} \quad \textbf{(4.22)}$$

The w-th sub-array of BS pre-code the desired signal v_{uwl} using a conjugated beamforming $T_{wu}$and sends the vector T_w to the intended user (u, j). This precoding scheme is termed large scale fading precoding. The vector T_w is given by:

$$T_w = T_{wu} v_{uwl} = T_{w1} v_{1wl} + T_{w2} v_{2wl} + \cdots + T_{wU} v_{Uwl} \quad \textbf{(4.23)}$$

The sub-group user (u, j)receives the signal:

$$x_{ujl} = \sqrt{\rho_b} \sum_{i=1}^{\mathrm{L}} \sum_{w=1}^{\mathrm{L}} \sum_{q=1}^{\mathrm{U}} \mathbf{g}_{wl,uji} T_{wq} v_{qwl} + \mathbf{w}_{ujl} \quad \textbf{(4.24)}$$

Where;

$$\lim_{M \to \infty} \frac{x_{ujl}}{\sqrt{M}} = \sqrt{\rho_b} \sum_{w=1}^{\mathrm{L}} \beta'_{wl,ujl} v_{uwl} = \sqrt{\rho_b} s_{ujl} \quad \textbf{(4.25)}$$

4.5 Achievable rates with finite number of sub-array BS antennas

In this section, the achievable rate of the received signal when there is a finite number of antennas is derived. When the MMSE estimator is considered the received signal as given by equation (4.3) then becomes;

$$\hat{\mathbf{g}}_{wl,uwl} = \mathbf{Y}_{l,w}\left(\phi_{u,l}^{\dagger}\varphi'_{wl,uwl}\right) = \varphi'_{wl,uwl}\sqrt{\tau\rho_t}\sum_{j=1}^{\boldsymbol{L}}\mathbf{g}_{wl,ujl} + \boldsymbol{n}'_{\boldsymbol{l,w}} \tag{4.26}$$

Where;

$$\varphi'_{wl,uwl} = \frac{\sqrt{\tau\rho_t}\beta_{wl,uwl}}{\zeta^2_{wl,uwl}}, \qquad \zeta^2_{wl,uwl} = 1 + \rho_t\tau\sum_{z=1}^{L}\beta_{wl,uzl} \tag{4.27}$$

The vectors $\mathbf{g}_{wl,uji}$ and $\hat{\mathbf{g}}_{wl,uwl}$have the following distributions**;**

$$\mathbf{g}_{wl,uji} \sim \mathcal{CN}\left(0, \beta_{lwl,uji}\boldsymbol{I_M}\right) \tag{4.28}$$

$$\hat{\mathbf{g}}_{wl,uwl} \sim \mathcal{CN}\left(0, \beta'^{2}_{wl,uwl}\boldsymbol{I_M}\right) \tag{4.29}$$

The sub-group user (u, j)receives the signal:

$$x_{ujl} = \sqrt{\rho_b}\sum_{i=1}^{\mathrm{L}}\sum_{w=1}^{\mathrm{L}}\sum_{q=1}^{\mathrm{U}}\mathbf{g}_{wl,uji}\frac{\hat{\mathbf{g}}^{\dagger}_{wl,qwl}}{\zeta^2_{wl,qwl}}v_{qwi} + w_{ujl} \tag{4.30}$$

The conjugated beamforming is assumed to be: $T_{wq} = \frac{\hat{\mathbf{g}}^{\dagger}_{wl,qwl}}{\zeta^2_{wl,qwl}}$

After some manipulation, equation (4.30) can be written as:

$$x_{ujl} = F_1 + F_2 + F_3 + F_4 + F_5 + F_6 \tag{4.31}$$

Where;

$$F_1 = s_{ujl}\sqrt{\rho_b}\sum_{w=1}^{\mathrm{L}} \boldsymbol{a}_{wl,ujl}\mathrm{E}\left[\mathbf{g}_{wl,ujl}\frac{\hat{\mathbf{g}}^{\dagger}_{wl,uwl}}{\zeta^2_{wl,uwl}}\right]$$

$$F_2 = s_{ujl}\sqrt{\rho_b}\sum_{w=1}^{\mathrm{L}} \boldsymbol{a}_{wl,ujl}\left(\mathbf{g}_{wl,ujl}\frac{\hat{\mathbf{g}}^{\dagger}_{wl,uwl}}{\zeta^2_{wl,uwl}} - \mathrm{E}\left[\mathbf{g}_{wl,ujl}\frac{\hat{\mathbf{g}}^{\dagger}_{wl,uwl}}{\zeta^2_{wl,uwl}}\right]\right)$$

$$\mathrm{F}_3 = \sqrt{\rho_b}\sum_{w=1}^{\mathrm{L}} \mathbf{g}_{wl,ujl}\frac{\hat{\mathbf{g}}^{\dagger}_{wl,uwl}}{\zeta^2_{wl,uwl}}\sum_{\substack{p=1\\p\neq j}}^{\mathrm{L}} s_{upl}\boldsymbol{a}_{wl,upl}$$

$$F_4 = \sqrt{\rho_b}\sum_{w=1}^{\mathrm{L}}\sum_{\substack{q=1\\q\neq u}}^{\mathrm{U}} \mathbf{g}_{wl,ujl}T_{wq}v_{qwl}$$

$$F_5 = \sqrt{\rho_b}\sum_{\substack{i=1\\i\neq l}}^{\mathrm{L}}\sum_{w=1}^{\mathrm{L}}\sum_{q=1}^{\mathrm{U}} \mathbf{g}_{wl,uji}T_{wq}v_{qwi}$$

$$F_6 = w_{ujl}$$

The achievable rate is given by:

$$\mathrm{C} = \mathbf{log_2}\left(\mathbf{1} + \frac{\mathrm{E}[|F_1|^2]}{\mathrm{E}[|F_2|^2] + \mathrm{E}[|F_3|^2] + \mathrm{E}[|F_4|^2] + \mathrm{E}[|F_5|^2] + \mathrm{E}[|F_6|^2]}\right) \qquad \textbf{(4.32)}$$

Similar to [21] then ,

$$\mathrm{E}[|F_1|^2] = \rho_b M^2\left|\sum_{w=1}^{\mathrm{L}}\frac{\rho_t\tau\beta_{wl,ujl}\beta_{wl,uwl}}{1+\rho_t\tau\sum_{z=1}^{L}\beta_{wl,uzl}}\frac{\boldsymbol{a}_{wl,ujl}}{\zeta_{wl,uwl}}\right|^2 \qquad \textbf{(4.33)}$$

$$\mathrm{E}[|F_2|^2] = \rho_b M\sum_{w=1}^{\mathrm{L}}\left|\frac{\boldsymbol{a}_{wl,ujl}}{\zeta_{wl,uwl}}\right|^2\frac{\rho_t\tau\beta_{wl,ujl}\beta^2_{wl,uwl}}{1+\rho_t\tau\sum_{z=1}^{L}\beta_{wl,uzl}} \qquad \textbf{(4.34)}$$

$$\mathrm{E}[|F_3|^2] = \rho_b M \sum_{w=1}^{\mathrm{L}} \sum_{\substack{\boldsymbol{p=1} \\ \boldsymbol{p \neq j}}}^{\mathrm{L}} \left| \frac{\boldsymbol{a}_{wl,upl}}{\zeta_{wl,uwl}} \right|^2 \frac{\rho_t \tau \beta_{wl,ujl} \beta_{wl,uwl}^2}{1 + \rho_t \tau \sum_{z=1}^{L} \beta_{wl,uzl}} + \rho_b M^2 \sum_{\substack{\boldsymbol{p=1} \\ \boldsymbol{p \neq j}}}^{\mathrm{L}} \left| \sum_{w=1}^{\mathrm{L}} \frac{\rho_t \tau \beta_{wl,ujl} \beta_{wl,uwl}}{1 + \rho_t \tau \sum_{z=1}^{L} \beta_{wl,uzl}} \frac{\boldsymbol{a}_{wl,upl}}{\zeta_{wl,uwl}} \right|^2 \quad \textbf{(4.35)}$$

$$\mathrm{E}[|F_4|^2] = \rho_b M \sum_{w=1}^{\mathrm{L}} \sum_{\substack{\mathrm{q=1} \\ q \neq u}}^{U} \frac{\rho_t \tau \beta_{lwl,ujl} \beta_{wl,qwl}^2}{1 + \rho_t \tau \sum_{z=1}^{L} \beta_{wl,qzl}} \left| \frac{\boldsymbol{v}_{qwl}}{\zeta_{wl,qwl}} \right|^2 \quad \textbf{(4.36)}$$

$$\mathrm{E}[|F_5|^2] = \rho_b M \sum_{\substack{i=1 \\ i \neq l}}^{\mathrm{L}} \sum_{w=1}^{\mathrm{L}} \sum_{\mathrm{q=1}}^{U} \frac{\rho_t \tau \beta_{lwl,uji} \beta_{wl,qwl}^2}{1 + \rho_t \tau \sum_{z=1}^{L} \beta_{wl,qzl}} \left| \frac{\boldsymbol{v}_{qwi}}{\zeta_{wl,qwi}} \right|^2 \quad \textbf{(4.37)}$$

$$\mathrm{E}[|F_6|^2] = var(w_{ujl}) = \sigma_{ujl}^2 \quad \textbf{(4.38)}$$

Finally, the achievable rate becomes;

$$\mathrm{C} = \mathbf{log_2} \left(\mathbf{1} + \frac{\rho_b M^2 \left| \sum_{w=1}^{\mathrm{L}} \frac{\rho_t \tau \beta_{wl,ujl} \beta_{wl,uwl}}{1 + \rho_t \tau \sum_{z=1}^{L} \beta_{wl,uzl}} \frac{\boldsymbol{a}_{wl,ujl}}{\zeta_{wl,uwl}} \right|^2}{M^2 \psi_1 + M \psi_2 + \sigma_{ujl}} \right) \quad \textbf{(4.39)}$$

Where;

$$\psi_1 = \rho_b \sum_{\substack{\boldsymbol{p=1} \\ \boldsymbol{p \neq j}}}^{\mathrm{L}} \left| \sum_{w=1}^{\mathrm{L}} \frac{\rho_t \tau \beta_{wl,ujl} \beta_{wl,uwl}}{1 + \rho_t \tau \sum_{z=1}^{L} \beta_{wl,uzl}} \frac{\boldsymbol{a}_{wl,upl}}{\zeta_{wl,uwl}} \right|^2$$

$$\psi_2 = \rho_b \sum_{i=1}^{\mathrm{L}} \sum_{w=1}^{\mathrm{L}} \sum_{\mathrm{q=1}}^{U} \frac{\rho_t \tau \beta_{lwl,uji} \beta_{wl,qwl}^2}{1 + \rho_t \tau \sum_{z=1}^{L} \beta_{wl,qzl}} \left| \frac{\boldsymbol{v}_{qwi}}{\zeta_{wl,qwi}} \right|^2$$

Full derivation of the achievable rate equation (4.39) is given in appendix B.

CHAPTER FIVE

COMPUTER SIMULATION RESULTS AND DISCUSSION

5.1 The 3GPP Standard of Urban Macro Model

The parameters used in simulations are taken from the 3rd Generation Partnership Project (3GPP) standard specifications [34]. It is a global wireless communications organization that collaboratively develops standards or specifications for radio, core network and service architecture.

The 3GPP standard of Urban Macro model used to generate the large scale fading as given by equation (5.1) [34].

$$10\log_{10}\beta_{wl,uji} = -139.5 - 35\log_{10} d_{wl,uji} + \varphi_{wl,uji} \quad \textbf{(5.1)}$$

Where $d_{wl,uji}$ is the distance (in km) between the user and the base station, and $\varphi_{wl,uji}$ is a shadowing coefficient modeled as a Gaussian random variable with zero mean and a variance of 8dB. The cell radius is taken to be $r = 0.75$km and $d_{wl,uji}$ is the distance of all users randomly distributed near the edge of the cell. The bandwidth is chosen to be $B = 20$MHz and the noise variance at each receiver $\sigma_{ujl}^2 = 92$dBm. The average power of w-th sub-array of BS and at each user terminal are $\rho_b = 48$dBm and $\rho_t = 23$dBm, respectively.

5.2 Results with Pilot Reuse Factor N=7

A network with pilot reuse factor $N = 7$ is considered. Within each cell, BS has $W = 7$ sub-array of antennas and the number of users in each cell is $K = LW$. For each cell unique $U = 7$ orthogonal signals are assigned and for users in each cell those orthogonal signals are reused.

The Cumulative Distribution Functions (CDF) of the achievable sum rates are given in equation (4.39) and simulated using MATLAB. The results of our method of the large scale fading precoding with non-cooperation cell (LSFP-NCC) are compared to

those obtained by Ashikhim et al [21] in their method of the large scale fading precoding with cell cooperation (LSFP-CC).

The results in figure 5.1 show the cumulative distribution function (CDF) of the achievable sum rate of LKusers with $M = 10^2$. It can be noted LSFP-CC with no pilot reuse factor (i.e.N $= 1$) achieves 5% outage rate around 10^{-4} bits per second. When the LSFP-NCC is used the achievable sum rate is improved to around 10^{-3} bits per second.

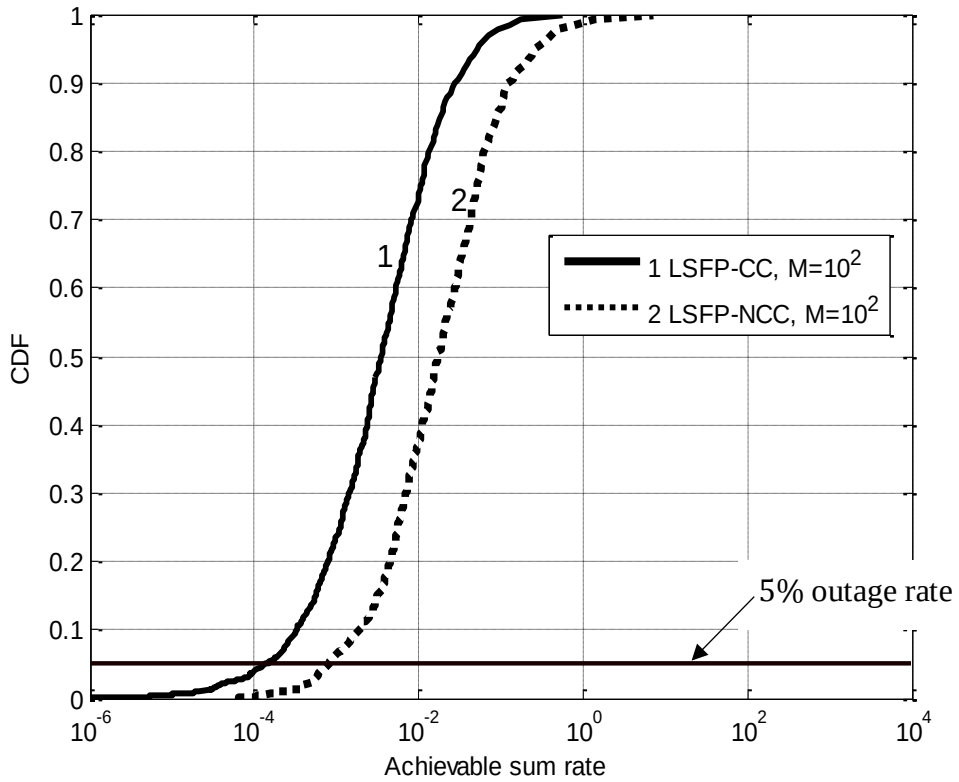

Figure 5.1 The CDF of all received Achievable sum rate of $\boldsymbol{LK}$ users for $\boldsymbol{M = 10^2}$

The results in figure 5.2 show the cumulative distribution function (CDF) of the achievable sum rate of LKusers with $M = 10^3$. It can be noted that the large scale fading precoding with cell cooperation (LSFP-CC) with no pilot reuse factor (i.e.N $=$ 1) achieves 5% outage rate around 10^{-3} bits per second. When the large scale fading precoding with non-cooperation cell is used (LSFP-NCC) the achievable sum rate is improved to around 10^{-2} bits per second.

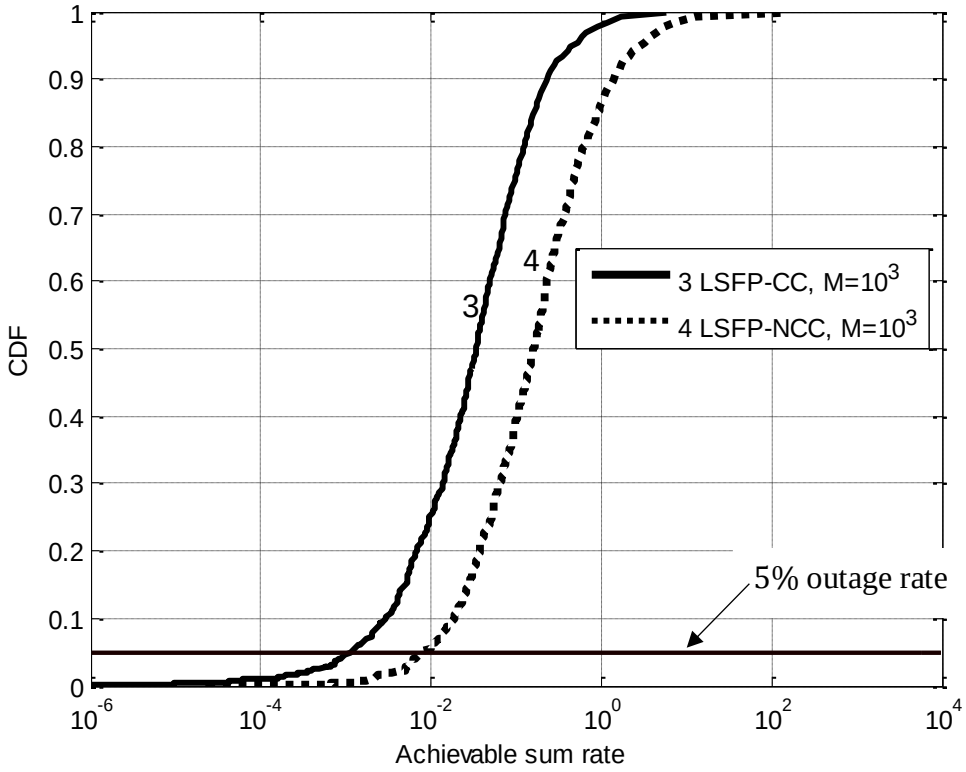

Figure 5.2 The CDF of all received Achievable sum rate of $\boldsymbol{LK}$ users for $\boldsymbol{M = 10^3}$

The results in figure 5.3 show the cumulative distribution function (CDF) of the achievable sum rate of LK users with $M = 10^4$. It can be noted that the large scale fading precoding with cell cooperation (LSFP-CC) with no pilot reuse factor (i.e.N $=$ 1) achieves 5% outage rate around 10^{-3} bits per second. When the large scale fading precoding with non-cooperation cell is used (LSFP-NCC) the achievable sum rate is improved to around 10^{-1} bits per second.

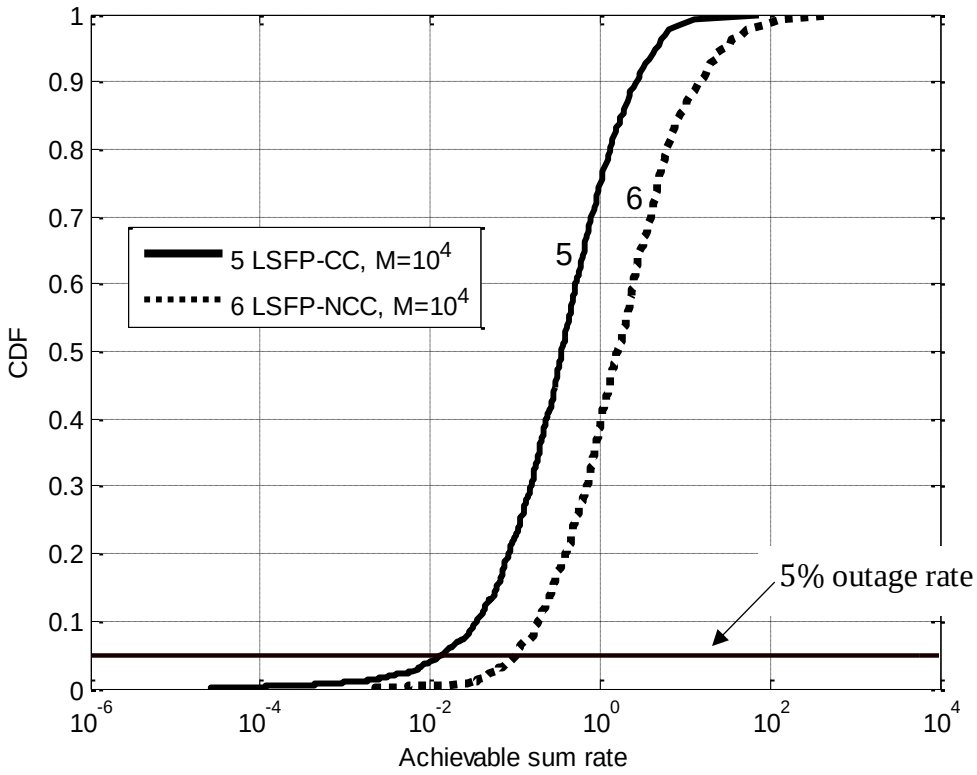

Figure 5.3. The CDF of all received Achievable sum rate of $\boldsymbol{LK}$ users for $\boldsymbol{M = 10^4}$

From figure 5.1, figure 5.2 and figure 5.3 it can be observed that the proposed LSFP-NCC given an improvement of 5% outage rate. This is ten times higher that was can be obtained with LSFP-CC approach. This improvement is due to the large scale precoding which reduces the interference that comes from the adjacent cells.

The results in figure 5.4 show the cumulative distribution function (CDF) of the achievable sum rate of LK users with $M = 10^2$, $M = 10^3$ and $M = 10^4$ for LSFP-NCC. It can be noted that the achievable sum rate for the number of antenna $M = 10^2$, $M = 10^3$ and $M = 10^4$ at 5% outage rate is 10^{-3}, 10^{-2} and 10^{-1} respectively. This shows the achievable sum rate increases as the number of antennas increases.

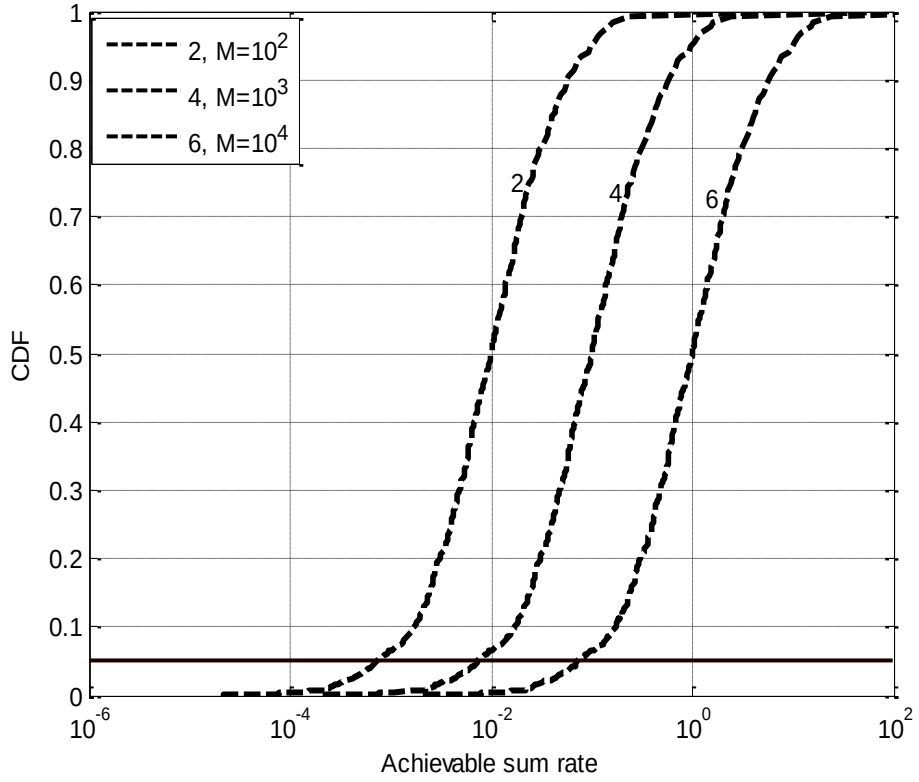

Figure 5.4. The CDF of LSFP-NCC all received Achievable sum rate of $\boldsymbol{LK}$users for $\boldsymbol{M = 10^2}$, $\boldsymbol{M = 10^3}$ and $\boldsymbol{M = 10^4}$

5.3 Comparison of results with different pilot reuse factors

The results of the achievable sum rate of equation (4.39) for pilot reuse factor $N = 3$, $N = 4$, and $N = 7$ were obtain by MATLAB simulation. For the purpose of simulation the number of users in each cell can be chosen any K number. In practice the number of users within cell determined by the coherence time and frequency smoothness interval [9]. The number of K users in each cell is chosen to be divisible by pilot reuse factors.

Figure. 5.5 shows result of the simulation for pilot reuse factor $N = 3$ and $N = 4$ with the number of users in each cell fixed at 48. It can be observed that pilot reuse factor $N = 4$ gives better achievable sum rate than pilot reuse factor $N = 3$. For example, for the number of antennas $M = 100$ the average achievable sum rate for pilot reuse factor $N = 3$ is 0.205×10^{-2}. The average achievable sum rate with a pilot reuse factor $N = 4$ for $M = 100$ is 0.237×10^{-2}. This is larger than the value of the pilot reuse factor $N = 3$.

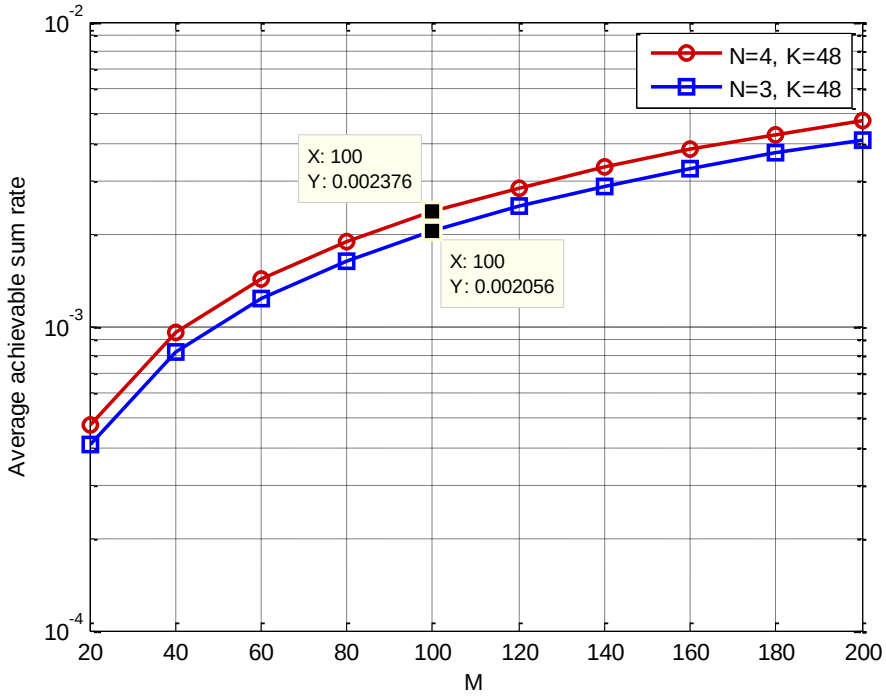

Figure 5.5 The Average achievable sum rate of 48 users for pilot reuse factor $\boldsymbol{N = 4}$ and $\boldsymbol{N = 3}$ with different M

Figure 5.6 shows result of the simulation for pilot reuse factor $N = 4$ and $N = 7$ with number of users in each cell fixed at 56. It can be observed that pilot reuse factor $N = 7$ gives better achievable sum rate than pilot reuse factor $N = 7$. For example, with the number of antennas $M = 100$ the average achievable sum rate for pilot reuse factor $N = 4$ is 0.245×10^{-2}. For pilot reuse factor $N = 7$ when $M = 100$ is 0.516×10^{-2}, which is larger than the value obtained with a pilot reuse factor $N = 4$.

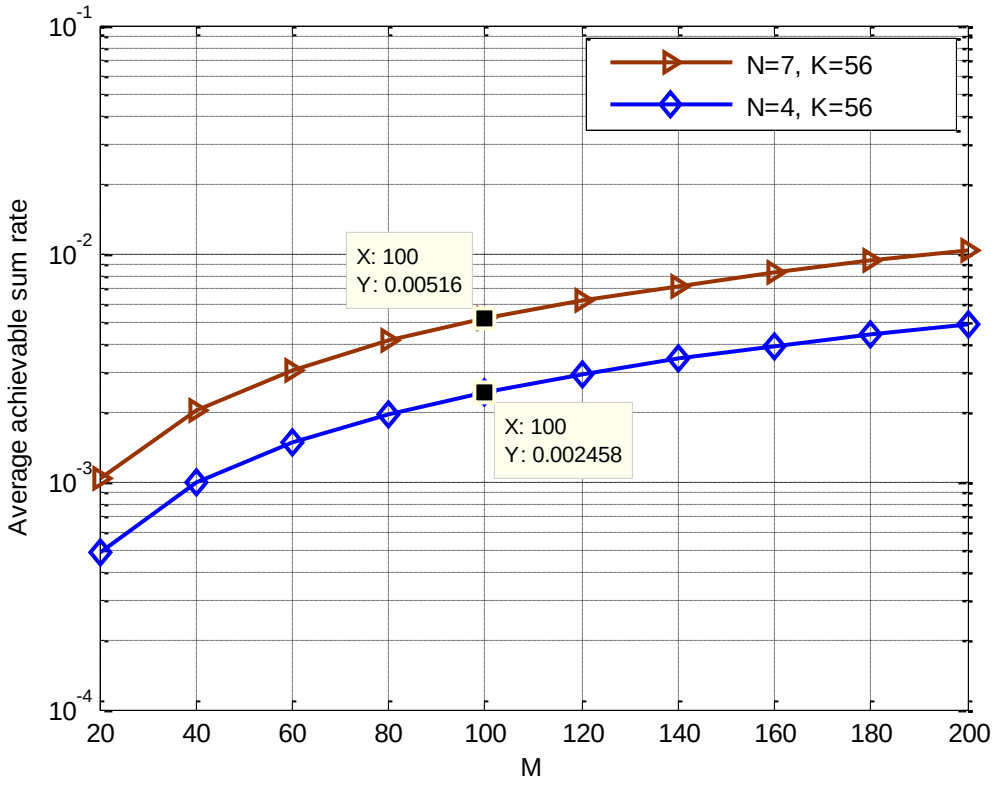

Figure 5.6 The Average achievable sum rate of 56 users for pilot reuse factor $\boldsymbol{N = 7}$ and $\boldsymbol{N = 4}$ with different M

Figure 5.7 shows a comparison of pilot reuse factor $N = 7$ with a large scale fading precoding for cooperation of cells ($N = 1$). It can be observed that the achievable sum rate improves when the pilot reuse factor is employed. For example, for the number of antennas $M = 100$ the average achievable sum rate without a pilot reuse factor ($N = 1$) is 0.118×10^{-2} . For pilot reuse factor $N = 7$ when $M = 100$ is 0.36×10^{-2} which is larger than the value obtained with no the pilot reuse factor ($N = 1$).

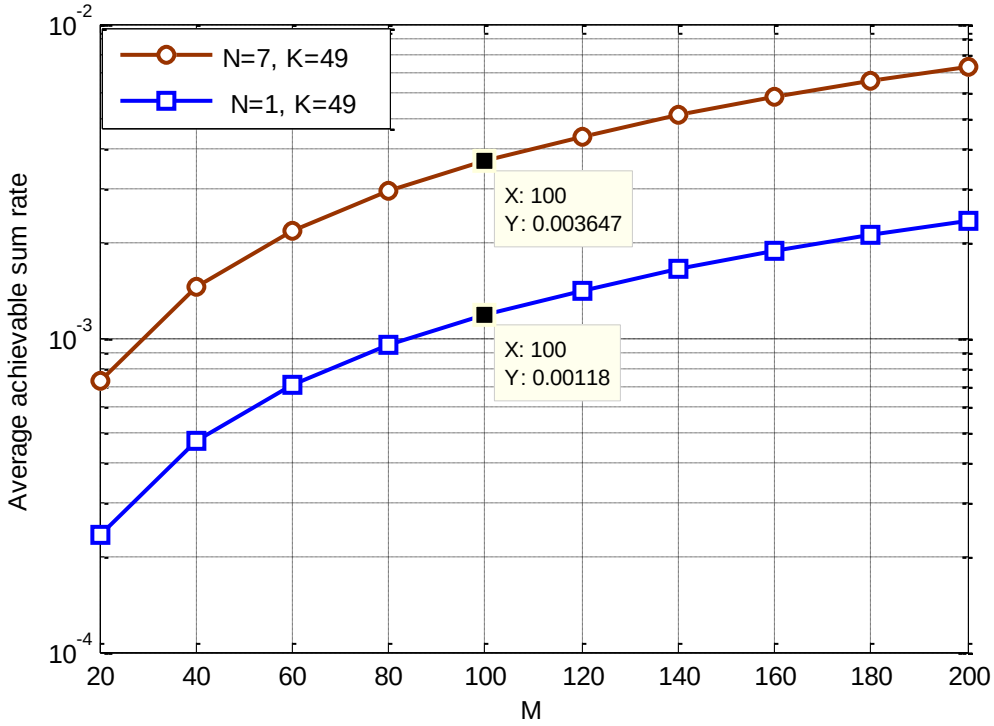

Figure 5.7 The Average achievable sum rate of 49 users for $\boldsymbol{N = 7}$ and $\boldsymbol{N = 1}$ with different M

Figure 5.8 shows a comparison of pilot reuse factor $N = 4$ with a large scale fading precoding for cooperation of cells ($N = 1$). It can be observed that pilot reuse factor $N = 4$ gives better achievable sum rate than with no the pilot reuse factor ($N = 1$). For example, for the number of antennas $M = 100$ the average achievable sum rate for pilot reuse factor $N = 1$ is 0.112×10^{-2} . For pilot reuse factor $N = 4$ when $M = 100$ is 0.23×10^{-2} which is larger than the value obtained with no the pilot reuse factor ($N = 1$).

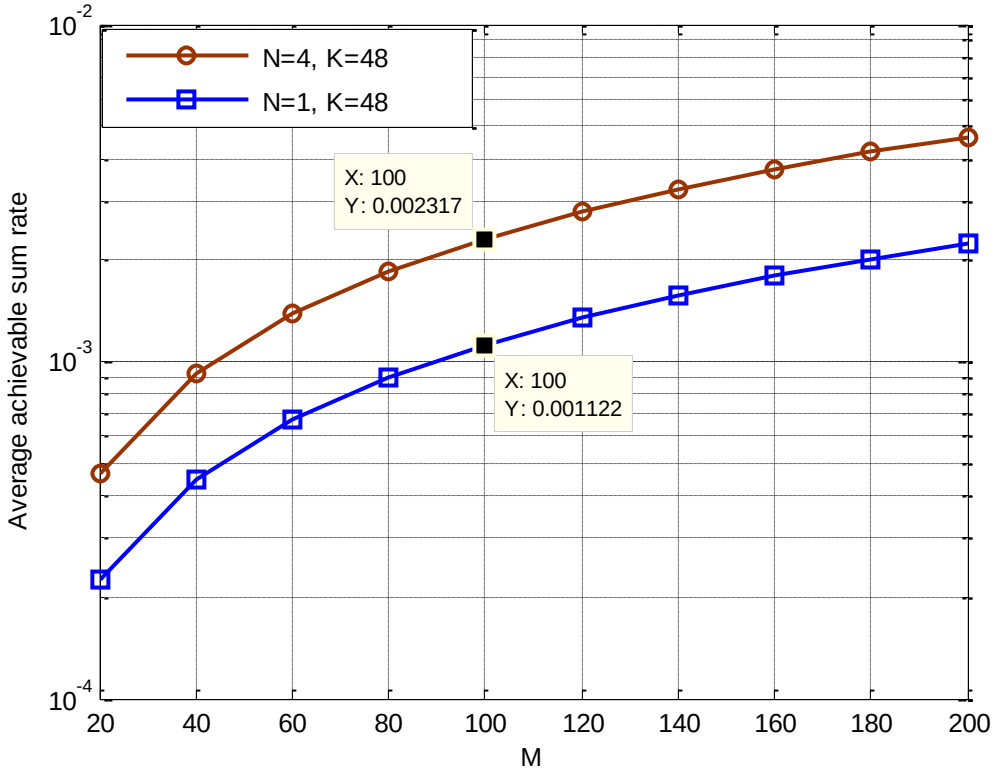

Figure 5.8 The Average achievable sum rate of 48 users for $\boldsymbol{N = 4}$ and $\boldsymbol{N = 1}$ with different M

Figure 5.9 shows comparison the average achievable sum rate of $N = 4$ and with the average achievable sum rate of the system without mitigation of pilot contamination effect (with PCE). From the figure 5.8 can be observed that the average achievable sum rate of $N = 4$ gives 6.3×10^7 times the PCE.

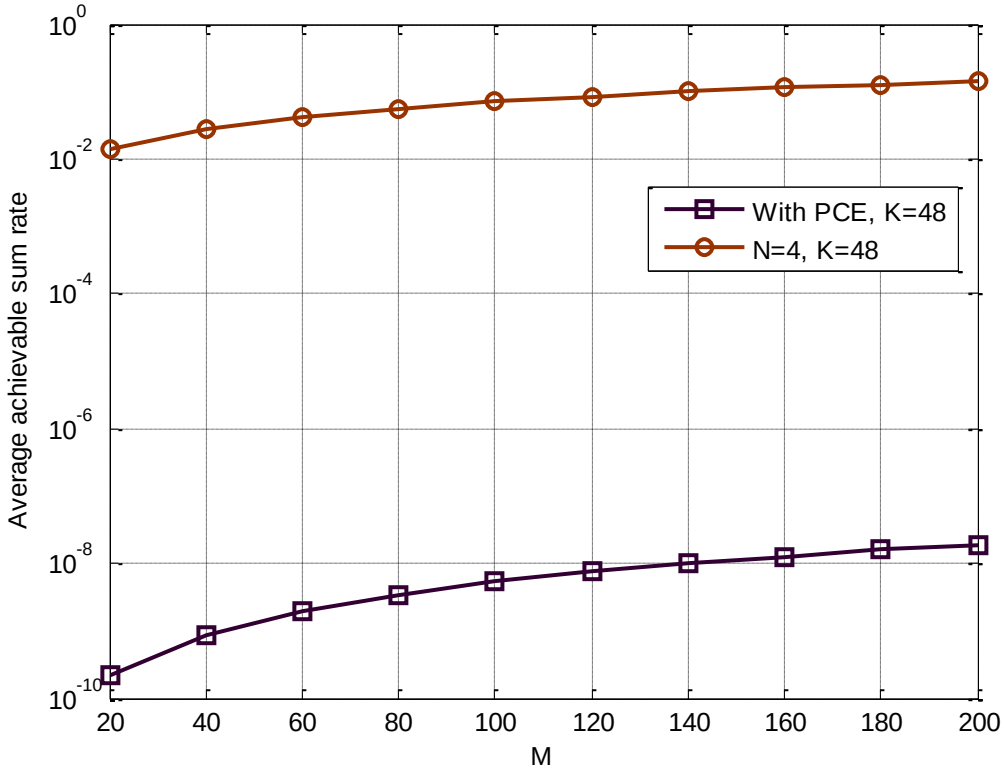

Figure 5.9 The Average achievable sum rate of 48 users for $\boldsymbol{N = 4}$ and PCF with different M

Figure 5.10 shows comparison of the average achievable sum rate of $N = 7$ and with PCE. The average achievable sum rate of $N = 7$ gives 9.7×10^{7} times the PCE.

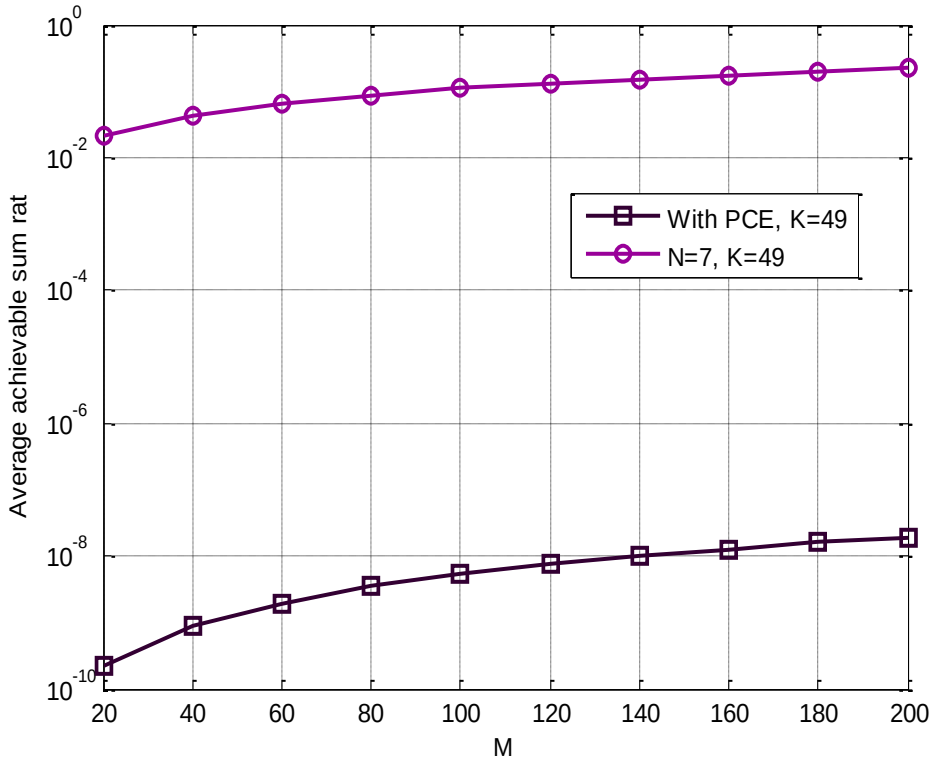

Figure 5.10 The Average achievable sum rate of 49 users for $\boldsymbol{N = 7}$ and PCF with different M

Figure 5.11 shows comparison of the average achievable sum rate of $N = 3$ and with PCE. The average achievable sum rate of $N = 3$ gives 3.9×10^{7} times the PCE.

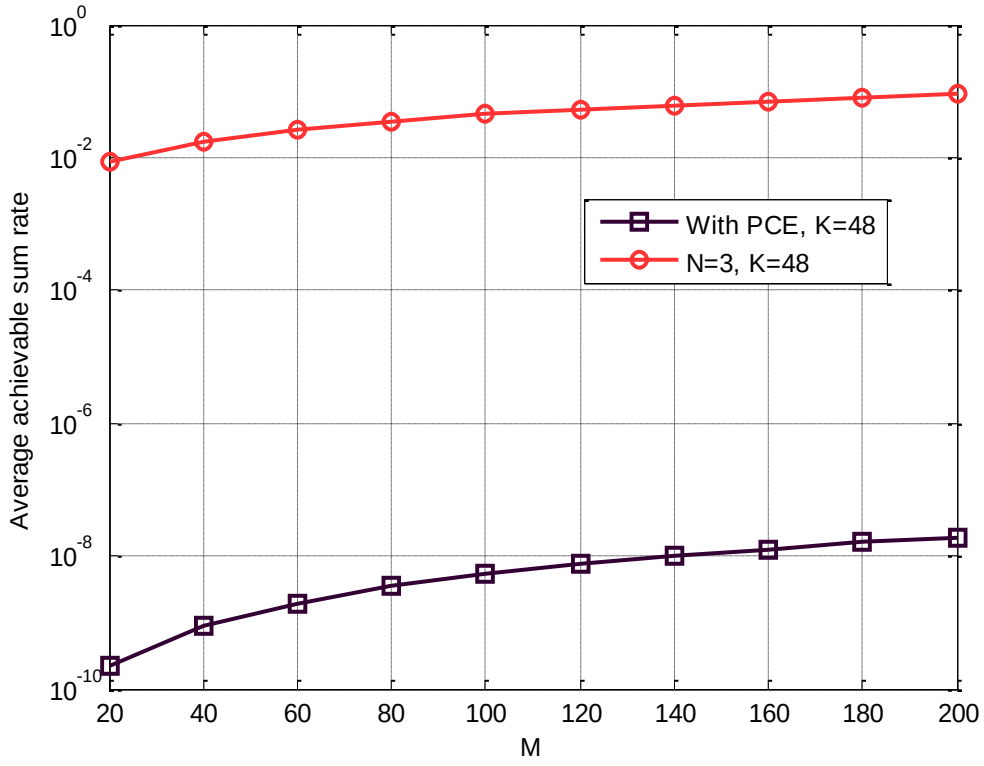

Figure 5.11 The Average achievable sum rate of 48 users for $\boldsymbol{N = 3}$ and PCF with different M

From Figures 5.9, 5.10 and 5.11, it can be noted that a great improvement in the average achievable sum rate has been obtained. This is due to the mitigation of pilot contamination effect in the proposed method where a novel pilot reuse factor with a large scale fading precoding has been employed.

All the above results show that as the number of antennas increases the achievable rate also increases. It can also be observed that a higher pilot reuse factor give better average achievable sum rates. This demonstrates that a large number of antennas gives a better achievable rate and is the main advantage of massive MIMO.

CHAPTER SIX

CONCLUSION AND RECOMMENDATIONS

6.1 Conclusion

Massive MIMO is the most promising technology for 5^{th} generation. It gives high spectral efficiency and communication reliability. The main challenge of this technology is the pilot contamination effect. This effect occurs when two or more users send the same orthogonal signals. The effect of pilot contamination can be inter-pilot contamination or intra-pilot contamination. The inter-pilot contamination occurs when users at different cells send the same orthogonal signal. The intra-pilot contamination occurs when users send the same orthogonal signals within the cell. The effect pilot contamination causes the signal interference plus noise ratio to decrease which affect the performance of the system. It has been observed that the fundamental limitation of massive MIMO is the effect of pilot contamination. This effect cannot be mitigated by increasing the number of antennas.

In this thesis, a pre-coder has been designed for downlink massive MIMO TDD system by considering pilot contamination. A pilot reuse factor has been developed and used in the design of a novel uplink training scheme that uses a large scale fading precoding without cooperation between cells. The pilot reuse factor is designed to mitigate the effect of inter-pilot contamination. A large scale fading precoding is used to mitigate the effect of intra-pilot contamination. The pilot reuse factor with a large scale fading precoding without cell cooperation (LSFP-NCC) gives a better average achievable sum rate compared with a large scale fading precoding using corporation between cells (LSFP-CC). The higher pilot reuse factor give better average achievable sum rates. The achievable rate also gives a better performance as the number of antennas increased.

It has been observed from the simulations that the proposed scheme of LSFP-NCC have an improvement on the 5% outage rate 10 times over the existing method of

LSFP-CC. This is a significant improvement, however it is achieved at the expense of sub-array BS installation and power consumption.

In this investigation the effect of power consumption and cost of the installation of the sub-array BS has not been considered. It is only the mitigation of pilot contamination using pilot reuse factor with a large scale fading precoding that has been interest. One of the limitation is to have a better average achievable sum rate it needs higher pilot reuse factor. This increases the number of sub array BSs which cause the power consumption to increase and also the cost of installation.

6.2 Future Work

Further investigations need to be carried out to find the optimal point of pilot reuse factor so as to reduce the number of sub-array BS within the cell without more reducing of the average achievable sum rate.

The method that has been used in this thesis assumes that the users are located at the cell edges. However, in practice this is rarely the situation as users are randomly distributed within a cell. Further investigations shall be carried out to assess the effect of random user location on the improvement of the achievable sum rates. In this work, also the effect of an antenna structure is not considered in estimating of the channel. The effect of an antennas structure can be studied further on the improvement of the achievable rate of the system.

REFERENCES

[1] E. Biglier, R. Calderbank, A. Constantinides, A. Goldsmith, A. Paulraj, and H.V. Poor, MIMO Wireless Communications, New York: Cambridge university press, 2007.

[2] F. Rusek et al., "Scaling Up MIMO: Opportunities and Challenges with Very Large Arrays," in IEEE Signal Processing Magazine, vol. 30, no. 1, pp. 40-60, Jan. 2013.

[3] E. G. Larsson, O. Edfors, F. Tufvesson and T. L. Marzetta, "Massive MIMO for next generation wireless systems," in IEEE Communications Magazine, vol. 52, no. 2, pp. 186-195, February 2014

[4] T. L. Marzetta, "Massive MIMO: An Introduction," in Bell Labs Technical Journal, vol. 20, no. , pp. 11-22, 2015.

[5] O. Elijah, C. Y. Leow, T. A. Rahman, S. Nunoo and S. Z. Iliya, "A Comprehensive Survey of Pilot Contamination in Massive MIMO—5G System," in IEEE Communications Surveys & Tutorials, vol. 18, no. 2, pp. 905-923, Second quarter 2016.

[6] O. Elijah, C. Y. Leow, A. R. Tharek, S. Nunoo and S. Z. Iliya, "Mitigating pilot contamination in massive MIMO system — 5G: An overview," 10th Asian Control Conference (ASCC), Kota Kinabalu, Malaysia, May 31-June 3, 2015, pp. 1-6.

[7] H. Q. Ngo, E. G. Larsson and T. L. Marzetta, "Energy and Spectral Efficiency of Very Large Multiuser MIMO Systems," in IEEE Transactions on Communications, vol. 61, no. 4, pp. 1436-1449, April 2013

[8] H. Q. Ngo, E. G. Larsson and T. L. Marzetta, "Uplink power efficiency of multiuser MIMO with very large antenna arrays," 2011 49th Annual Allerton Conference on Communication, Control, and Computing, Monticello, Illinois, United States, 28 - 30 Sep 2011, pp. 1272-1279.

[9] T. L. Marzetta, "Non cooperative Cellular Wireless with Unlimited Numbers of Base Station Antennas," in IEEE Transactions on Wireless Communications, vol. 9, no. 11, pp. 3590-3600, November 2010

[10] J. Hoydis, S.T. Brink and M. Debbah, "Massive MIMO in the UL/DL of Cellular Networks: How Many Antennas Do We Need?," in IEEE Journal on Selected Areas in Communications, vol. 31, no. 2, pp. 160-171, February 2013.

[11] T.S. Rappaport, Wireless communications: principles and practice. Vol. 2. New Jersey: Prentice Hall PTR, 1996.

[12] K. Appaiah, A. Ashikhmin and T. L. Marzetta, "Pilot Contamination Reduction in Multi-User TDD Systems," 2010 IEEE International Conference on Communications (ICC), Cape Town,South Africa, 23-27 May 2010, pp. 1-5.

[13] J. Mohinder, Space-Time Codes and MIMO Systems, Artech House, 2004.

[14] J. Y. R. Hampton, Introduction to MIMO Communications, Cambridge University Press, 2013.

[15] X. Gao, O. Edfors, F. Rusek and F. Tufvesson, "Linear Pre-Coding Performance in Measured Very-Large MIMO Channels," Vehicular Technology Conference (VTC Fall), 2011 IEEE, San Francisco, California, United States, 5-8 Sep 2011, pp. 1-5.

[16] H. Q. C. Ngo, Massive MIMO: Fundamentals and System Designs, vol. 1642, Linköping University Electronic Press, 2015.

[17] E. Björnson, E. G. Larsson and T. L. Marzetta, "Massive MIMO: Ten myths and one critical question," in IEEE Communications Magazine, vol. 54, no. 2, pp. 114-123, February 2016.

[18] H. Q. Ngo, E. G. Larsson and T. L. Marzetta, "Massive MU-MIMO downlink TDD systems with linear precoding and downlink pilots," , "51st Annual Allerton Conference on Communication, Control, and Computing", Monticello, Illinois, United States, 02-04 Oct 2013, pp. 293-298.

[19] L. Wang; H. Q. Ngo; M. Elkashlan; T. Q. Duong; K. K. Wong, "Massive MIMO in Spectrum Sharing Networks: Achievable Rate and Power Efficiency," in IEEE Systems Journal ,2015, vol.99, pp.1-12

[20] A. Ashikhmin and T. Marzetta, "Pilot contamination precoding in multi-cell large scale antenna systems," Information Theory Proceedings (ISIT), 2012 IEEE International Symposium , Massachusetts, United States, 1-6 July 2012, pp. 1137-1141.

[21] A. Ashikhmin, T. L. Marzetta, and L. Li, “Interference reduction in multi-cell massive MIMO systems I: Large-scale fading precoding and decoding,” arXiv preprint arXiv:1411.4182, 2014.

[22] A. Ashikhmin, T. L. Marzetta, and L. Li, “Interference reduction in multi-cell massive MIMO systems II: Large-scale fading precoding and decoding,” arXiv preprint arXiv:1411.4183, 2014.

[23] F. Fernandes, A. Ashikhmin and T. L. Marzetta, "Inter-Cell Interference in Noncooperative TDD Large Scale Antenna Systems," in IEEE Journal on Selected Areas in Communications, vol. 31, no. 2, pp. 192-201, February 2013.

[24] H. Q. Ngo, T. L. Marzetta and E. G. Larsson, "Analysis of the pilot contamination effect in very large multicell multiuser MIMO systems for physical channel models," 2011 IEEE International Conference on Acoustics, Speech and Signal Processing (ICASSP), Prague, Czech Republic,22-27 May 2011, pp. 3464-3467.

[25] J. Jose, A. Ashikhmin, T. L. Marzetta and S. Vishwanath, "Pilot Contamination and Precoding in Multi-Cell TDD Systems," in IEEE Transactions on Wireless Communications, vol. 10, no. 8, pp. 2640-2651, August 2011.

[26] T. L. Marzetta, "How Much Training is Required for Multiuser Mimo?," Fortieth Asilomar Conference on Signals, Systems and Computers, Pacific Grove, California, United States, 29 Oct-01 Nov 2006, pp. 359-363.

[27] T. L. Marzetta and B. M. Hochwald, "Fast transfer of channel state information in wireless systems," in IEEE Transactions on Signal Processing, vol. 54, no. 4, pp. 1268-1278, April 2006.

[28] H. Q. Ngo and E. G. Larsson, "EVD-based channel estimation in multicell multiuser MIMO systems with very large antenna arrays," 2012 IEEE International Conference on Acoustics, Speech and Signal Processing (ICASSP), Kyoto, Japan, 25-30 Mar 2012, pp. 3249-3252.

[29] R. R. Müller, L. Cottatellucci and M. Vehkaperä, "Blind Pilot Decontamination," in IEEE Journal of Selected Topics in Signal Processing, vol. 8, no. 5, pp. 773-786, Oct. 2014.

[30] X. Yan, H. Yin, M. Xia and G. Wei, "Pilot sequences allocation in TDD massive MIMO systems," 2015 IEEE Wireless Communications and Networking Conference (WCNC), New Orleans, LA,USA, 09-12 Mar 2015, pp. 1488-1493.

[31] X. Zheng, H. Zhang, W. Xu and X. You, "Semi-orthogonal pilot design for massive MIMO systems using successive interference cancellation," 2014 IEEE

Global Communications Conference, Austin, TX,USA, 8-12 Dec 2014, pp. 3719-3724.

[32] X. Zhu, Z. Wang, L. Dai and C. Qian, "Smart Pilot Assignment for Massive MIMO," in IEEE Communications Letters, vol. 19, no. 9, pp. 1644-1647, Sept. 2015.

[33] B. Liu, Y. Cheng and X. Yuan, "Pilot contamination elimination precoding in multi-cell massive MIMO systems," Personal, Indoor, and Mobile Radio Communications (PIMRC), 2015 IEEE 26th Annual International Symposium , Hong Kong, China, 30 Aug - 02 Sep 2015, pp. 320-325.

[34] 3GPP TR 25.996,"Spatial channel model for multiple input multiple output (MIMO) simulations", 2016

APPENDICES

Appendix A

Derivation of the achievable rate Massive MIMO without using large scale fading precoding

The k-th user of the l-th cell receives the signal:

$$\mathrm{x}_{ki} = \sqrt{\rho_b} \sum_{l=1}^{\mathrm{L}} \sum_{\mathrm{j}=1}^{K} \mathbf{g}_{\boldsymbol{l}ki} \frac{\hat{\mathbf{g}}_{\boldsymbol{lji}}^{\dagger}}{\zeta_{lji}} \; s_{jl} + \mathbf{n}_{ki} \tag{A.1}$$

$$\hat{\mathbf{g}}_{\boldsymbol{lji}} = \mathbf{x}_{\boldsymbol{kl}} \left(\phi_j^{\dagger} \varphi'_{lji} \right) = \varphi'_{lji} \sqrt{\tau \rho_t} \sum_{z=1}^{L} \mathbf{g}_{\boldsymbol{ljz}} + \boldsymbol{n}'_{\boldsymbol{k}} \tag{A.2}$$

Where**;**

$$\varphi'_{lji} = \frac{\sqrt{\tau \rho_t} \beta_{lji}}{\zeta_{lji}^2} \, , \qquad \zeta_{lji}^2 = 1 + \rho_t \tau \sum_{z=1}^{L} \beta_{ljz}$$

The vectors $\mathbf{g}_{\boldsymbol{lji}}$ and $\hat{\mathbf{g}}_{\boldsymbol{lji}}$ have the following distributions**;**

$$\mathbf{g}_{\boldsymbol{lji}} = \mathcal{CN}\left(0, \beta_{lji} I_M\right) \tag{A.3}$$

$$\hat{\mathbf{g}}_{\boldsymbol{lji}} = \mathcal{CN}\left(0, \left(\frac{\beta_{lji}}{\zeta_{lji}}\right)^2 I_M\right) \tag{A.4}$$

Changing the random variable in front of s_{uj} with its expected value we obtain:

$$x_{\mathrm{ki}} = \sqrt{\rho_b} \mathbf{g}_{\boldsymbol{i}ki} \frac{\hat{\mathbf{g}}_{\boldsymbol{iki}}^{\dagger}}{\zeta_{iki}} \, s_{ki} + \sqrt{\rho_b} \sum_{\substack{l=1 \\ l \neq i}}^{\mathrm{L}} \mathbf{g}_{\boldsymbol{l}ki} \frac{\hat{\mathbf{g}}_{\boldsymbol{lkl}}^{\dagger}}{\zeta_{lkl}} \, s_{kl} + \sqrt{\rho_b} \sum_{l=1}^{\mathrm{L}} \sum_{\substack{\mathrm{j}=1 \\ j \neq k}}^{K} \mathbf{g}_{\boldsymbol{l}ki} \frac{\hat{\mathbf{g}}_{\boldsymbol{ljl}}^{\dagger}}{\zeta_{ljl}} \, s_{jl} + \mathbf{n}_{\mathrm{ki}}$$

$$x_{\mathrm{ki}} = \mathrm{E}\left[\sqrt{\rho_b}\mathbf{g}_{\boldsymbol{iki}}\frac{\hat{\mathbf{g}}_{\boldsymbol{iki}}^{\dagger}}{\zeta_{iki}}\, s_{ki}\right] + \left(\sqrt{\rho_b}\mathbf{g}_{\boldsymbol{iki}}\frac{\hat{\mathbf{g}}_{\boldsymbol{iki}}^{\dagger}}{\zeta_{iki}}\, s_{ki} - \mathrm{E}\left[\sqrt{\rho_b}\mathbf{g}_{\boldsymbol{iki}}\frac{\hat{\mathbf{g}}_{\boldsymbol{iki}}^{\dagger}}{\zeta_{iki}}\, s_{ki}\right]\right) + \sqrt{\rho_b}\sum_{\substack{l=1\\ l\neq i}}^{\mathrm{L}}\mathbf{g}_{\boldsymbol{lki}}\frac{\hat{\mathbf{g}}_{\boldsymbol{lkl}}^{\dagger}}{\zeta_{lkl}}\, s_{kl} + \sqrt{\rho_b}\sum_{l=1}^{\mathrm{L}}\sum_{\substack{\mathrm{j}=1\\ j\neq k}}^{K}\mathbf{g}_{\boldsymbol{lki}}\frac{\hat{\mathbf{g}}_{\boldsymbol{ljl}}^{\dagger}}{\zeta_{ljl}}\, s_{jl} + \mathbf{n}_{\mathrm{ki}} \tag{A.5}$$

$$\mathrm{v}_1 = \mathrm{E}\left[\sqrt{\rho_b}\mathbf{g}_{\boldsymbol{iki}}\frac{\hat{\mathbf{g}}_{\boldsymbol{iki}}^{\dagger}}{\zeta_{iki}}\, s_{ki}\right]$$

$$\mathrm{v}_2 = \left(\sqrt{\rho_b}\mathbf{g}_{\boldsymbol{iki}}\frac{\hat{\mathbf{g}}_{\boldsymbol{iki}}^{\dagger}}{\zeta_{iki}}\, s_{ki} - \mathrm{E}\left[\sqrt{\rho_b}\mathbf{g}_{\boldsymbol{iki}}\frac{\hat{\mathbf{g}}_{\boldsymbol{iki}}^{\dagger}}{\zeta_{iki}}\, s_{ki}\right]\right)$$

$$\mathrm{v}_3 = \sqrt{\rho_b}\sum_{\substack{l=1\\ l\neq i}}^{\mathrm{L}}\mathbf{g}_{\boldsymbol{lki}}\frac{\hat{\mathbf{g}}_{\boldsymbol{lkl}}^{\dagger}}{\zeta_{lkl}}\, s_{kl}$$

$$\mathrm{v}_4 = \sqrt{\rho_b}\sum_{l=1}^{\mathrm{L}}\sum_{\substack{\mathrm{j}=1\\ j\neq k}}^{K}\mathbf{g}_{\boldsymbol{lki}}\frac{\hat{\mathbf{g}}_{\boldsymbol{ljl}}^{\dagger}}{\zeta_{ljl}}\, s_{jl}$$

$$\mathrm{v}_5 = \mathbf{n}_{\mathrm{ki}}$$

The achievable rate given by:

$$\mathrm{C} = \mathbf{log_2}\left(\mathbf{1} + \frac{\mathrm{E}[|\mathrm{v}_1|^2]}{\mathrm{E}[|v_2|^2] + \mathrm{E}[|\mathrm{v}_3|^2] + \mathrm{E}[|\mathrm{v}_4|^2] + \mathrm{E}[|\mathrm{v}_5|^2]}\right) \tag{A.6}$$

$$[|\mathrm{v}_1|^2] = \left|\mathrm{E}\left[\sqrt{\rho_b}\mathbf{g}_{\boldsymbol{iki}}\frac{\hat{\mathbf{g}}_{\boldsymbol{iki}}^{\dagger}}{\zeta_{iki}}\right]\right|^2 = \rho_b \mathrm{M}^2\left|\frac{\rho_t \tau \beta_{iki}^2}{\zeta_{iki}^3}\right|^2$$

$$\mathrm{E}[|\mathrm{v}_1|^2] = \rho_b \mathrm{M}^2 \left| \frac{\rho_t \tau \beta_{iki}^2}{\zeta_{iki}^3} \right|^2 \tag{A.7}$$

$$\begin{aligned}
\mathrm{E}[|\mathrm{v}_2|^2] &= \left| \left(\sqrt{\rho_b} \mathbf{g}_{iki} \frac{\hat{\mathbf{g}}_{\boldsymbol{iki}}^{\dagger}}{\zeta_{iki}} - \mathrm{E}\left[\sqrt{\rho_b} \mathbf{g}_{iki} \frac{\hat{\mathbf{g}}_{\boldsymbol{iki}}^{\dagger}}{\zeta_{iki}} \right] \right) \right|^2 \\
&= \mathrm{E}[s_{ki} {s_{ki}}^{\dagger}] \rho_b \left[\mathbf{g}_{\boldsymbol{i}iki} \frac{\hat{\mathbf{g}}_{\boldsymbol{iki}}^{\dagger}}{\zeta_{iki}} \right. \\
&\quad \left. - \mathrm{E}\left[\mathbf{g}_{\boldsymbol{i}iki} \frac{\hat{\mathbf{g}}_{\boldsymbol{iki}}^{\dagger}}{\zeta_{iki}} \right] \left(\mathbf{g}_{\boldsymbol{i}iki} \frac{\hat{\mathbf{g}}_{\boldsymbol{iki}}^{\dagger}}{\zeta_{iki}} - \mathrm{E}\left[\mathbf{g}_{\boldsymbol{i}iki} \frac{\hat{\mathbf{g}}_{\boldsymbol{iki}}^{\dagger}}{\zeta_{iki}} \right] \right)^{\dagger} \right] = \rho_b Var\left(\mathbf{g}_{\boldsymbol{i}iki} \frac{\hat{\mathbf{g}}_{\boldsymbol{iki}}^{\dagger}}{\zeta_{iki}} \right) \\
&= \rho_b \rho_t \tau \mathrm{M} \left(\frac{\beta_{iki}}{\zeta_{iki}^2} \right)^3
\end{aligned}$$

$$\mathrm{E}[|\mathrm{v}_2|^2] = \rho_b \rho_t \tau \mathrm{M} \left(\frac{\beta_{iki}}{\zeta_{iki}^2} \right)^3 \tag{A.8}$$

$$\begin{aligned}
\mathrm{E}[|\mathrm{v}_3|^2] &= \mathrm{E}\left| \sqrt{\rho_b} \sum_{\substack{l=1 \\ l \neq i}}^{\mathrm{L}} \mathbf{g}_{\boldsymbol{l}ki} \frac{\hat{\mathbf{g}}_{\boldsymbol{lkl}}^{\dagger}}{\zeta_{lkl}} \right|^2 = \rho_b \sum_{\substack{l=1 \\ l \neq i}}^{\mathrm{L}} \sum_{\substack{n=1 \\ n \neq i}}^{\mathrm{L}} \mathbf{E}\left[\mathbf{g}_{\boldsymbol{l}ki} \frac{\hat{\mathbf{g}}_{\boldsymbol{lkl}}^{\dagger}}{\zeta_{lkl}} \hat{\mathbf{g}}_{\boldsymbol{n}kn} \frac{\mathbf{g}_{\boldsymbol{nki}}^{\dagger}}{\zeta_{nkn}} \right] \\
&= \rho_b \sum_{\substack{l=1 \\ l \neq i}}^{\mathrm{L}} \sum_{\substack{n=1 \\ n \neq i \\ n \neq l}}^{\mathrm{L}} \mathbf{E}\left[\mathbf{g}_{\boldsymbol{l}ki} \frac{\hat{\mathbf{g}}_{\boldsymbol{lkl}}^{\dagger}}{\zeta_{lkl}} \hat{\mathbf{g}}_{\boldsymbol{n}kn} \frac{\mathbf{g}_{\boldsymbol{nki}}^{\dagger}}{\zeta_{nkn}} \right] + \rho_b \sum_{\substack{l=1 \\ l \neq i}}^{\mathrm{L}} \mathrm{E}\left[\mathbf{g}_{\boldsymbol{l}ki} \frac{\hat{\mathbf{g}}_{\boldsymbol{lkl}}^{\dagger}}{\zeta_{lkl}} \hat{\mathbf{g}}_{\boldsymbol{l}kl} \frac{\mathbf{g}_{\boldsymbol{lki}}^{\dagger}}{\zeta_{lkl}} \right] \\
&= \rho_b \sum_{\substack{l=1 \\ l \neq i}}^{\mathrm{L}} \mathrm{E}\left[\mathbf{g}_{\boldsymbol{l}ki} \frac{\hat{\mathbf{g}}_{\boldsymbol{lkl}}^{\dagger}}{\zeta_{lkl}} \hat{\mathbf{g}}_{\boldsymbol{l}kl} \frac{\mathbf{g}_{\boldsymbol{lki}}^{\dagger}}{\zeta_{lkl}} \right] \\
&= \rho_b \sum_{\substack{l=1 \\ l \neq i}}^{\mathrm{L}} \mathrm{Var}\left[\mathbf{g}_{\boldsymbol{l}ki} \frac{\hat{\mathbf{g}}_{\boldsymbol{lkl}}^{\dagger}}{\zeta_{lkl}} \right] + \rho_b \left| \sum_{\substack{l=1 \\ l \neq i}}^{\mathrm{L}} \mathrm{E}\left[\mathbf{g}_{\boldsymbol{l}ki} \frac{\hat{\mathbf{g}}_{\boldsymbol{lkl}}^{\dagger}}{\zeta_{lkl}} \right] \right|^2 \\
&= \rho_b \mathrm{M} \sum_{\substack{l=1 \\ l \neq i}}^{\mathrm{L}} \frac{\rho_t \tau \beta_{lki} \beta_{lkl}^2}{(\zeta_{lkl}^3)^2} + \rho_b \mathrm{M}^2 \left| \sum_{\substack{l=1 \\ l \neq i}}^{\mathrm{L}} \frac{\rho_t \tau \beta_{lki} \beta_{lkl}}{\zeta_{lkl}^3} \right|^2
\end{aligned}$$

$$\mathrm{E}[|\mathrm{v}_3|^2] = \rho_b \mathrm{M} \sum_{\substack{l=1 \\ l \neq i}}^{\mathrm{L}} \frac{\rho_t \tau \beta_{lki} \beta_{lkl}^2}{(\zeta_{lkl}^3)^2} + \rho_b \mathrm{M}^2 \left| \sum_{\substack{l=1 \\ l \neq i}}^{\mathrm{L}} \frac{\rho_t \tau \beta_{lki} \beta_{lkl}}{\zeta_{lkl}^3} \right|^2 \tag{A.9}$$

$$\mathrm{E}[|\mathrm{v}_4|^2] = \mathrm{E}\left[\left|\sqrt{\rho_b}\sum_{l=1}^{\mathrm{L}}\sum_{\substack{\mathrm{j}=1\\ j\neq k}}^{K}\mathbf{g}_{\boldsymbol{l}ki}\frac{\hat{\mathbf{g}}_{\boldsymbol{ljl}}^{\dagger}}{\zeta_{ljl}}\right|^2\right] = \sum_{l=1}^{\mathrm{L}}\sum_{\substack{\mathrm{j}=1\\ j\neq k}}^{K}\mathrm{E}\left[\mathbf{g}_{\boldsymbol{l}ki}\frac{\hat{\mathbf{g}}_{\boldsymbol{ljl}}^{\dagger}}{\zeta_{ljl}}\hat{\mathbf{g}}_{\boldsymbol{l}jl}\frac{\mathbf{g}_{\boldsymbol{lki}}^{\dagger}}{\zeta_{ljl}}\right]$$

$$= \sum_{l=1}^{\mathrm{L}}\sum_{\substack{\mathrm{j}=1\\ j\neq k}}^{K}\mathrm{E}\left[\mathrm{Tr}\left(\frac{\hat{\mathbf{g}}_{\boldsymbol{ljl}}^{\dagger}}{\zeta_{ljl}}\hat{\mathbf{g}}_{\boldsymbol{l}jl}\frac{\mathbf{g}_{\boldsymbol{lki}}^{\dagger}}{\zeta_{ljl}}\mathbf{g}_{\boldsymbol{l}ki}\right)\right]$$

$$= \sum_{l=1}^{\mathrm{L}}\sum_{\substack{\mathrm{j}=1\\ j\neq k}}^{K}\mathrm{E}\left[\mathrm{Tr}\left(\mathrm{E}\left[\frac{\hat{\mathbf{g}}_{\boldsymbol{ljl}}^{\dagger}}{\zeta_{ljl}}\hat{\mathbf{g}}_{\boldsymbol{l}jl}\right]\mathrm{E}\left[\frac{\mathbf{g}_{\boldsymbol{lki}}^{\dagger}}{\zeta_{ljl}}\mathbf{g}_{\boldsymbol{l}ki}\right]\right)\right]$$

$$= \rho_b\mathrm{M}\sum_{l=1}^{\mathrm{L}}\sum_{\substack{\mathrm{j}=1\\ j\neq k}}^{K}\frac{\rho_t\tau\beta_{lki}\beta_{ljl}^2}{\left(\zeta_{ijl}^3\right)^2}$$

$$\mathrm{E}[|\mathrm{v}_4|^2] = \rho_b\mathrm{M}\sum_{l=1}^{\mathrm{L}}\sum_{\substack{\mathrm{j}=1\\ j\neq k}}^{K}\frac{\rho_t\tau\beta_{lki}\beta_{ljl}^2}{\left(\zeta_{ijl}^3\right)^2} \tag{A.10}$$

$$\mathrm{E}[|\mathrm{v}_5|^2] = Var[\mathbf{n}_{\mathrm{ki}}] = \sigma_{ki}^2 \tag{A.11}$$

$$\mathrm{E}[|v_2|^2] + \mathrm{E}[|\mathrm{v}_3|^2] + \mathrm{E}[|\mathrm{v}_4|^2] + \mathrm{E}[|\mathrm{v}_5|^2]$$

$$= \rho_b\mathrm{M}^2\left|\frac{\rho_t\tau\beta_{iki}^2}{\zeta_{iki}^3}\right|^2 + \rho_b\rho_t\tau\mathrm{M}\left(\frac{\beta_{iki}}{\zeta_{iki}^2}\right)^3 + \rho_b\mathrm{M}\sum_{\substack{l=1\\ l\neq i}}^{\mathrm{L}}\frac{\rho_t\tau\beta_{lki}\beta_{lkl}^2}{(\zeta_{lkl}^3)^2}$$

$$+ \rho_b\mathrm{M}^2\left|\sum_{\substack{l=1\\ l\neq i}}^{\mathrm{L}}\frac{\rho_t\tau\beta_{lki}\beta_{lkl}}{\zeta_{lkl}^3}\right|^2 + \rho_b\mathrm{M}\sum_{l=1}^{\mathrm{L}}\sum_{\substack{\mathrm{j}=1\\ j\neq k}}^{K}\frac{\rho_t\tau\beta_{lki}\beta_{ljl}^2}{\left(\zeta_{ijl}^3\right)^2} + \sigma_{ki}^2$$

$$= \rho_b\mathrm{M}^2\left|\frac{\rho_t\tau\beta_{iki}^2}{\zeta_{iki}^3}\right|^2 + \rho_b\mathrm{M}\sum_{l=1}^{\mathrm{L}}\sum_{\mathrm{j}=1}^{K}\frac{\rho_t\tau\beta_{lki}\beta_{ljl}^2}{\left(\zeta_{ijl}^3\right)^2} + \sigma_{ki}^2$$

$$\mathrm{E}[|v_2|^2] + \mathrm{E}[|\mathrm{v}_3|^2] + \mathrm{E}[|\mathrm{v}_4|^2] + \mathrm{E}[|\mathrm{v}_5|^2]$$

$$= \rho_b \mathrm{M}^2 \left| \frac{\rho_t \tau \beta_{iki}^2}{\zeta_{iki}^3} \right|^2 + \rho_b \mathrm{M} \sum_{l=1}^{\mathrm{L}} \sum_{\mathrm{j}=1}^{K} \frac{\rho_t \tau \beta_{lki} \beta_{ljl}^2}{\left(\zeta_{ijl}^3\right)^2} \qquad \text{(A.12)}$$

$$+ \sigma_{ki}^2$$

Equation (A.6) becomes:

$$\mathrm{C} = \mathbf{log_2} \left(\mathbf{1} + \frac{\rho_b \mathrm{M}^2 \left| \frac{\rho_t \tau \beta_{iki}^2}{\zeta_{iui}^3} \right|^2}{M^2 \psi_1 + M \psi_2 + \sigma_{ki}^2} \right) \qquad \text{(A.13)}$$

$$\psi_1 = \rho_b \left| \sum_{\substack{l=1 \\ l \neq i}}^{\mathrm{L}} \frac{\rho_t \tau \beta_{lki}^2}{\zeta_{iki}^3} \right|^2$$

$$\psi_2 = \rho_b \mathrm{M} \sum_{l=1}^{\mathrm{L}} \sum_{\mathrm{j}=1}^{K} \frac{\rho_t \tau \beta_{lki} \beta_{ljl}^2}{\left(\zeta_{ijl}^3\right)^2}$$

Appendix B

Achievable rate of massive MIMO with large scale fading precoding

The sub-group user (u, j)receives the signal:

$$x_{ujl} = \sqrt{\rho_b} \sum_{i=1}^{\mathrm{L}} \sum_{w=1}^{\mathrm{L}} \sum_{q=1}^{\mathrm{U}} \mathbf{g}_{wl,uji} \frac{\hat{\mathbf{g}}_{wl,qwl}^{\dagger}}{\zeta_{wl,qwl}} v_{qwi} + \mathrm{w}_{ujl} \tag{B.1}$$

The vectors $\mathbf{g}_{wl,uji}$ and $\hat{\mathbf{g}}_{wl,uwl}$have the following distributions**;**

$$\mathbf{g}_{wl,uji} \sim \mathcal{CN}\left(0, \beta_{wl,uji} \boldsymbol{I_M}\right) \tag{B.2}$$

$$\hat{\mathbf{g}}_{wl,uwl} \sim \mathcal{CN}\left(0, \left(\frac{\beta_{wl,uji}}{\zeta_{wl,uwl}}\right)^2 \boldsymbol{I_M}\right) \tag{B.3}$$

Changing the random variable in front of s_{ujl} with its expected value we obtain:

$$\begin{aligned} x_{ujl} = s_{ujl}\sqrt{\rho_b} \sum_{w=1}^{\mathrm{L}} \mathbf{g}_{wl,ujl} \frac{\hat{\mathbf{g}}_{wl,uwl}^{\dagger}}{\zeta_{wl,uwl}} \boldsymbol{a}_{wl,ujl} \\ + \sqrt{\rho_b} \sum_{w=1}^{\mathrm{L}} \mathbf{g}_{wl,ujl} \frac{\hat{\mathbf{g}}_{wl,uwl}^{\dagger}}{\zeta_{wl,uwl}} \sum_{\substack{p=1 \\ p \neq j}}^{\mathrm{L}} s_{upl} \boldsymbol{a}_{wl,upl} \\ + \sqrt{\rho_b} \sum_{w=1}^{\mathrm{L}} \sum_{\substack{q=1 \\ q \neq u}}^{\mathrm{U}} \mathbf{g}_{wl,ujl} \frac{\hat{\mathbf{g}}_{wl,qwl}^{\dagger}}{\zeta_{wl,qwl}} v_{qwi} \\ + \sqrt{\rho_b} \sum_{\substack{i=1 \\ i \neq l}}^{\mathrm{L}} \sum_{w=1}^{\mathrm{L}} \sum_{q=1}^{\mathrm{U}} \mathbf{g}_{wl,uji} \frac{\hat{\mathbf{g}}_{wl,qwl}^{\dagger}}{\zeta_{wl,qwl}} v_{qwi} + \mathrm{w}_{ujl} \end{aligned}$$

$$
\begin{aligned}
x_{ujl} = s_{ujl}\sqrt{\rho_b}\sum_{w=1}^{\mathrm{L}} \boldsymbol{a}_{wl,ujl}\mathrm{E}\left[\mathbf{g}_{wl,ujl}\frac{\hat{\mathbf{g}}_{wl,uwl}^{\dagger}}{\zeta_{wl,uwl}}\right] \\
+ s_{ujl}\sqrt{\rho_b}\sum_{w=1}^{\mathrm{L}} \boldsymbol{a}_{wl,ujl}\left(\mathbf{g}_{wl,ujl}\frac{\hat{\mathbf{g}}_{wl,uwl}^{\dagger}}{\zeta_{wl,uwl}}\right. \\
\left. - \mathrm{E}\left[\mathbf{g}_{wl,ujl}\frac{\hat{\mathbf{g}}_{wl,uwl}^{\dagger}}{\zeta_{wl,uwl}}\right]\right) \\
+ \sqrt{\rho_b}\sum_{w=1}^{\mathrm{L}} \mathbf{g}_{wl,ujl}\frac{\hat{\mathbf{g}}_{wl,uwl}^{\dagger}}{\zeta_{wl,uwl}}\sum_{\substack{p=1\\p\neq j}}^{\mathrm{L}} s_{upl}\boldsymbol{a}_{wl,upl} \\
+ \sqrt{\rho_b}\sum_{w=1}^{\mathrm{L}}\sum_{\substack{q=1\\q\neq u}}^{\mathrm{U}} \mathbf{g}_{wl,ujl}\frac{\hat{\mathbf{g}}_{wl,qwl}^{\dagger}}{\zeta_{wl,qwl}} v_{qwl} \\
+ \sqrt{\rho_b}\sum_{\substack{i=1\\i\neq l}}^{\mathrm{L}}\sum_{w=1}^{\mathrm{L}}\sum_{q=1}^{\mathrm{U}} \mathbf{g}_{wl,uji}\frac{\hat{\mathbf{g}}_{wl,qwl}^{\dagger}}{\zeta_{wl,qwl}} v_{qwi} + \mathrm{w}_{ujl}
\end{aligned}
\tag{B.4}
$$

$$
\mathrm{F}_1 = s_{ujl}\sqrt{\rho_b}\sum_{w=1}^{\mathrm{L}} \boldsymbol{a}_{wl,ujl}\mathrm{E}\left[\mathbf{g}_{wl,ujl}\frac{\hat{\mathbf{g}}_{wl,uwl}^{\dagger}}{\zeta_{wl,uwl}}\right]
$$

$$
\mathrm{F}_2 = s_{ujl}\sqrt{\rho_b}\sum_{w=1}^{\mathrm{L}} \boldsymbol{a}_{wl,ujl}\left(\mathbf{g}_{wl,ujl}\frac{\hat{\mathbf{g}}_{wl,uwl}^{\dagger}}{\zeta_{wl,uwl}} - \mathrm{E}\left[\mathbf{g}_{wl,ujl}\frac{\hat{\mathbf{g}}_{wl,uwl}^{\dagger}}{\zeta_{wl,uwl}}\right]\right)
$$

$$
\mathrm{F}_3 = \sqrt{\rho_b}\sum_{w=1}^{\mathrm{L}} \mathbf{g}_{wl,ujl}\frac{\hat{\mathbf{g}}_{wl,uwl}^{\dagger}}{\zeta_{wl,uwl}}\sum_{\substack{p=1\\p\neq j}}^{\mathrm{L}} s_{upl}\boldsymbol{a}_{wl,upl}
$$

$$
\mathrm{F}_4 = \sqrt{\rho_b}\sum_{w=1}^{\mathrm{L}}\sum_{\substack{q=1\\q\neq u}}^{\mathrm{U}} \mathbf{g}_{wl,ujl}\frac{\hat{\mathbf{g}}_{wl,qwl}^{\dagger}}{\zeta_{wl,qwl}} v_{qwl}
$$

$$
\mathrm{F}_5 = \sqrt{\rho_b}\sum_{\substack{i=1\\i\neq l}}^{\mathrm{L}}\sum_{w=1}^{\mathrm{L}}\sum_{q=1}^{\mathrm{U}} \mathbf{g}_{wl,uji}\frac{\hat{\mathbf{g}}_{wl,qwl}^{\dagger}}{\zeta_{wl,qwl}} v_{qwi}
$$

$$
\mathrm{F}_6 = \mathrm{w}_{ujl}
$$

The achievable rate given by:

$$\mathrm{C} = \mathbf{log_2}\left(\mathbf{1} + \frac{\mathrm{E}[|\mathrm{F}_1|^2]}{\mathrm{E}[|\mathrm{F}_2|^2] + \mathrm{E}[|\mathrm{F}_3|^2] + \mathrm{E}[|\mathrm{F}_4|^2] + \mathrm{E}[|\mathrm{F}_5|^2] + \mathrm{E}[|\mathrm{F}_6|^2]}\right) \quad \text{(B.5)}$$

Where:

$$\mathrm{E}[|\mathrm{F}_1|^2] = \mathrm{E}\left[\left|s_{ujl}\sqrt{\rho_b}\sum_{w=1}^{\mathrm{L}}\boldsymbol{a}_{wl,ujl}\mathrm{E}\left[\mathbf{g}_{wl,ujl}\frac{\hat{\mathbf{g}}_{wl,uwl}^{\dagger}}{\zeta_{wl,uwl}}\right]\right|^2\right]$$

$$= \rho_b M^2\left|\sum_{w=1}^{\mathrm{L}}\frac{\rho_t\tau\beta_{wl,ujl}\beta_{wl,uwl}}{1+\rho_t\tau\sum_{z=1}^{L}\beta_{wl,uzl}}\frac{\boldsymbol{a}_{wl,ujl}}{\zeta_{wl,uwl}}\right|^2$$

$$\mathrm{E}[|\mathrm{F}_1|^2] = \rho_b M^2\left|\sum_{w=1}^{\mathrm{L}}\frac{\rho_t\tau\beta_{wl,ujl}\beta_{wl,uwl}}{1+\rho_t\tau\sum_{z=1}^{L}\beta_{wl,uzl}}\frac{\boldsymbol{a}_{wl,ujl}}{\zeta_{wl,uwl}}\right|^2 \quad \text{(B.6)}$$

$$\mathrm{E}[|\mathrm{F}_2|^2] = \mathrm{E}\left[\left|s_{ujl}\sqrt{\rho_b}\sum_{w=1}^{\mathrm{L}}\boldsymbol{a}_{wl,ujl}\left(\mathbf{g}_{wl,ujl}\frac{\hat{\mathbf{g}}_{wl,uwl}^{\dagger}}{\zeta_{wl,uwl}} - \mathrm{E}\left[\mathbf{g}_{wl,ujl}\frac{\hat{\mathbf{g}}_{wl,uwl}^{\dagger}}{\zeta_{wl,uwl}}\right]\right)\right|^2\right]$$

$$= \mathrm{E}[s_{ui}{s_{ui}}^{\dagger}]\rho_b\sum_{w=1}^{\mathrm{L}}\sum_{n=1}^{\mathrm{L}}\boldsymbol{a}_{wl,ujl}\left(\boldsymbol{a}_{nl,ujl}\right)^{\dagger}\mathbf{E}\left[\left(\mathbf{g}_{wl,ujl}\frac{\hat{\mathbf{g}}_{wl,uwl}^{\dagger}}{\zeta_{wl,uwl}}\right.\right.$$

$$\left.\left. - \mathrm{E}\left[\mathbf{g}_{wl,ujl}\frac{\hat{\mathbf{g}}_{wl,uwl}^{\dagger}}{\zeta_{wl,uwl}}\right]\right)\left(\mathbf{g}_{nl,ujl}\frac{\hat{\mathbf{g}}_{nl,unl}^{\dagger}}{\zeta_{wl,uwl}} - \mathbf{g}_{nl,ujl}\frac{\hat{\mathbf{g}}_{nl,unl}^{\dagger}}{\zeta_{wl,uwl}}\right)^{\dagger}\right]$$

$$= \sqrt{\rho_b}\sum_{w=1}^{\mathrm{L}}\left|\boldsymbol{a}_{wl,ujl}\right|\mathrm{Var}\left[\mathbf{g}_{wl,ujl}\frac{\hat{\mathbf{g}}_{wl,uwl}^{\dagger}}{\zeta_{wl,uwl}}\right]$$

$$= \rho_b M\sum_{w=1}^{\mathrm{L}}\left|\frac{\boldsymbol{a}_{wl,ujl}}{\zeta_{wl,uwl}}\right|^2\frac{\rho_t\tau\beta_{wl,ujl}\beta_{wl,uwl}^2}{1+\rho_t\tau\sum_{z=1}^{L}\beta_{wl,uzl}}$$

$$\mathrm{E}[|\mathrm{F}_2|^2] = \rho_b M\sum_{w=1}^{\mathrm{L}}\left|\frac{\boldsymbol{a}_{wl,ujl}}{\zeta_{wl,uwl}}\right|^2\frac{\rho_t\tau\beta_{wl,ujl}\beta_{wl,uwl}^2}{1+\rho_t\tau\sum_{z=1}^{L}\beta_{wl,uzl}} \quad \text{(B.7)}$$

$$\mathrm{E}[|\mathrm{F}_3|^2] = \mathrm{E}\left[\left|\sqrt{\rho_b}\sum_{w=1}^{\mathrm{L}}\mathbf{g}_{wl,ujl}\frac{\hat{\mathbf{g}}_{wl,uwl}^{\dagger}}{\zeta_{wl,uwl}}\sum_{\substack{p=1\\p\neq j}}^{\mathrm{L}}s_{upl}\boldsymbol{a}_{wl,upl}\right|^2\right]$$

$$= \rho_b\sum_{w=1}^{\mathrm{L}}\sum_{n=1}^{\mathrm{L}}\mathbf{E}\left[\mathbf{g}_{wl,ujl}\frac{\hat{\mathbf{g}}_{wl,uwl}^{\dagger}}{\zeta_{wl,uwl}}\mathbf{g}_{nl,ujl}^{\dagger}\frac{\hat{\mathbf{g}}_{nl,unl}}{\zeta_{nl,unl}}\right]\sum_{\substack{p=1\\p\neq j}}^{\mathrm{L}}\mathrm{E}\left[s_{upl}{s_{upl}}^{\dagger}\right]\boldsymbol{a}_{wl,upl}\left(\boldsymbol{a}_{nl,upl}\right)^{\dagger}$$

$$= \rho_b\sum_{w=1}^{\mathrm{L}}\sum_{\substack{n=1\\n\neq w}}^{\mathrm{L}}\mathbf{E}\left[\mathbf{g}_{wl,ujl}\frac{\hat{\mathbf{g}}_{wl,uwl}^{\dagger}}{\zeta_{wl,uwl}}\mathbf{g}_{nl,ujl}^{\dagger}\frac{\hat{\mathbf{g}}_{nl,unl}}{\zeta_{nl,unl}}\right]\sum_{\substack{p=1\\p\neq j}}^{\mathrm{L}}\mathrm{E}\left[s_{upl}{s_{upl}}^{\dagger}\right]\boldsymbol{a}_{wl,upl}\left(\boldsymbol{a}_{nl,upl}\right)^{\dagger}$$

$$+ \rho_b\sum_{w=1}^{\mathrm{L}}\mathrm{E}\left[\mathbf{g}_{wl,ujl}\frac{\hat{\mathbf{g}}_{wl,uwl}^{\dagger}}{\zeta_{wl,uwl}}\mathbf{g}_{wl,ujl}^{\dagger}\frac{\hat{\mathbf{g}}_{wl,uwl}}{\zeta_{wl,uwl}}\right]\sum_{\substack{p=1\\p\neq j}}^{\mathrm{L}}\mathrm{E}\left[s_{upl}{s_{upl}}^{\dagger}\right]\left|\boldsymbol{a}_{wl,upl}\right|^2$$

$$= \rho_b\sum_{w=1}^{\mathrm{L}}\mathrm{E}\left[\mathbf{g}_{wl,ujl}\frac{\hat{\mathbf{g}}_{wl,uwl}^{\dagger}}{\zeta_{wl,uwl}}\mathbf{g}_{wl,ujl}^{\dagger}\frac{\hat{\mathbf{g}}_{wl,uwl}}{\zeta_{wl,uwl}}\right]\sum_{\substack{p=1\\p\neq j}}^{\mathrm{L}}\mathrm{E}\left[s_{upl}{s_{upl}}^{\dagger}\right]\left|\boldsymbol{a}_{wl,upl}\right|^2$$

$$= \rho_b\sum_{w=1}^{\mathrm{L}}\mathrm{Var}\left[\mathbf{g}_{wl,ujl}\frac{\hat{\mathbf{g}}_{wl,uwl}^{\dagger}}{\zeta_{wl,uwl}}\right]\sum_{\substack{p=1\\p\neq j}}^{\mathrm{L}}\mathrm{E}\left[s_{upl}{s_{upl}}^{\dagger}\right]\left|\boldsymbol{a}_{wl,upl}\right|^2$$

$$+ \rho_b\left|\sum_{w=1}^{\mathrm{L}}\mathrm{E}\left[\mathbf{g}_{wl,ujl}\frac{\hat{\mathbf{g}}_{wl,uwl}^{\dagger}}{\zeta_{wl,uwl}}\right]\right|^2\sum_{\substack{p=1\\p\neq j}}^{\mathrm{L}}\mathrm{E}\left[s_{upl}{s_{upl}}^{\dagger}\right]\left|\boldsymbol{a}_{wl,upl}\right|^2$$

$$= \rho_b M\sum_{w=1}^{\mathrm{L}}\sum_{\substack{\boldsymbol{p=1}\\\boldsymbol{p\neq j}}}^{\mathrm{L}}\left|\frac{\boldsymbol{a}_{wl,upl}}{\zeta_{wl,uwl}}\right|^2\frac{\rho_t\tau\beta_{wl,ujl}\beta_{wl,uwl}^2}{1+\rho_t\tau\sum_{z=1}^{L}\beta_{wl,uzl}}$$

$$+ \rho_b M^2\sum_{\substack{\boldsymbol{p=1}\\\boldsymbol{p\neq j}}}^{\mathrm{L}}\left|\sum_{w=1}^{\mathrm{L}}\frac{\rho_t\tau\beta_{wl,ujl}\beta_{wl,uwl}}{1+\rho_t\tau\sum_{z=1}^{L}\beta_{wl,uzl}}\frac{\boldsymbol{a}_{wl,upl}}{\zeta_{wl,uwl}}\right|^2$$

$$\mathrm{E}[|\mathrm{F}_3|^2] = \rho_b M\sum_{w=1}^{\mathrm{L}}\sum_{\substack{\boldsymbol{p=1}\\\boldsymbol{p\neq j}}}^{\mathrm{L}}\left|\frac{\boldsymbol{a}_{wl,upl}}{\zeta_{wl,uwl}}\right|^2\frac{\rho_t\tau\beta_{wl,ujl}\beta_{wl,uwl}^2}{1+\rho_t\tau\sum_{z=1}^{L}\beta_{wl,uzl}}$$

$$+ \rho_b M^2\sum_{\substack{\boldsymbol{p=1}\\\boldsymbol{p\neq j}}}^{\mathrm{L}}\left|\sum_{w=1}^{\mathrm{L}}\frac{\rho_t\tau\beta_{wl,ujl}\beta_{wl,uwl}}{1+\rho_t\tau\sum_{z=1}^{L}\beta_{wl,uzl}}\frac{\boldsymbol{a}_{wl,upl}}{\zeta_{wl,uwl}}\right|^2 \quad \text{(B.8)}$$

$$\mathrm{E}[|\mathrm{F}_4|^2] = \mathrm{E}\left[\left|\sqrt{\rho_b}\sum_{w=1}^{\mathrm{L}}\sum_{\substack{q=1\\q\neq u}}^{\mathrm{U}}\mathbf{g}_{wl,ujl}\frac{\hat{\mathbf{g}}_{wl,qwl}^{\dagger}}{\zeta_{wl,qwl}}v_{qwi}\right|^2\right]$$

$$= \rho_b\sum_{w=1}^{\mathrm{L}}\sum_{\substack{\mathrm{q}=1\\q\neq u}}^{U}\mathrm{E}\left[\mathbf{g}_{wl,ujl}\frac{\hat{\mathbf{g}}_{wl,qwl}^{\dagger}}{\zeta_{wl,qwl}}\mathbf{g}_{wl,ujl}^{\dagger}\frac{\hat{\mathbf{g}}_{wl,qwl}}{\zeta_{wl,qwl}}\right]\left|v_{qwi}\right|^2$$

$$= \rho_b\sum_{w=1}^{\mathrm{L}}\sum_{\substack{\mathrm{q}=1\\\mathrm{q}\neq\mathrm{u}}}^{\mathrm{U}}\mathrm{E}\left[\mathrm{Tr}\left(\frac{\hat{\mathbf{g}}_{wl,qwl}^{\dagger}}{\zeta_{wl,qwl}}\frac{\hat{\mathbf{g}}_{wl,qwl}}{\zeta_{wl,qwl}}\mathbf{g}_{wl,ujl}^{\dagger}\mathbf{g}_{wl,ujl}\right)\right]\left|v_{qwi}\right|^2$$

$$= \rho_b\sum_{w=1}^{\mathrm{L}}\sum_{\substack{\mathrm{j}=1\\\mathrm{q}\neq\mathrm{u}}}^{\mathrm{U}}\mathrm{Tr}\left(\mathrm{E}\left[\frac{\hat{\mathbf{g}}_{wl,qwl}^{\dagger}}{\zeta_{wl,qwl}}\frac{\hat{\mathbf{g}}_{wl,qwl}}{\zeta_{wl,qwl}}\right]\mathrm{E}\left[\mathbf{g}_{wl,ujl}^{\dagger}\mathbf{g}_{wl,ujl}\right]\right)\left|v_{qwi}\right|^2$$

$$= \rho_b M\sum_{w=1}^{\mathrm{L}}\sum_{\substack{\mathrm{q}=1\\q\neq u}}^{U}\frac{\rho_t\tau\beta_{wl,ujl}\beta_{wl,qwl}^2}{1+\rho_t\tau\sum_{z=1}^{L}\beta_{wl,qzl}}\left|\frac{\boldsymbol{v}_{qwl}}{\zeta_{wl,qwl}}\right|^2$$

$$\mathrm{E}[|\mathrm{F}_4|^2] = \rho_b M\sum_{w=1}^{\mathrm{L}}\sum_{\substack{\mathrm{q}=1\\q\neq u}}^{U}\frac{\rho_t\tau\beta_{wl,ujl}\beta_{wl,qwl}^2}{1+\rho_t\tau\sum_{z=1}^{L}\beta_{wl,qzl}}\left|\frac{\boldsymbol{v}_{qwl}}{\zeta_{wl,qwl}}\right|^2 \qquad \text{(B.9)}$$

$$\mathrm{E}[|\mathrm{F}_5|^2] = \mathrm{E}\left[\left|\sqrt{\rho_b}\sum_{\substack{i=1\\ i\neq l}}^{\mathrm{L}}\sum_{w=1}^{\mathrm{L}}\sum_{q=1}^{\mathrm{U}}\mathbf{g}_{wl,uji}\frac{\hat{\mathbf{g}}_{wl,qwl}^{\dagger}}{\zeta_{wl,qwl}}v_{qwi}\right|^2\right]$$

$$= \rho_b\sum_{\substack{i=1\\ i\neq l}}^{\mathrm{L}}\sum_{w=1}^{\mathrm{L}}\sum_{q=1}^{\mathrm{U}}\mathrm{E}\left[\mathbf{g}_{wl,ujl}\frac{\hat{\mathbf{g}}_{wl,qwl}^{\dagger}}{\zeta_{wl,qwl}}\mathbf{g}_{wl,ujl}^{\dagger}\frac{\hat{\mathbf{g}}_{wl,qwl}}{\zeta_{wl,qwl}}\right]\left|v_{qwi}\right|^2$$

$$= \rho_b\sum_{\substack{i=1\\ i\neq l}}^{\mathrm{L}}\sum_{w=1}^{\mathrm{L}}\sum_{q=1}^{\mathrm{U}}\mathrm{E}\left[\mathrm{Tr}\left(\frac{\hat{\mathbf{g}}_{wl,qwl}^{\dagger}}{\zeta_{wl,qwl}}\frac{\hat{\mathbf{g}}_{wl,qwl}}{\zeta_{wl,qwl}}\mathbf{g}_{wl,ujl}^{\dagger}\mathbf{g}_{wl,ujl}\right)\right]\left|v_{qwi}\right|^2$$

$$= \rho_b\sum_{\substack{i=1\\ i\neq l}}^{\mathrm{L}}\sum_{w=1}^{\mathrm{L}}\sum_{q=1}^{\mathrm{U}}\mathrm{Tr}\left(\mathrm{E}\left[\frac{\hat{\mathbf{g}}_{wl,qwl}^{\dagger}}{\zeta_{wl,qwl}}\frac{\hat{\mathbf{g}}_{wl,qwl}}{\zeta_{wl,qwl}}\right]\mathrm{E}\left[\mathbf{g}_{wl,ujl}^{\dagger}\mathbf{g}_{wl,ujl}\right]\right)\left|v_{qwi}\right|^2$$

$$= \rho_b M\sum_{\substack{i=1\\ i\neq l}}^{\mathrm{L}}\sum_{w=1}^{\mathrm{L}}\sum_{\mathrm{q}=1}^{U}\frac{\rho_t\tau\beta_{wl,uji}\beta_{wl,qwl}^2}{1+\rho_t\tau\sum_{z=1}^{L}\beta_{wl,qzl}}\left|\frac{\boldsymbol{v}_{qwi}}{\zeta_{wl,qwl}}\right|^2$$

$$\mathrm{E}[|\mathrm{F}_5|^2] = \rho_b M\sum_{\substack{i=1\\ i\neq l}}^{\mathrm{L}}\sum_{w=1}^{\mathrm{L}}\sum_{\mathrm{q}=1}^{U}\frac{\rho_t\tau\beta_{wl,uji}\beta_{wl,qwl}^2}{1+\rho_t\tau\sum_{z=1}^{L}\beta_{wl,qzl}}\left|\frac{\boldsymbol{v}_{qwi}}{\zeta_{wl,qwl}}\right|^2 \qquad \text{(B.10)}$$

$$\mathrm{E}[|\mathrm{F}_6|^2] = var\left(\mathbf{w}_{ujl}\right) = \sigma_{ujl}^2 \qquad \text{(B.11)}$$

$$
\begin{aligned}
&\mathrm{E}[|\mathrm{F}_2|^2] + \mathrm{E}[|\mathrm{F}_3|^2] + \mathrm{E}[|\mathrm{F}_4|^2] + \mathrm{E}[|\mathrm{F}_5|^2] + \mathrm{E}[|\mathrm{F}_6|^2] \\
&\quad = +\rho_b M \sum_{w=1}^{\mathrm{L}} \left| \frac{\boldsymbol{a}_{wl,ujl}}{\zeta_{wl,uwl}} \right|^2 \frac{\rho_t \tau \beta_{wl,ujl} \beta_{wl,uwl}^2}{1 + \rho_t \tau \sum_{z=1}^{L} \beta_{wl,uzl}} \\
&\quad + \rho_b M \sum_{w=1}^{\mathrm{L}} \sum_{\substack{p=1 \\ p \neq j}}^{\mathrm{L}} \left| \frac{\boldsymbol{a}_{wl,upl}}{\zeta_{wl,uwl}} \right|^2 \frac{\rho_t \tau \beta_{wl,ujl} \beta_{wl,uwl}^2}{1 + \rho_t \tau \sum_{z=1}^{L} \beta_{wl,uzl}} \\
&\quad + \rho_b M^2 \sum_{\substack{p=1 \\ p \neq j}}^{\mathrm{L}} \left| \sum_{w=1}^{\mathrm{L}} \frac{\rho_t \tau \beta_{wl,ujl} \beta_{wl,uwl}}{1 + \rho_t \tau \sum_{z=1}^{L} \beta_{wl,uzl}} \frac{\boldsymbol{a}_{wl,upl}}{\zeta_{wl,uwl}} \right|^2 \\
&\quad + \rho_b M \sum_{w=1}^{\mathrm{L}} \sum_{\substack{\mathrm{q}=1 \\ q \neq u}}^{U} \frac{\rho_t \tau \beta_{wl,ujl} \beta_{wl,qwl}^2}{1 + \rho_t \tau \sum_{z=1}^{L} \beta_{wl,qzl}} \left| \frac{\boldsymbol{v}_{qwl}}{\zeta_{wl,qwl}} \right|^2 \\
&\quad + \rho_b M \sum_{\substack{i=1 \\ i \neq l}}^{\mathrm{L}} \sum_{w=1}^{\mathrm{L}} \sum_{\mathrm{q}=1}^{U} \frac{\rho_t \tau \beta_{wl,uji} \beta_{wl,qwl}^2}{1 + \rho_t \tau \sum_{z=1}^{L} \beta_{wl,qzl}} \left| \frac{\boldsymbol{v}_{qwi}}{\zeta_{wl,qwl}} \right|^2 + \sigma_{ujl}^2 \\
&\quad = M^2 \rho_b \sum_{\substack{p=1 \\ p \neq j}}^{\mathrm{L}} \left| \sum_{w=1}^{\mathrm{L}} \frac{\rho_t \tau \beta_{wl,ujl} \beta_{wl,uwl}}{1 + \rho_t \tau \sum_{z=1}^{L} \beta_{wl,uzl}} \frac{\boldsymbol{a}_{wl,upl}}{\zeta_{wl,uwl}} \right|^2 \\
&\quad + M \rho_b \sum_{i=1}^{\mathrm{L}} \sum_{w=1}^{\mathrm{L}} \sum_{\mathrm{q}=1}^{U} \frac{\rho_t \tau \beta_{wl,uji} \beta_{wl,qwl}^2}{1 + \rho_t \tau \sum_{z=1}^{L} \beta_{wl,qzl}} \left| \frac{\boldsymbol{v}_{qwi}}{\zeta_{wl,qwl}} \right|^2 + \sigma_{ujl}^2
\end{aligned}
$$

$$
\begin{aligned}
&\mathrm{E}[|\mathrm{F}_2|^2] + \mathrm{E}[|\mathrm{F}_3|^2] + \mathrm{E}[|\mathrm{F}_4|^2] + \mathrm{E}[|\mathrm{F}_5|^2] + \mathrm{E}[|\mathrm{F}_6|^2] \\
&= M^2 \rho_b \sum_{\substack{p=1 \\ p \neq j}}^{\mathrm{L}} \left| \sum_{w=1}^{\mathrm{L}} \frac{\rho_t \tau \beta_{wl,ujl} \beta_{wl,uwl}}{1 + \rho_t \tau \sum_{z=1}^{L} \beta_{wl,uzl}} \frac{\boldsymbol{a}_{wl,upl}}{\zeta_{wl,uwl}} \right|^2 \\
&+ M \rho_b \sum_{i=1}^{\mathrm{L}} \sum_{w=1}^{\mathrm{L}} \sum_{\mathrm{q}=1}^{U} \frac{\rho_t \tau \beta_{wl,uji} \beta_{wl,qwl}^2}{1 + \rho_t \tau \sum_{z=1}^{L} \beta_{wl,qzl}} \left| \frac{\boldsymbol{v}_{qwi}}{\zeta_{wl,qwl}} \right|^2 + \sigma_{ujl}^2
\end{aligned}
\tag{B.12}
$$

Equation (B.5) becomes:

$$\mathrm{C} = \mathbf{log_2}\left(\mathbf{1} + \frac{\rho_b M^2 \left|\sum_{w=1}^{\mathrm{L}} \frac{\rho_t \tau \beta_{wl,ujl}\beta_{wl,uwl}}{1+\rho_t \tau \sum_{z=1}^{L}\beta_{wl,uzl}} \frac{\boldsymbol{a}_{wl,ujl}}{\zeta_{wl,uwl}}\right|^2}{M^2\psi_1 + M\psi_2 + \sigma_{ujl}^2}\right) \quad \text{(B.13)}$$

Where;

$$\psi_1 = \rho_b \sum_{\substack{\boldsymbol{p=1} \\ \boldsymbol{p\neq j}}}^{\mathrm{L}} \left|\sum_{w=1}^{\mathrm{L}} \frac{\rho_t \tau \beta_{wl,ujl}\beta_{wl,uwl}}{1+\rho_t \tau \sum_{z=1}^{L}\beta_{wl,uzl}} \frac{\boldsymbol{a}_{wl,upl}}{\zeta_{wl,uwl}}\right|^2$$

$$\psi_2 = \rho_b \sum_{i=1}^{\mathrm{L}} \sum_{w=1}^{\mathrm{L}} \sum_{\mathrm{q}=1}^{U} \frac{\rho_t \tau \beta_{wl,uji}\beta_{wl,qwl}^2}{1+\rho_t \tau \sum_{z=1}^{L}\beta_{wl,qzl}} \left|\frac{\boldsymbol{v}_{qwi}}{\zeta_{wl,qwl}}\right|^{\mathbf{2}}$$

Appendix C

Published conference paper

Large Scale Fading Pre-coder for Massive MIMO without Cell cooperation

[1]Tedros Salih, [2]Elijah Mwangi, [3]Kibet Langat

[1]Department of Electrical Engineering, Pan African University, Po Box 62000 00200 Nairobi, Kenya
[2]School of Engineering, University of Nairobi, Po Box 30197 Nairobi, Kenya
[3]Department of Telecommunication and Information Engineering, Jomo Kenyatta University of Agriculture and Technology, Po Box 62000, Nairobi Kenya
{tedysal2001@gmail.com; elijah.mwangi@uonbi.ac.ke; kibetlp@jkuat.ac.ke }

Abstract. In massive MIMO technology the channel is estimated using uplink training by sending an orthogonal pilot sequence from users to the base station. These sequences are re-used in the cell and also outside the cell. This gives rise to a channel estimation error referred to as pilot contamination. Large scale fading precoding which is based on the cooperation between cells has been proposed to mitigate pilot contamination. However this approach is known to limit in data transmission rate. In this paper, we propose a novel uplink training scheme to mitigate pilot contamination using a large scale fading precoding without the need of cooperation between cells. This achieves a higher transmission rate over existing method. The simulation results show that the proposed scheme improves 5% outage rate 10 times, over the existing method.

Keywords: Large Scale fading Precoding, Massive MIMO, Pilot contamination, Uplink training

1 Introduction

The effect of multipath fading, limited power at the transmitter and scarce spectrum makes the task of designing high data rate, high reliability wireless communication systems extremely challenging [1]. A solution to this challenge is the use of Multiple Input and Multiple Output (MIMO) technology that uses multiple antennas both for transmission and reception. When the number of antennas at the transmitter and receiver increases, the degree of freedom in propagation channel also increases and gives an improvement in the data rate and link reliability [2].

In point-to-point MIMO, the hardware complexity and power consumption of the signal processing units increase at both the transmitter and receiver sides [2]. In addition, it is also un-scalable and has unfavorable propagation properties. The unfavorable propagation can be minimized using the multi user MIMO (MU-MIMO) technique in which the multiple antennas at the receiver side are divided into many independent terminal users. However, MU-MIMO is not a scalable technology since it was designed to have an equal number of service antennas and terminals and to operate in frequency division duplex mode [3]. It also uses dirty-paper coding/decoding, and requires the knowledge of the channel state information (CSI) at both ends of the link. This increases the computational complexity as the number of antennas increase [4].

The massive MIMO technology has been proposed as a solution to scalability. Massive MIMO is a multi-user MIMO technology where each base station (BS) is equipped with an array of many active antenna elements and utilizes these to communicate with several single-antenna terminals over the same frequency band [4],[5],[6],[7].

In massive MIMO the BS needs channel state information to detect the signal that comes from all users. This CSI is obtained through uplink training. In uplink training multiple users send orthogonal signals that are known at the base station and then the base station estimates the channel based on the

received pilot signal. Massive MIMO operates in a TDD system (time division duplex) [8], [9]. In the TDD system, the uplink channel and downlink channel are considered to be reciprocals for a given coherence time. This coherence time is divided into a number of time slots using the TDD protocol for uplink training, uplink data and downlink data. Due to the coherence time limitation the time slot that are given for uplink training are very short. If we increase the amount of time required for uplink training the amount of time required to send data for uplink and downlink will be decreased and causes the data rate to decrease. For this reason the orthogonal signals that are used for uplink training are limited and the users of different cells cannot have a unique assigned orthogonal signal rather the orthogonal signals are re-used within a cell or adjacent cell. Using of the same orthogonal signal for different users leads to imperfect of the channel estimation. This channel estimation error is referred as pilot contamination.

A pilot contamination mitigation scheme based on large scale fading precoding has been proposed in [10] and in [11].It is based on the assumption that the signals from all terminals in all cells are accessible at each BS and that slow-fading coefficients are accessible to all the BS or alternatively to a network hub. Instead of mitigating interference caused by pilot contamination in estimating of the channel, each BS uses the pilot contamination for transmitting information to all terminals. This mitigation technique has a high computational complexity since it uses cooperation between cells. To avoid the cooperation between cells, we purpose a new uplink training scheme that uses a large scale fading precoding within the cell. Our purposed uplink training scheme that avoids cell cooperation gives a high achievable sum rate compared to the scheme that uses cooperation between cells as reported in literature [11].

The rest of the paper is organized as follows. The system model is presented and discussed in section 2. The pilot contamination analysis is presented in section 3, and in section 4, a discussion of the large scale fading pecoding is discussed. In section 5, a derivation of the achievable rate with a finite number of base station antennas is given. In section 6, the computer simulation results that support our proposed method are presented. Finally, section 7 gives a conclusion and suggestions for future extension of the work.

2 System Model

Consider L hexagonal cells, each consisting of one BS and K single antenna users. In each cell the BS consists of W distributed sub-array antennas and each sub-array has M antennas, as shown in Fig. 1.

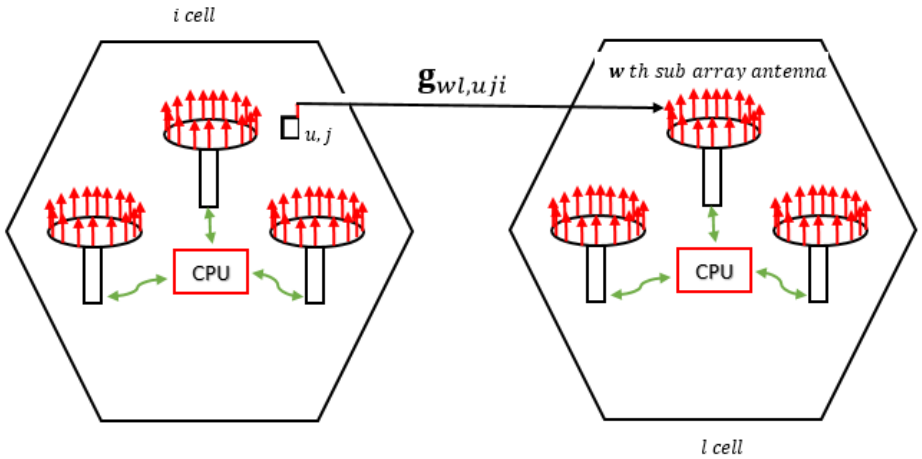

Fig. 1.Multi cell Massive MIMO

We design the uplink training so that each cell has U orthogonal signals, where $U = \frac{K}{L}$ and since $K > U$, all U orthogonal signals are reused within the cell J times. We assume J,L, and, W to be equal. Each

orthogonal signal will have a length of $\tau = K$ and the U orthogonal signals $\{\phi_{1,l}, \phi_{2,l} \dots \phi_{U,l}\}$ have the following property:

(i). For adjacent cells $\phi_{n,l}\phi_{r,i}^{\dagger} = 0$

(ii). Within the cell$\phi_{n,l}\phi_{r,l}^{\dagger} = \delta_{nr}$.

The propagation channel $\mathbf{g}_{wl,uji}$ is modelled as the product of small scale fading (fast fading) and large scale fading (slow fading) [10-15]. The propagation channel coefficient from i-th cell of (u,j) user to the l-th cell of w-th sub-array sub array of antenna given as:

$$\mathbf{g}_{wl,uji} = \boldsymbol{h}_{mwl,uji}\sqrt{\beta_{wl,uji}}\,. \qquad (\mathbf{1})$$

Where $\boldsymbol{h}_{mwl,uji} \sim \mathcal{CN}(0,1)$ small scale fading and $\beta_{wl,uji}$ is a large scale fading. We consider the slow fading to be different at all w sub-array of the BS. However, since the distance between the antennas of the sub-array BS is very small compared to the distance of between the (u,j) user and the sub-array BS, the slow fading ($\beta_{wl,uji}$) can be considered to be independent of M antennas of the sub-array of BS.

The received signal at the w-th sub-array of the BS that comes from users in the cell given by:

$$\mathbf{Y}_{l,w} = \sum_{i=1}^{\mathrm{L}}\sum_{j=1}^{\mathrm{L}}\sum_{u=1}^{\mathrm{U}}\sqrt{\tau\rho_t}\mathbf{g}_{wl,uji}\phi_{u,l} + \mathbf{n}_{l,w}\,. \qquad (\mathbf{2})$$

Where $\mathbf{n}_{l,w} \epsilon \mathbb{C}^{M\,x\,U}$ is the additive noise with distribution $\mathbf{n}_{l,w} \sim \mathcal{CN}(0,1)$ and ρ_t is the average transmitted power at each user.

The w-th sub-array of BS estimates the channel $\mathbf{g}_{wl,uji}$ from its own U users by multiplying eq.(**2**) signal with $\frac{\phi_{u,l}^{\dagger}}{\sqrt{\tau\rho_t}}$ i.e

$$\hat{\mathrm{g}}_{wl,uwl} = \mathrm{Y}_{l,w}\frac{\phi_{u,l}^{\dagger}}{\sqrt{\tau\rho_t}} = \mathrm{g}_{wl,uwl} + \sum_{j=1,j\neq w}^{L}\mathrm{g}_{wl,ujl} + \frac{\phi_{u,l}^{\dagger}}{\sqrt{\tau\rho_t}}\mathbf{n}_{l,w}\,. \qquad (\mathbf{3})$$

The w-th sub-array of BS pre-code the desired signal s_{uwl} using a conjugated beamforming precoder T_{wu} [10-13]. The precoder T_{wu} given by:

$$T_{wu} = \frac{\hat{\mathbf{g}}_{wl,uwl}^{\dagger}}{\left\|\hat{\mathbf{g}}_{wl,uwl}\right\|}. \qquad (\mathbf{4})$$

The w-th sub-array of BS sends the transmitted signal vector T_w to the intended user (u,j).The vector T_w given by:

$$T_w = T_{wu}s_{uwl} = T_{w1}s_{1wl} + T_{w2}s_{2wl} + \cdots + T_{wU}s_{Uwl}\,. \qquad (\mathbf{5})$$

The sub-group user (u,j) receives the signal:

$$x_{ujl} = \sqrt{\rho_b}\sum_{i=1}^{\mathrm{L}}\sum_{w=1}^{\mathrm{L}}\mathbf{g}_{wl,uji}T_w + \mathrm{w}_{ujl}\,,\mathrm{w}_{ujl} \epsilon\, \mathcal{CN}(0,\sigma_{ujl})\,. \qquad (\mathbf{6})$$

$$x_{ujl} = \sqrt{\rho_b} \sum_{i=1}^{\mathrm{L}} \sum_{w=1}^{\mathrm{L}} \sum_{q=1}^{\mathrm{U}} \mathbf{g}_{wl,uji} T_{wq} s_{qwl} + \mathrm{w}_{ujl} \,. \tag{7}$$

Where ρ_b the average transmit power form w-th sub-array of BS.

3 Pilot contamination analysis

The analysis of the pilot contamination effect when the number of antennas approaches infinity has been deduced under the assumption of uplink training reuse in adjacent cells [10],[11],[13],[14],[15]. Here we analyze the pilot contamination effect when the uplink training is reused within cell but different in adjacent cells.

Lemma 1. Let $x, y\ \mathbb{C}^{M\,x\,1}$ be two independent vectors with distribution $\mathcal{CN}(0, c\mathbf{I})$. Then;

$$\lim_{M\to\infty} \frac{x^{\dagger} y}{M} = 0 \text{ and } \lim_{M\to\infty} \frac{x^{\dagger} x}{M} = c. \tag{8}$$

Using the above Lemma when the number of antenna approaches infinity eq.(**7**) becomes

$$\lim_{M\to\infty} \frac{x_{ujl}}{\sqrt{M}} = \lim_{M\to\infty} \sqrt{\rho_b} \sum_{i=1}^{\mathrm{L}} \sum_{w=1}^{\mathrm{L}} \sum_{q=1}^{\mathrm{U}} \frac{\mathbf{g}_{wl,uji} T_{wq} s_{qwl}}{\sqrt{M}} + \frac{\mathbf{w}_{ujl}}{\sqrt{M}} \,. \tag{9}$$

$$\lim_{M\to\infty} \frac{\mathbf{g}_{wl,uji} T_{wq}}{\sqrt{M}} = \lim_{M\to\infty} \left(\frac{\mathbf{g}_{wl,uji} \hat{\mathbf{g}}^{\dagger}_{wl,qwl}}{M} \frac{1}{\frac{\left\| \hat{\mathbf{g}}^{\dagger}_{wl,qwl} \right\|}{\sqrt{M}}} \right). \tag{10}$$

$$\lim_{M\to\infty} \frac{\mathbf{g}_{wl,uji} \hat{\mathbf{g}}^{\dagger}_{wl,qwl}}{M} = \begin{cases} \beta_{wl,ujl} & for\ \mathrm{q} = u\,, i = l \\ 0 & for\ \mathrm{q} \neq u \end{cases}. \tag{11}$$

$$\lim_{M\to\infty} \frac{\left\| \hat{\boldsymbol{g}}^{\dagger}_{\boldsymbol{wl,qwl}} \right\|}{\sqrt{\boldsymbol{M}}} = \boldsymbol{\mathcal{B}_{ujl}} = \left(\sum_{j=1}^{\boldsymbol{L}} \boldsymbol{\beta_{wl,uji}} + \mathbf{1} \right)^{\frac{1}{2}} . \tag{12}$$

$$\lim_{M\to\infty} \frac{x_{ujl}}{\sqrt{M}} = \sqrt{\rho_b} X_{ujl} = \sqrt{\rho_b} \sum_{w=1}^{\mathrm{L}} \beta'_{wl,ujl} s_{uwl} \,. \tag{13}$$

Where $\beta'_{wl,uji} = \frac{\beta_{wl,ujl}}{\mathcal{B}_{ujl}}$.

From eq.(**13**) we can observe two things. The first is that the signal that comes from adjacent cell vanish when M approaches infinity. The second is that the (u, j)-th user in the l-th receives not only the intended signal that comes from the BS of the l-th cell but also from other sub-arrays in the BS of the l-th cell. This causes signal interference. This interference happened due to pilot contamination error estimation of the channel at the sub array of BS of the l-th cell. The signal-to-interference-plus-noise

ratio (SINR) is given in eq.(**14**) and from this we can observe that the SINR is limited as M approaches infinity. But this limitation can be avoided by using large scale fading precoding.

$$SINR_{u1} = \frac{\beta'^{2}_{1l,ujl}}{\beta'^{2}_{2l,ujl} + \beta'^{2}_{3l,ujl} + \cdots + \beta'^{2}_{Ll,ujl}} = \frac{\beta^{2}_{1l,ujl}}{\sum_{w=2}^{L} \beta^{2}_{wl,ujl}} . \quad (\mathbf{14})$$

4 Large Scale Fading Precoding

In this precoding scheme it is assumed that the slow fading coefficients are estimated. To mitigate the pilot contamination, the w-th sub-array can add to a pre-coder unknown variable form A_1, A_2 ... A_L so as to get the received signal as:

$$\begin{aligned} X_{u1} &= \beta'_{1l,u1l}A_1 s_{u1l} + \beta'_{2l,u1l}A_2 s_{u2l} + \cdots + \beta'_{Ll,u1l}A_L s_{uLl} = s_{u1l} \\ X_{u2} &= \beta'_{1l,u2l}A_1 s_{u1l} + \beta'_{2l,u2l}A_2 s_{u2l} + \cdots + \beta'_{Ll,u2l}A_L s_{uLl} = s_{u2l} \\ \vdots \quad & \quad \vdots \quad \quad \vdots \quad \quad \vdots \quad \quad \vdots . \\ X_{uL} &= \beta'_{1l,uLl}A_1 s_{u1l} + \beta'_{2l,uLl}A_2 s_{u2l} + \cdots + \beta'_{Ll,uLl}A_L s_{uLl} = s_{uLl} \end{aligned} \quad (\mathbf{15})$$

Then eq.(**15**) can be written in matrix form

$$\begin{pmatrix} \beta'_{1l,u1l} & \beta'_{2l,u1l} & \cdots & \beta'_{Ll,u1l} \\ \beta'_{1l,u2l} & \beta'_{2l,u2l} & \cdots & \beta'_{Ll,u2l} \\ \vdots & \vdots & \ddots & \vdots \\ \beta'_{1l,uLl} & \beta'_{2l,uLl} & \cdots & \beta'_{Ll,uLl} \end{pmatrix} \begin{pmatrix} A_1 s_{u1l} \\ A_2 s_{u2l} \\ \vdots \\ A_L s_{uLl} \end{pmatrix} = \begin{pmatrix} s_{u1l} \\ s_{u2l} \\ \vdots \\ s_{uLl} \end{pmatrix} . \quad (\mathbf{16})$$

$$\begin{pmatrix} v_{u1l} \\ v_{u2l} \\ \vdots \\ v_{uLl} \end{pmatrix} = \begin{pmatrix} a_{1l,u1l} & a_{2l,u1l} & \cdots & a_{Ll,u1l} \\ a_{1l,u2l} & a_{2l,u2l} & \cdots & a_{Ll,u2l} \\ \vdots & \vdots & \ddots & \vdots \\ a_{1l,uLl} & a_{2l,uLl} & \cdots & a_{Ll,uLl} \end{pmatrix} \begin{pmatrix} s_{u1l} \\ s_{u2l} \\ \vdots \\ s_{uLl} \end{pmatrix} . \quad (\mathbf{17})$$

Where

$\mathrm{A}_\mathrm{w} s_{uwl} = v_{uwl}$ and

$$\begin{pmatrix} a_{1l,u1l} & a_{2l,u1l} & \cdots & a_{Ll,u1l} \\ a_{1l,u2l} & a_{2l,u2l} & \cdots & a_{Ll,u2l} \\ \vdots & \vdots & \ddots & \vdots \\ a_{1l,uLl} & a_{2l,uLl} & \cdots & a_{Ll,uLl} \end{pmatrix} = \begin{pmatrix} \beta'_{1l,u1l} & \beta'_{2l,u1l} & \cdots & \beta'_{Ll,u1l} \\ \beta'_{1l,u2l} & \beta'_{2l,u2l} & \cdots & \beta'_{Ll,u2l} \\ \vdots & \vdots & \ddots & \vdots \\ \beta'_{1l,uLl} & \beta'_{2l,uLl} & \cdots & \beta'_{Ll,uLl} \end{pmatrix}^{-1} . \quad (\mathbf{18})$$

The w-th sub-array of BS pre-code the desired signal v_{uwl} using a conjugated beamforming T_{wu} and sends the vector T_w to the intended user (u, j). This precoding scheme is called large scale fading precoding. The vector T_w given by:

$$T_w = T_{wu} v_{uwl} = T_{w1} v_{1wl} + T_{w2} v_{2wl} + \cdots + T_{wU} v_{Uwl} . \quad (\mathbf{19})$$

The sub-group user (u, j)receives the signal

$$x_{ujl} = \sqrt{\rho_b}\sum_{i=1}^{\mathrm{L}}\sum_{w=1}^{\mathrm{L}}\sum_{q=1}^{\mathrm{U}}\mathbf{g}_{wl,uji}T_{wq}v_{qwl} + \mathbf{w}_{ujl}\,. \tag{20}$$

$$\lim_{M\to\infty}\frac{x_{ujl}}{\sqrt{M}} = \sqrt{\rho_b}\sum_{w=1}^{\mathrm{L}}\beta'_{wl,ujl}v_{uwl} = \sqrt{\rho_b}s_{ujl}\ . \tag{21}$$

5 Achievable rates with finite M

In this section we derived the achievable rate of the received signal when a finite number of antennas are used. We consider the MMSE estimator and the received signal as given by eq.(**2**) then becomes;

$$\hat{\mathbf{g}}_{wl,uwl} = \mathbf{Y}_{l,w}\left(\phi^{\dagger}_{u,l}\varphi'_{wl,uwl}\right) = \varphi'_{wl,uwl}\sqrt{\tau\rho_t}\sum_{j=1}^{\boldsymbol{L}}\mathbf{g}_{wl,ujl} + \boldsymbol{n'_{l,w}}$$

Where;

$$\varphi'_{wl,uwl} = \frac{\sqrt{\tau\rho_t}\beta_{wl,uwl}}{\zeta^2_{wl,uwl}}, \qquad \zeta^2_{wl,uwl} = 1 + \rho_t\tau\sum_{z=1}^{L}\beta_{wl,uzl}$$

The vectors$\mathbf{g}_{wl,uji}$ and $\hat{\mathbf{g}}_{wl,uwl}$have the following distributions**;**

$$\mathbf{g}_{wl,uji} \sim \mathcal{CN}\left(0, \beta_{wl,uji}\boldsymbol{I_M}\right). \tag{22}$$

$$\hat{\mathbf{g}}_{wl,uwl} \sim \mathcal{CN}\left(0, \left(\frac{\beta_{wl,uji}}{\zeta_{wl,uwl}}\right)^2\boldsymbol{I_M}\right). \tag{23}$$

The sub-group user (u,j)receives the signal:

$$x_{ujl} = \sqrt{\rho_b}\sum_{i=1}^{\mathrm{L}}\sum_{w=1}^{\mathrm{L}}\sum_{q=1}^{\mathrm{U}}\mathbf{g}_{wl,uji}\frac{\hat{\mathbf{g}}^{\dagger}_{wl,qwl}}{\zeta_{wl,qwl}}v_{qwi} + \mathrm{w}_{ujl}\,. \tag{24}$$

We assume that the conjugated beamforming of $T_{wq} = \frac{\hat{\mathbf{g}}^{\dagger}_{wl,qwl}}{\zeta_{wl,qwl}}$

After some manipulation, eq.(**24**) can be written as:

$$x_{ujl} = \mathrm{F}_1 + \mathrm{F}_2 + \mathrm{F}_3 + \mathrm{F}_4 + \mathrm{F}_5 + \mathrm{F}_6\,. \tag{25}$$

Where;

$$\mathrm{F}_1 = s_{ujl}\sqrt{\rho_b}\sum_{w=1}^{\mathrm{L}}\boldsymbol{a}_{wl,ujl}\mathrm{E}\left[\mathbf{g}_{wl,ujl}\frac{\hat{\mathbf{g}}^{\dagger}_{wl,uwl}}{\zeta_{wl,uwl}}\right]$$

$$\mathrm{F}_2 = s_{ujl}\sqrt{\rho_b}\sum_{w=1}^{\mathrm{L}} \boldsymbol{a}_{wl,ujl}\left(\mathbf{g}_{wl,ujl}\frac{\hat{\mathbf{g}}^{\dagger}_{wl,uwl}}{\zeta_{wl,qwl}} - \mathrm{E}\left[\mathbf{g}_{wl,ujl}\frac{\hat{\mathbf{g}}^{\dagger}_{wl,uwl}}{\zeta_{wl,uwl}}\right]\right)$$

$$\mathrm{F}_3 = \sqrt{\rho_b}\sum_{w=1}^{\mathrm{L}} \mathbf{g}_{wl,ujl}\frac{\hat{\mathbf{g}}^{\dagger}_{wl,uwl}}{\zeta_{wl,uwl}}\sum_{\substack{p=1\\p\neq j}}^{\mathrm{L}} s_{upl}\boldsymbol{a}_{wl,upl}$$

$$\mathrm{F}_4 = \sqrt{\rho_b}\sum_{w=1}^{\mathrm{L}}\sum_{\substack{q=1\\q\neq u}}^{\mathrm{U}} \mathbf{g}_{wl,ujl}T_{wq}v_{qwl}$$

$$\mathrm{F}_5 = \sqrt{\rho_b}\sum_{\substack{i=1\\i\neq l}}^{\mathrm{L}}\sum_{w=1}^{\mathrm{L}}\sum_{q=1}^{\mathrm{U}} \mathbf{g}_{wl,uji}T_{wq}v_{qwi}$$

$$\mathrm{F}_6 = \mathrm{w}_{ujl}$$

The achievable rate given by:

$$\mathrm{C} = \mathbf{log_2}\left(\mathbf{1} + \frac{\mathrm{E}[|\mathrm{F}_1|^2]}{\mathrm{E}[|\mathrm{F}_2|^2] + \mathrm{E}[|\mathrm{F}_3|^2] + \mathrm{E}[|\mathrm{F}_4|^2] + \mathrm{E}[|\mathrm{F}_5|^2] + \mathrm{E}[|\mathrm{F}_6|^2]}\right). \quad (\mathbf{26})$$

Similar to [11] we can have;

$$|\mathrm{F}_1|^2 = \rho_b M^2\left|\sum_{w=1}^{\mathrm{L}}\frac{\rho_t\tau\beta_{wl,ujl}\beta_{wl,uwl}}{1+\rho_t\tau\sum_{z=1}^{L}\beta_{wl,uzl}}\frac{\boldsymbol{a}_{wl,ujl}}{\zeta_{wl,qwl}}\right|^2. \quad (\mathbf{27})$$

$$\mathrm{E}[|\mathrm{F}_2|^2] = \rho_b M\sum_{w=1}^{\mathrm{L}}\left|\frac{\boldsymbol{a}_{wl,ujl}}{\zeta_{wl,qwl}}\right|^2\frac{\rho_t\tau\beta_{wl,ujl}\beta^2_{wl,uwl}}{1+\rho_t\tau\sum_{z=1}^{L}\beta_{wl,uzl}}. \quad (\mathbf{28})$$

$$\mathrm{E}[|\mathrm{F}_3|^2] = \rho_b M\sum_{w=1}^{\mathrm{L}}\sum_{\substack{\boldsymbol{p=1}\\\boldsymbol{p\neq j}}}^{\mathrm{L}}\left|\frac{\boldsymbol{a}_{wl,upl}}{\zeta_{wl,uwl}}\right|^2\frac{\rho_t\tau\beta_{wl,ujl}\beta^2_{wl,uwl}}{1+\rho_t\tau\sum_{z=1}^{L}\beta_{wl,uzl}} + \rho_b M^2\sum_{\substack{\boldsymbol{p=1}\\\boldsymbol{p\neq j}}}^{\mathrm{L}}\left|\sum_{w=1}^{\mathrm{L}}\frac{\rho_t\tau\beta_{wl,ujl}\beta_{wl,uwl}}{1+\rho_t\tau\sum_{z=1}^{L}\beta_{wl,uzl}}\frac{\boldsymbol{a}_{wl,upl}}{\zeta_{wl,uwl}}\right|^2. \quad (\mathbf{29})$$

$$\mathrm{E}[|\mathrm{F}_4|^2] = \rho_b M\sum_{w=1}^{\mathrm{L}}\sum_{\substack{\mathrm{q}=1\\q\neq u}}^{U}\frac{\rho_t\tau\beta_{wl,ujl}\beta^2_{wl,qwl}}{1+\rho_t\tau\sum_{z=1}^{L}\beta_{wl,qzl}}\left|\frac{\boldsymbol{v}_{qwl}}{\zeta_{wl,qwl}}\right|^{\mathbf{2}}. \quad (\mathbf{30})$$

$$\mathrm{E}[|\mathrm{F}_5|^2] = \rho_b M\sum_{\substack{i=1\\i\neq l}}^{\mathrm{L}}\sum_{w=1}^{\mathrm{L}}\sum_{\mathrm{q}=1}^{U}\frac{\rho_t\tau\beta_{wl,uji}\beta^2_{wl,qwl}}{1+\rho_t\tau\sum_{z=1}^{L}\beta_{wl,qzl}}\left|\frac{\boldsymbol{v}_{qwi}}{\zeta_{wl,qwl}}\right|^{\mathbf{2}}. \quad (\mathbf{31})$$

$$\mathrm{E}[|\mathrm{F}_6|^2] = var(\mathbf{w}_{ujl}) = \sigma^2_{ujl}. \quad (\mathbf{32})$$

Finally, the achievable rate becomes;

$$\mathrm{C} = \mathbf{log_2}\left(\mathbf{1} + \frac{\rho_b M^2 \left|\sum_{w=1}^{\mathrm{L}} \frac{\rho_t \tau \beta_{wl,ujl}\beta_{wl,uwl}}{1+\rho_t \tau \sum_{z=1}^{L}\beta_{wl,uzl}} \frac{\boldsymbol{a}_{wl,ujl}}{\zeta_{wl,uwl}}\right|^2}{M^2\psi_1 + M\psi_2 + \sigma_{ujl}}\right). \qquad (\mathbf{33})$$

Where;

$$\psi_1 = \rho_b \sum_{\substack{\boldsymbol{p=1} \\ \boldsymbol{p\neq j}}}^{\mathrm{L}} \left|\sum_{w=1}^{\mathrm{L}} \frac{\rho_t \tau \beta_{wl,ujl}\beta_{wl,uwl}}{1+\rho_t \tau \sum_{z=1}^{L}\beta_{wl,uzl}} \frac{\boldsymbol{a}_{wl,upl}}{\zeta_{wl,uwl}}\right|^2$$

$$\psi_2 = \rho_b \sum_{i=1}^{\mathrm{L}} \sum_{w=1}^{\mathrm{L}} \sum_{\mathrm{q}=1}^{U} \frac{\rho_t \tau \beta_{wl,uji}\beta_{wl,qwl}^2}{1+\rho_t \tau \sum_{z=1}^{L}\beta_{wl,qzl}} \left|\frac{\boldsymbol{v}_{qwi}}{\zeta_{wl,qwl}}\right|^{\mathbf{2}}$$

6 Simulation Result

In this section we consider a network with $L = 7$ cells. Within each cell, BS has $W = 7$ sub-array of antennas and the number of users in each cell is $K = LW$. For each cell unique $U = 7$ orthogonal signals are assigned and for users in each cell those orthogonal signals are reused. We use the 3GPP standard of Urban Macro model to generate large scale fading as given by eq. (**34**) [18].

$$10\log_{10}\beta_{wl,uji} = -139.5 - 35\log_{10} d_{wl,uji} + \varphi_{wl,uji}\,. \qquad (\mathbf{34})$$

Where $d_{wl,uji}$is the distance (in km) between the user and the base station, and $\varphi_{wl,uji}$ is shadowing coefficient modeled as a Gaussian random variable with zero mean and variance 8dB. We consider the cell radius to be $r = 0.75$km and the distance $d_{wl,uji}$ of all users randomly distributed near the edge of the cell. We choose the bandwidth to be B= 20MHz and the noise variance at each receiver $\sigma_{ujl}^2 =$ 92dBm. The average power of w-th sub-array of BS and at each user terminal are $\rho_b = 48$dBm and $\rho_t = 23$dBm, respectively.

We have simulated the cumulative distribution function (CDF) of the achievable sum rate eq. (**33**) using MATLAB. The results in Fig. 2, Fig. 3 and Fig. 4 show the cumulative distribution function (CDF) of the achievable sum rate of LKusers with $M = 10^2$,10^3, and 10^3 respectively.From Fig. 2, Fig. 3 and Fig. 4 it can be noted that the large scale fading precoding with cell cooperation (LSFP-CC) achieves 5% outage rate around 10^{-4} , 10^{-3}, and 10^{-2}bits per channel respectively. When the large scale fading precoding with non-cooperation cell is used (LSFP-NCC) the achievable sum rate is improved to around 10^{-3},10^{-2}, and 10^{-1}bits per channel respectively. From those results, it can be observed that the purposed LSFP-NCC improve 5% outage rate 10 times compared to LSFP-CC. This is due to the large scale precoding which reduces the interference that comes from the adjacent cells. The time complexity analysis shows that the proposed scheme required less time to execute than the existing method. This is due to each cell computes its own users but not the existing method which uses a network hub that computes to all $L = 7$ cell users.

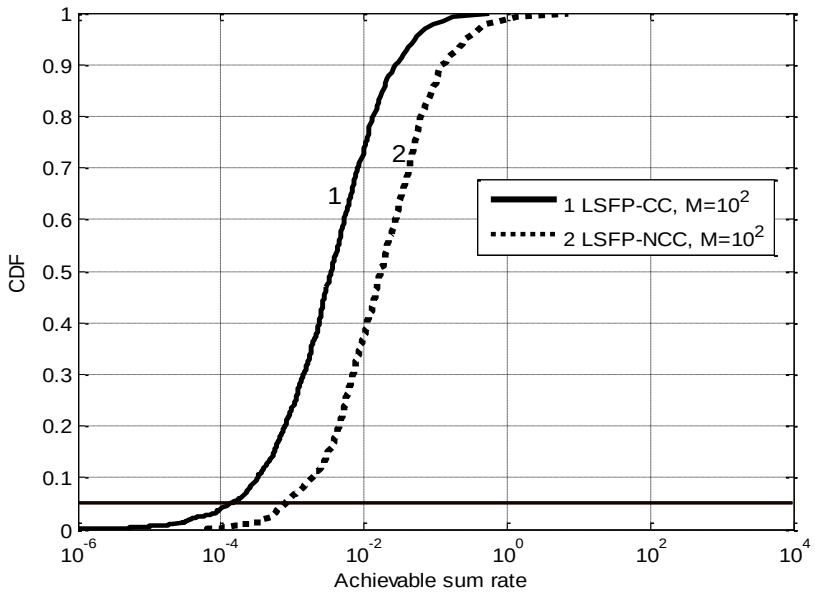

Fig. 2. The CDF of all received Achievable sum rate of $\boldsymbol{LK}$users for $\boldsymbol{M = 10^2}$

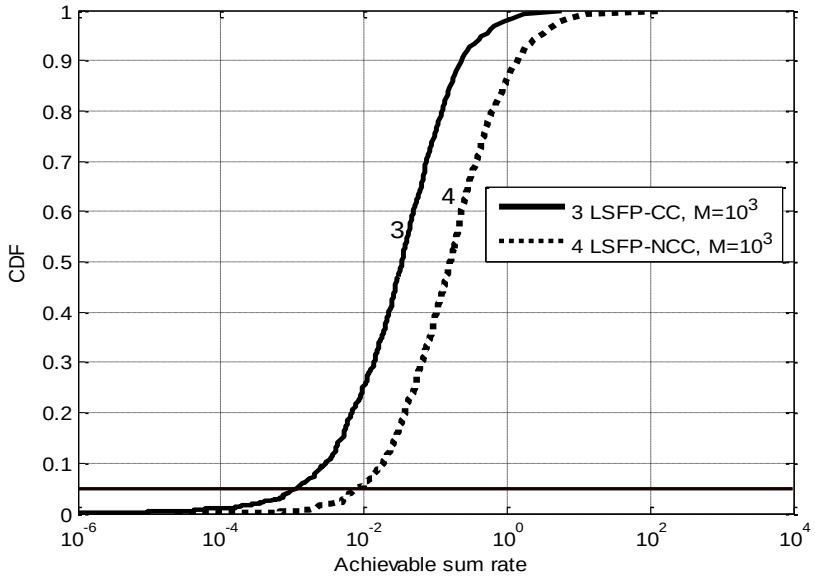

Fig. 3. The CDF of all received Achievable sum rate of $\boldsymbol{LK}$users for $\boldsymbol{M = 10^3}$

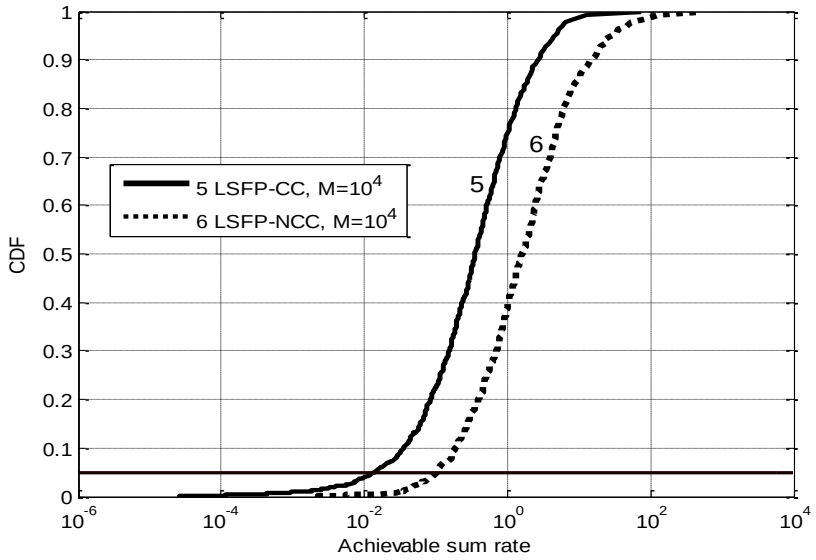

Fig. 4. The CDF of all received Achievable sum rate of $\boldsymbol{LK}$users for $\boldsymbol{M = 10^4}$

7 Conclusion

We have purposed a novel uplink training scheme that uses large scale fading precoding without cooperation between cells and the achievable rate of the scheme has been derived. The proposed scheme improves 5% outage rate 10 times over the existing method. This is a significant improvement, however it is achieved at the expense of sub array BS installation and power consumption.

We have assumed that users are located near the cell edges and but in practice user locations vary randomly within the cell. Further investigations shall be carried out to assess the effect of random user location on the improvement of the achievable sum rates.

References

1. Ezio Biglier, Robert Calderbank, Anthony Constantinides, Andrea Goldsmith, Arogyaswami Paulraj, and H. Vincent Poor, MIMO Wireless Communications, New York: Cambridge university press, 2007.
2. F. Rusek et al., "Scaling Up MIMO: Opportunities and Challenges with Very Large Arrays," in IEEE Signal Processing Magazine, vol. 30, no. 1, pp. 40-60, Jan. 2013.
3. E. G. Larsson, O. Edfors, F. Tufvesson and T. L. Marzetta, "Massive MIMO for next generation wireless systems," in IEEE Communications Magazine, vol. 52, no. 2, pp. 186-195, February 2014.
4. T. L. Marzetta, "Massive MIMO: An Introduction," in Bell Labs Technical Journal, vol. 20, no. , pp. 11-22, 2015.
5. E. Björnson, E. G. Larsson and T. L. Marzetta, "Massive MIMO: ten myths and one critical question," in IEEE Communications Magazine, vol. 54, no. 2, pp. 114-123, February 2016.
6. H. Q. Ngo, E. G. Larsson and T. L. Marzetta, "Massive MU-MIMO downlink TDD systems with linear precoding and downlink pilots," Communication, Control, and Computing (Allerton), 2013 51st Annual Allerton Conference on, Monticello, IL, 2013, pp. 293-298.
7. L. Wang; H. Q. Ngo; M. Elkashlan; T. Q. Duong; K. K. Wong, "Massive MIMO in Spectrum Sharing Networks: Achievable Rate and Power Efficiency," in IEEE Systems Journal ,vol.PP, no.99, pp.1-12
8. L. Lu, G. Y. Li, A. L. Swindlehurst, A. Ashikhmin and R. Zhang, "An Overview of Massive MIMO: Benefits and Challenges," in IEEE Journal of Selected Topics in Signal Processing, vol. 8, no. 5, pp. 742-758, Oct. 2014.

9. Peng Xu, J. Wang and J. Wang, "Effect of pilot contamination on channel estimation in massive MIMO systems," Wireless Communications & Signal Processing (WCSP), 2013 International Conference on, Hangzhou, 2013, pp. 1-6.
10. A. Ashikhmin and T. Marzetta, "Pilot contamination precoding in multi-cell large scale antenna systems," Information Theory Proceedings (ISIT), 2012 IEEE International Symposium on, Cambridge, MA, 2012, pp. 1137-1141.
11. A. Ashikhmin, T. L. Marzetta, and L. Li, "Interference reduction in multi-cell massive mimo systems I: Large-scale fading precoding anddecoding," arXiv preprint arXiv:1411.4182, 2014.
12. A. Ashikhmin, T. L. Marzetta, and L. Li, "Interference reduction in multi-cell massive mimo systems II: Large-scale fading precoding anddecoding," arXiv preprint arXiv:1411.4183, 2014.
13. T. L. Marzetta, "Noncooperative Cellular Wireless with Unlimited Numbers of Base Station Antennas," in IEEE Transactions on Wireless Communications, vol. 9, no. 11, pp. 3590-3600, November 2010.
14. F. Fernandes, A. Ashikhmin and T. L. Marzetta, "Inter-Cell Interference in Noncooperative TDD Large Scale Antenna Systems," in IEEE Journal on Selected Areas in Communications, vol. 31, no. 2, pp. 192-201, February 2013.
15. H. Q. Ngo, T. L. Marzetta and E. G. Larsson, "Analysis of the pilot contamination effect in very large multicell multiuser MIMO systems for physical channel models," 2011 IEEE International Conference on Acoustics, Speech and Signal Processing (ICASSP), Prague, Czech Republic, 2011, pp. 3464-3467.
16. J. Jose, A. Ashikhmin, T. L. Marzetta and S. Vishwanath, "Pilot Contamination and Precoding in Multi-Cell TDD Systems," in IEEE Transactions on Wireless Communications, vol. 10, no. 8, pp. 2640-2651, August 2011.
17. 3GPP TR 25.996,"Spatial channel model for multiple input multiple output (MIMO) simulations", 2016

Appendix D

MATLAB program codes

D.1MATLAB Code for figure 5.1, figure 5.2 and figure 5.3

```
% This code is prepared by Tedros Salih Abdu
% Department of electrical engineering
% Pan African University
% September 2016
% This code is used to simulate the Cumulative Distribution Function
(CDF)
% of the achievable sum rate equation (3.39)
function LSFPCCvsLSFPNCC (CL,K,MM,r)
% CL number of Pilot reuse factor
% K number of users in one cell
% MM number of antennas
% r radius of the cell
 for it=1:2
    if it==2
%  Parameter of LSFP-NCC
% L number of sub-array antennas
L=CL;
% N number of users in one group
N=K/CL;
% t coherence time
t=L*N;
    else
 %  Parameter of LSFP-CC
%  L number of cells
L=CL;
% N number of users in a cell
N=K;
% t coherence time
t=K;
    end
%   Z number of adjacent cells
Z=6;
% T number of iteration
T=1000;
Slul=0;
phi22=0;
% power user terminal with 23dBm
Pt=0.199;
% power of BS with 48dBm
Pb=20;
c=zeros(1,T);
 a=zeros(L,L,N);
 b=zeros(L,L,N);

for S=1:T
    phi1=zeros(N,L);
phi2=zeros(N,L);
```

```
phi3=zeros(N,L);
phi4=zeros(N,L);
% d a distance user to the BS
 d=(poissrnd(r,L,N,L))/1000;
%  B,G large scale fading modeling
 B=10.^(-13.9 - 3.5*log(d) + 0.8*randn(L,N,L));
 G=10.^(-13.9 - 3.5*log(d) + 0.8*randn(L,N,L));
 for k=1:N
     for g=1:L
   for z=1:L
   Slul=Slul+Pt*t*B(g,k,z);
   end
%   the matrix of large scale fading equation(4.20)
 b(:,g,k)=B(:,k,g)/sqrt((1+Slul));
 g=g+1;
     end
     Slul=0;
 k=k+1;

 end

 for k=1:N
%      large scale fading precoder
     a(:,:,k)=inv(b(:,:,k));
     k=k+1;
 end
% calculating components achievable rate of equation(4.39)
for i=1:L

for u=1:N


    for l=1:L

   for z=1:L
   Slul=Slul+Pt*t*B(l,u,z);
  end
        phi1(u,i)=phi1(u,i)+(B(i,u,l)*B(l,u,l)...
            *a(l,i,u))/((1+Slul)*sqrt((1+Slul)));

        Slul=0;
    end

    for q=1:L
    for l=1:L
            for z=1:L
                Slul=Slul+Pt*t*B(l,u,z);
            end

        for j=1:N

        phi3(u,i)=phi3(u,i)+B(i,u,l)*B(l,j,l)*B(l,j,l)...
            *(abs(a(l,q,j)/sqrt((1+Slul))))^2/((1+Slul));
        if it==2
       phi4(u,i)=phi4(u,i)+G(i,u,l)*B(l,j,l)*B(l,j,l)...
           *(abs(a(l,q,j)/sqrt((1+Slul))))^2/((1+Slul));
        end
        end
```

```
        if q~=i

    phi22=(B(i,u,l)*B(l,u,l)...
        *a(l,q,u))/((1+Slul)*sqrt((1+Slul)));
        end
         Slul=0;
    end
      phi2(u,i)= phi2(u,i)+ phi22^2;

    end



end

end

% calculating achievable sum rate of for LK users using
equation(4.39)
M=MM;
SNR=(M*phi1.*phi1)./(M*phi2+phi3./(Pt*t)...
    +Z*phi4./(Pt*t)+6.3/(Pb*Pt^2*M*t^2*10^13));

if it==2
c(S)=7*sum(sum(20*10^6*log(1+SNR)./log(2)));
else

c(S)=7*sum(sum(20*10^6*log(1+SNR(:,1))./log(2)));
end

end
c=sort(c);

% ecdf Empirical cumulative distribution function
[ydata,xdata] = ecdf(c);

plotInd = unique(floor(logspace(0, log10(length(xdata)), 2000)));
if it==2
% Plot of ECDF of the achievable sum rate of LK users for LSFP-NCC
plot(xdata(plotInd),ydata(plotInd),'LineStyle', '-.', 'Color',...
    [0 0 0],'LineWidth', 2.5,'HandleVisibility','off');
hold on;
else
 % Plot of ECDF of the achievable sum rate of LK users for LSFP-CC
   plot(xdata(plotInd),ydata(plotInd),'LineStyle', '-', 'Color', ...
       [0 0 0],'LineWidth', 2.5,'HandleVisibility','off');
   hold on;
end

 end
% plot of 5% outage rate of the achievable sum rate
plot(10^-6:10^1,zeros(1,length(10^-6:10^1))+0.05,'Color',...
    [0.1 0 0],'LineWidth', 2,'HandleVisibility','off');
plot(-200,0,'-s','Color', [0 0 0],'LineWidth', 2);
hold on;
plot(-200,0,'-o','Color', [0 0 0],'LineWidth', 2);
hold on;
```

```
leg =  legend(['LSFP-CC, M=',num2str(M)],['LSFP-NCC,
M=',num2str(M)]);
 axis([10^-6 10^1 0 1])
grid on;

set(gca,'XScale','log')

 end
```

D.2 MATLAB Code for figure 5.5, figure 5.6, figure 5.7 and figure 5.8

```
% This code is prepared by Tedros Salih Abdu
% Department of electrical engineering
% Pan African University
% September 2016
% This code is used to simulate the achievable sum rate equation
(3.39)

function Document (CL1,CL2,K,r)
% CL1 and CL2 number of Pilot reuse factor
% K number of users in one cell
% K should be devisble by CL1 and CL2
% r radius of the cell
 for it=1:2
    if it==2
%  Parameter for pilot reuse factor CL1
% L number of sub-array antennas
L=CL1;
% N number of users in one group
N=K/CL1;
% t coherence time
t=L*N;
    else
 %  Parameter for pilot reuse factor CL2
% L number of sub-array antennas
L=CL2;
% N number of users in one group
N=K/CL2;
% t coherence time
t=L*N;
    end
%   Z number of adjacent cells
Z=6;
% T number of iteration
T=1000;
% power user terminal with 23dBm
Pt=0.199;
% power of BS with 48dBm
Pb=0.6;
%  Number of antennas
NoAntenna=[20 40 60 80 100 120 140 160 180 200];
% intalization
Slul=0;
phi22=0;
 a=zeros(L,L,N);
```

```
 b=zeros(L,L,N);
c1=zeros(1,T);
c2=zeros(1,T);
c3=zeros(1,T);
c4=zeros(1,T);
c5=zeros(1,T);
c6=zeros(1,T);
c7=zeros(1,T);
c8=zeros(1,T);
c9=zeros(1,T);
c10=zeros(1,T);
for S=1:T
    phi1=zeros(N,L);
phi2=zeros(N,L);
phi3=zeros(N,L);
phi4=zeros(N,L);
% d a distance user to the BS
 d=(poissrnd(r,L,N,L))/1000;
%  B,G large scale fading modeling
 B=10.^(-13.9 - 3.5*log(d) + 0.8*randn(L,N,L));
 G=10.^(-13.9 - 3.5*log(d) + 0.8*randn(L,N,L));
 for k=1:N
     for g=1:L
   for z=1:L
   Slul=Slul+Pt*t*B(g,k,z);
   end
%   the matrix of large scale fading equation(4.20)
 b(:,g,k)=B(:,k,g)/sqrt((1+Slul));
 g=g+1;
     end
     Slul=0;
 k=k+1;

 end

 for k=1:N
%      large scale fading precoder
     a(:,:,k)=inv(b(:,:,k));
     k=k+1;
 end
% calculating components achievable rate of equation(4.39)
for i=1:L

for u=1:N


    for l=1:L

   for z=1:L
   Slul=Slul+Pt*t*B(l,u,z);
  end
        phi1(u,i)=phi1(u,i)+(B(i,u,l)*B(l,u,l)...
            *a(l,i,u))/((1+Slul)*sqrt((1+Slul)));

        Slul=0;
    end

    for q=1:L
```

```
    for l=1:L
            for z=1:L
                Slul=Slul+Pt*t*B(l,u,z);
            end

        for j=1:N

        phi3(u,i)=phi3(u,i)+B(i,u,l)*B(l,j,l)*B(l,j,l)...
            *(abs(a(l,q,j)/sqrt((1+Slul))))^2/((1+Slul));
        if it==2
       phi4(u,i)=phi4(u,i)+G(i,u,l)*B(l,j,l)*B(l,j,l)...
           *(abs(a(l,q,j)/sqrt((1+Slul))))^2/((1+Slul));
        end
        end

        if q~=i

    phi22=(B(i,u,l)*B(l,u,l)...
        *a(l,q,u))/((1+Slul)*sqrt((1+Slul)));
        end
         Slul=0;
    end
      phi2(u,i)= phi2(u,i)+ phi22^2;

    end



end

end

% calculating Average achievable sum rate of for LK users using
equation(4.39)

M=NoAntenna(1);
SNR=(M*phi1.*phi1)./(M*phi2+phi3./(Pt*t)+(Z-1)*phi4./(Pt*t)+...
    6.3/(Pb*Pt^2*M*t^2*10^13));

c1(S)=sum(sum(20*10^6*log(1+SNR)./log(2)));
M=NoAntenna(2);
SNR=(M*phi1.*phi1)./(M*phi2+phi3./(Pt*t)+(Z-1)*phi4./(Pt*t)+...
    6.3/(Pb*Pt^2*M*t^2*10^13));

c2(S)=sum(sum(20*10^6*log(1+SNR)./log(2)));
M=NoAntenna(3);
SNR=(M*phi1.*phi1)./(M*phi2+phi3./(Pt*t)+(Z-1)*phi4./(Pt*t)+...
    6.3/(Pb*Pt^2*M*t^2*10^13));

c3(S)=sum(sum(20*10^6*log(1+SNR)./log(2)));

M=NoAntenna(4);
SNR=(M*phi1.*phi1)./(M*phi2+phi3./(Pt*t)+(Z-1)*phi4./(Pt*t)+...
    6.3/(Pb*Pt^2*M*t^2*10^13));

c4(S)=sum(sum(20*10^6*log(1+SNR)./log(2)));

M=NoAntenna(5);
```

```
SNR=(M*phi1.*phi1)./(M*phi2+phi3./(Pt*t)+(Z-1)*phi4./(Pt*t)+...
    6.3/(Pb*Pt^2*M*t^2*10^13));

c5(S)=sum(sum(20*10^6*log(1+SNR)./log(2)));
M=NoAntenna(6);
SNR=(M*phi1.*phi1)./(M*phi2+phi3./(Pt*t)+(Z-1)*phi4./(Pt*t)+6.3/...
    (Pb*Pt^2*M*t^2*10^13));

c6(S)=sum(sum(20*10^6*log(1+SNR)./log(2)));
M=NoAntenna(7);
SNR=(M*phi1.*phi1)./(M*phi2+phi3./(Pt*t)+(Z-1)*phi4./(Pt*t)+...
    6.3/(Pb*Pt^2*M*t^2*10^13));

c7(S)=sum(sum(20*10^6*log(1+SNR)./log(2)));
M=NoAntenna(8);
SNR=(M*phi1.*phi1)./(M*phi2+phi3./(Pt*t)+(Z-1)*phi4./(Pt*t)+...
    6.3/(Pb*Pt^2*M*t^2*10^13));

c8(S)=sum(sum(20*10^6*log(1+SNR)./log(2)));
M=NoAntenna(9);
SNR=(M*phi1.*phi1)./(M*phi2+phi3./(Pt*t)+(Z-1)*phi4./(Pt*t)+...
    6.3/(Pb*Pt^2*M*t^2*10^13));

c9(S)=sum(sum(20*10^6*log(1+SNR)./log(2)));
M=NoAntenna(10);
SNR=(M*phi1.*phi1)./(M*phi2+phi3./(Pt*t)+(Z-1)*phi4./(Pt*t)+...
    6.3/(Pb*Pt^2*M*t^2*10^13));

c10(S)=sum(sum(20*10^6*log(1+SNR)./log(2)));


end

c=[sum(c1) sum(c2) sum(c3) sum(c4) sum(c5)...
    sum(c6) sum(c7) sum(c8) sum(c9) sum(c10)]./T;
if it==2
 semilogy (NoAntenna,c,'-s','Color', [0 0 1],'LineWidth',2);

hold on;
else
    semilogy (NoAntenna,c,'-o','Color', [0 0 0],'LineWidth',2);
  hold on;
end
grid on;
 legend(['N=',num2str(CL2),',','K=',num2str(K)],...
     ['N=',num2str(CL1),',','K=',num2str(K)]);
 end
```

D.3 MATLAB Code for figure 5.9, figure 5.10 and figure 5.11

```
% This code is prepared by Tedros Salih Abdu
% Department of electrical engineering
% Pan African University
% September 2016
% This code is used to compare the average achievable sum rate
```

```
% of equation (3.39) with the average achievable rate of
equation(3.25)
function Myfile3 (CL1,K,r)
% CL1 number of Pilot reuse factor
% K number of users in one cell
% K should be devisble by CL1 and CL2
% r radius of the cell
 for it=1:2
    if it==2
%  Parameter for pilot reuse factor CL1
% L number of sub-array antennas
L=CL1;
% N number of users in one group
N=K/CL1;
% t coherence time
t=L*N;
    else
 %  Parameter for pilot reuse factor CL2
% L number of sub-array antennas
L=7;
% N number of users in one group
N=K;
% t coherence time
t=N;
    end
%   Z number of adjacent cells
Z=6;
% T number of iteration
T=1000;
% power user terminal with 23dBm
Pt=0.199;
% power of BS with 48dBm
Pb=0.6;
%  Number of antennas
NoAntenna=[20 40 60 80 100 120 140 160 180 200];
% intalization

c1=zeros(1,T);
c2=zeros(1,T);
c3=zeros(1,T);
c4=zeros(1,T);
c5=zeros(1,T);
c6=zeros(1,T);
c7=zeros(1,T);
c8=zeros(1,T);
c9=zeros(1,T);
c10=zeros(1,T);
 phi1=zeros(N,L);
phi2=zeros(N,L);
phi3=zeros(N,L);
phi4=zeros(N,L);
for S=1:T


 if it==2
    [phi1,phi2,phi3,phi4]= function1(L,N,r);
    M=NoAntenna(1);
SNR=(M*phi1.*phi1)./(M*phi2+phi3./(Pt*t)+Z*phi4./(Pt*t)+...
```

```
    6.3/(Pb*Pt^2*M*t^2*10^13));

c1(S)=sum(sum(20*10^6*log(1+SNR)./log(2)));
M=NoAntenna(2);
SNR=(M*phi1.*phi1)./(M*phi2+phi3./(Pt*t)+Z*phi4./(Pt*t)+...
    6.3/(Pb*Pt^2*M*t^2*10^13));

c2(S)=sum(sum(20*10^6*log(1+SNR)./log(2)));
M=NoAntenna(3);
SNR=(M*phi1.*phi1)./(M*phi2+phi3./(Pt*t)+Z*phi4./(Pt*t)+...
    6.3/(Pb*Pt^2*M*t^2*10^13));

c3(S)=sum(sum(20*10^6*log(1+SNR)./log(2)));

M=NoAntenna(4);
SNR=(M*phi1.*phi1)./(M*phi2+phi3./(Pt*t)+Z*phi4./(Pt*t)+...
    6.3/(Pb*Pt^2*M*t^2*10^13));

c4(S)=sum(sum(20*10^6*log(1+SNR)./log(2)));

M=NoAntenna(5);
SNR=(M*phi1.*phi1)./(M*phi2+phi3./(Pt*t)+(Z-1)*phi4./(Pt*t)+...
    6.3/(Pb*Pt^2*M*t^2*10^13));

c5(S)=sum(sum(20*10^6*log(1+SNR)./log(2)));
M=NoAntenna(6);
SNR=(M*phi1.*phi1)./(M*phi2+phi3./(Pt*t)+Z*phi4./(Pt*t)+6.3/...
    (Pb*Pt^2*M*t^2*10^13));

c6(S)=sum(sum(20*10^6*log(1+SNR)./log(2)));
M=NoAntenna(7);
SNR=(M*phi1.*phi1)./(M*phi2+phi3./(Pt*t)+Z*phi4./(Pt*t)+...
    6.3/(Pb*Pt^2*M*t^2*10^13));

c7(S)=sum(sum(20*10^6*log(1+SNR)./log(2)));
M=NoAntenna(8);
SNR=(M*phi1.*phi1)./(M*phi2+phi3./(Pt*t)+Z*phi4./(Pt*t)+...
    6.3/(Pb*Pt^2*M*t^2*10^13));

c8(S)=sum(sum(20*10^6*log(1+SNR)./log(2)));
M=NoAntenna(9);
SNR=(M*phi1.*phi1)./(M*phi2+phi3./(Pt*t)+Z*phi4./(Pt*t)+...
    6.3/(Pb*Pt^2*M*t^2*10^13));

c9(S)=sum(sum(20*10^6*log(1+SNR)./log(2)));
M=NoAntenna(10);
SNR=(M*phi1.*phi1)./(M*phi2+phi3./(Pt*t)+Z*phi4./(Pt*t)+...
    6.3/(Pb*Pt^2*M*t^2*10^13));

c10(S)=sum(sum(20*10^6*log(1+SNR)./log(2)));
 else
     [phi1,phi2,phi3]= function2(L,N,r);
     M=NoAntenna(1);
SNR=(M*phi1.*phi1)./(M*phi2+phi3./(Pt*t)+6.3/(Pb*Pt^2*M*t^2*10^13));

c1(S)=sum(sum(20*10^6*log(1+SNR(:,1))./log(2)));
M=NoAntenna(2);
SNR=(M*phi1.*phi1)./(M*phi2+phi3./(Pt*t)+6.3/(Pb*Pt^2*M*t^2*10^13));
```

```
c2(S)=sum(sum(20*10^6*log(1+SNR(:,1))./log(2)));
M=NoAntenna(3);
SNR=(M*phi1.*phi1)./(M*phi2+phi3./(Pt*t)+6.3/(Pb*Pt^2*M*t^2*10^13));


c3(S)=sum(sum(20*10^6*log(1+SNR(:,1))./log(2)));

M=NoAntenna(4);
SNR=(M*phi1.*phi1)./(M*phi2+phi3./(Pt*t)+6.3/(Pb*Pt^2*M*t^2*10^13));


c4(S)=sum(sum(20*10^6*log(1+SNR(:,1))./log(2)));

M=NoAntenna(5);
SNR=(M*phi1.*phi1)./(M*phi2+phi3./(Pt*t)+6.3/(Pb*Pt^2*M*t^2*10^13));


c5(S)=sum(sum(20*10^6*log(1+SNR(:,1))./log(2)));
M=NoAntenna(6);
SNR=(M*phi1.*phi1)./(M*phi2+phi3./(Pt*t)+6.3/(Pb*Pt^2*M*t^2*10^13));

c6(S)=sum(sum(20*10^6*log(1+SNR(:,1))./log(2)));
M=NoAntenna(7);
SNR=(M*phi1.*phi1)./(M*phi2+phi3./(Pt*t)+6.3/(Pb*Pt^2*M*t^2*10^13));


c7(S)=sum(sum(20*10^6*log(1+SNR(:,1))./log(2)));
M=NoAntenna(8);
SNR=(M*phi1.*phi1)./(M*phi2+phi3./(Pt*t)+6.3/(Pb*Pt^2*M*t^2*10^13));


c8(S)=sum(sum(20*10^6*log(1+SNR(:,1))./log(2)));
M=NoAntenna(9);
SNR=(M*phi1.*phi1)./(M*phi2+phi3./(Pt*t)+6.3/(Pb*Pt^2*M*t^2*10^13));

c9(S)=sum(sum(20*10^6*log(1+SNR(:,1))./log(2)));
M=NoAntenna(10);
SNR=(M*phi1.*phi1)./(M*phi2+phi3./(Pt*t)+6.3/(Pb*Pt^2*M*t^2*10^13));

c10(S)=sum(sum(20*10^6*log(1+SNR(:,1))./log(2)));
 end

end

c=[sum(c1) sum(c2) sum(c3) sum(c4) sum(c5)...
    sum(c6) sum(c7) sum(c8) sum(c9) sum(c10)]./T
if it==2
 semilogy (NoAntenna,c,'-o','Color', [0 0 1],'LineWidth',2);

hold on;
else
    semilogy (NoAntenna,c,'-s','Color', [0 0 0],'LineWidth',2);
  hold on;
end
legend(['With PCE',',','K=',num2str(K)],...
     ['N=',num2str(CL1),',','K=',num2str(K)]);
grid on;
```

```
  end


function [phi1,phi2,phi3,phi4]=function1 (L,N,r)
 phi1=zeros(N,L);
phi2=zeros(N,L);
phi3=zeros(N,L);
phi4=zeros(N,L);
Slul=0;
phi22=0;
 a=zeros(L,L,N);
 b=zeros(L,L,N);
 Slul=0;
phi22=0;
 a=zeros(L,L,N);
 b=zeros(L,L,N);
 % t coherence time
t=N*L;

 % power user terminal with 23dBm
Pt=0.199;
 % d a distance user to the BS
 d=(poissrnd(r,L,N,L))/1000;
%  B,G large scale fading modeling

 B=10.^(-13.9 - 3.5*log(d) + 0.8*randn(L,N,L));
 G=10.^(-13.9 - 3.5*log(d) + 0.8*randn(L,N,L));

for k=1:N
     for g=1:L
   for z=1:L
   Slul=Slul+Pt*t*B(g,k,z);
   end
%   the matrix of large scale fading equation(4.20)
 b(:,g,k)=B(:,k,g)/sqrt((1+Slul));
 g=g+1;
     end
     Slul=0;
 k=k+1;

 end

 for k=1:N
%      large scale fading precoder
     a(:,:,k)=inv(b(:,:,k));
     k=k+1;
 end
% calculating components achievable rate of equation(4.39)
for i=1:L

for u=1:N


    for l=1:L

   for z=1:L
   Slul=Slul+Pt*t*B(l,u,z);
```

```
  end
        phi1(u,i)=phi1(u,i)+(B(i,u,l)*B(l,u,l)...
            *a(l,i,u))/((1+Slul)*sqrt((1+Slul)));

        Slul=0;
    end

    for q=1:L
    for l=1:L
            for z=1:L
                Slul=Slul+Pt*t*B(l,u,z);
            end

        for j=1:N

        phi3(u,i)=phi3(u,i)+B(i,u,l)*B(l,j,l)*B(l,j,l)...
            *(abs(a(l,q,j)/sqrt((1+Slul))))^2/((1+Slul));
        phi4(u,i)=phi4(u,i)+G(i,u,l)*B(l,j,l)*B(l,j,l)...
           *(abs(a(l,q,j)/sqrt((1+Slul))))^2/((1+Slul));

        end

        if q~=i

    phi22=(B(i,u,l)*B(l,u,l)...
        *a(l,q,u))/((1+Slul)*sqrt((1+Slul)));
        end
         Slul=0;
    end
      phi2(u,i)= phi2(u,i)+ phi22^2;

    end



end


end


function[phi1,phi2,phi3]=function2 (L,N,r)
 phi1=zeros(N,L);
phi2=zeros(N,L);
phi3=zeros(N,L);
phi4=zeros(N,L);
Slul=0;
phi22=0;
 a=zeros(L,L,N);
 b=zeros(L,L,N);
 Slul=0;
phi22=0;
 a=zeros(L,L,N);
 b=zeros(L,L,N);
 % t coherence time
t=N;
     % power user terminal with 23dBm
```

```
Pt=0.199;
 % d a distance user to the BS
 d=(poissrnd(r,L,N,L))/1000;
%  B large scale fading modeling

 B=10.^(-13.9 - 3.5*log(d) + 0.8*randn(L,N,L));

for k=1:N
     for g=1:L
 b(:,g,k)=B(:,k,g);
 g=g+1;
     end
 k=k+1;

 end

for i=1:L

for u=1:N

    for z=1:L
      Siuz=1+Pt*N*B(i,u,z);
    end
    Siui=(Siuz)^0.5;
  phi1(u,i)=phi1(u,i)+abs(B(i,u,i)^2/(Siui)^3);
 Siuz=0;
    for l=1:L
        for z=1:L
      Siuz=1+Pt*N*B(l,u,z);
    end
    Siui=(Siuz)^0.5;
        if i~=l
    phi2(u,i)=phi2(u,i)+(B(l,u,i)*B(l,u,l))/(Siui)^3;
        end
        Siuz=0;
    end


         for l=1:L

        for j=1:N
              for z=1:L
      Siuz=1+Pt*N*B(l,j,z);
    end
       Siui=(Siuz)^0.5;
        phi3(u,i)=phi3(u,i)+B(l,u,i)*B(l,j,l)^2/((Siui)^3)^2;

          Siuz=0;
        end


         end

end

end
```